Author/s:
Edirisinghege, Sampath Surendra Edirisinghe

Title:
Challenges in optical wireless communication networks

Date:
2020

Persistent Link:
https://hdl.handle.net/11343/258787

Challenges in Optical Wireless Communication Networks

Sampath Edirisinghe

Submitted in partial fulfilment of the requirements of the degree of

Doctor of Philosophy

Department of Electrical and Electronic Engineering
THE UNIVERSITY OF MELBOURNE

August 2020

Abstract

WIRELESS local area networks (WLANs) have continually evolved during the last few decades to meet the ever-growing user demands. However, popular radio frequency technologies such as Wi-Fi are now experiencing a spectrum crunch due to a multitude of bandwidth hungry applications and limited bandwidth available in the sub-6 GHz bands. Therefore, a number of complementary technologies such as 60 GHz Wi-Fi, visible light communication and optical wireless communication have emerged to build high capacity WLANs in indoor spaces.

Amongst these emerging WLAN technologies, optical wireless communication, operating in the infrared range, is becoming popular as it has access to virtually unlimited bandwidth compared to radio frequency technologies. With this huge spectrum resources, it is quite straightforward to establish wireless links over 10 Gbps with optical wireless communication. In addition to that, optical wireless communication has several advantages like not causing interference to existing WLANs, high security, and simple transceiver designs.

Though the physical layer of optical wireless communication is being developed fast and brings unprecedented capabilities to WLAN landscape, upper layer protocols and architectures that are essential in harnessing the benefits of physical layer to provide multi-gigabit communication have received minimal attention so far. Therefore, this thesis explores the upper layer protocols, algorithms and architectures for optical wireless networks in homogeneous and heterogeneous settings.

To this end, we first evaluate the suitability of the contention-based MAC protocol of Wi-Fi standard for optical wireless networks. The inefficiencies of the contention-based MAC protocol are highly pronounced at the higher data rates of optical wireless net-

works. Therefore, we introduce an improved version of the Wi-Fi MAC protocol with novel dynamic contention window tuning mechanism that can operate at multi-gigabit data rates.

Second, due to the lack of availability of a simulation platform to evaluate the performance of optical wireless communication networks, we develop a simulation module for optical wireless networks in the Network Simulator-3 (ns-3) project. The proposed module can deploy optical wireless networks of different architectures and layouts, apply different scheduling algorithms, and channel models. To the best of our knowledge, this is the first multi-gigabit optical wireless network simulation module.

Third, we explored novel network architectures for optical wireless networks considering the massive capacity, increased number of access points and smaller cells. Subsequently, we proposed the FLOWN (full-duplex split-plane optical wireless network) architecture for optical wireless networks. The FLOWN architecture is later generalised to all the upcoming WLANs such as Wi-Fi 6, 60 GHz Wi-Fi, and visible light communication to support homogeneous or heterogeneous WLAN deployments. It features a centralised pool of hardware and software resources, a high-capacity distribution network and advanced capabilities like full-duplex and split-plane operation.

Further, delay-sensitive users can only receive guaranteed quality-of-service under contention-free MAC protocols. Therefore, most of the upcoming WLAN MAC protocols deploy hybrid versions of contention-based and contention-free MAC protocols to reap the advantages of both types. Hence, we finally introduce a contention-free MAC protocol for optical wireless networks with adaptable parameters that can be tuned to the traffic requirements of the current users.

Overall, our work reported in this thesis provide simulation platform for optical wireless networks and also insight into design strategies that can be used to realise centralised multi-gigabit network architectures and MAC protocols.

Declaration

This is to certify that

1. the thesis comprises only my original work towards the PhD,
2. due acknowledgement has been made in the text to all other material used,
3. the thesis is less than 100,000 words in length, exclusive of tables, maps, bibliographies and appendices.

Sampath Edirisinghe, August 2020
ORCID iD: 0000-0003-0747-923X

Preface

This thesis presents the original work that I carried out towards my PhD at the University of Melbourne under the supervision of Prof. Christina Lim, Prof. Ampalavanapillai Nirmalathas, Prof. Elaine Wong, and Dr. Chathurika Ranaweera.

The original contributions are presented in the Chapters 3 to 6. I performed the majority of the work including conceiving the idea, analyses, simulations and manuscript compositions. Prof. Christina Lim, Prof. Ampalavanapillai Nirmalathas, Prof. Elaine Wong, and Dr. Chathurika Ranaweera supervised my work in various ways including providing feedback, discussing ideas, reviewing manuscripts and thesis.

The publications stemming from this thesis are listed under Publications section in Chapter 1. The first author conference and journal publications contain my original work including conceiving the idea, analyses, simulations and manuscript composition which contributed more than 90% of the work, while the rest of the authors provided helpful discussions and comments. The 2nd and 5th conference publications were invited review papers and they were prepared by Prof. Ampalavanapillai Nirmalathas in which my contributions are 20% and 15%, respectively. Both 2nd and 5th conference publications outline the contention window tuning mechanism proposed in Chapter 3.

I confirm that this thesis has not been submitted for other qualifications and all the work was carried out after the enrolment in the degree. No third party editorial assistance was provided in preparation of the thesis.

I acknowledge the Melbourne Research Scholarship for funding my PhD candidature with full tuition fee remission. Further, I acknowledge the funding from the Australian Research Council (ARC) under the Discovery Project (DP170100268).

Acknowledgements

I would like to express my deepest gratitude to my supervisors, Prof. Christina Lim, Prof. Ampalavanapillai Nirmalathas, Prof. Elaine Wong, and Dr. Chathurika Ranaweera for believing in me and giving me the opportunity to pursue my PhD in this wonderful research group. Their encouragements have always helped me to extend my boundaries in both professional and personal aspects of my life. Though it is inevitably stressful, I consider these 3.5 years to be one of the most fulfilling periods of my life. I would also like to thank Prof. Nando Ochoa for providing critical feedback on my progress as my advisory committee chair.

I would like to thank the University of Melbourne for providing me with the opportunity to pursue my graduate studies in a world-renowned university. I am grateful for the financial support I received under the Melbourne Research Scholarship program and ARC Discovery project. Further, the cloud computing facilities provided by the Nectar Research Cloud helped me significantly accelerate my research. I take this opportunity to thank the University of Peradeniya for laying a solid foundation of knowledge which led me to pursue graduate studies.

I was privileged to meet many great colleagues in the University of Melbourne. I am thankful that I met Tian Liang, Yu Tian, Lihua Ruan, Charlie Sun, Tingting Song, Sourav Mondal, Ke Wang, Imali Dias, and Rob Delaney from the Electronic and Photonic Systems Group. I was also lucky to interact with Samiru Gayan, Shalanika Dayarathna, Trang Ngoc Cao, Neil Bernardo, Rajitha Senanayake, and Saman Atapattu from the Wireless Communications group. Furthermore, I would like to thank David Lynch, Tessa Pullar, Thananjeyan Shanmuganathan, Nicholas O'Keefe, Alan Lee, and Chien Chan from Insta-Wireless for their support and encouragement.

My sincere gratitude also goes to the administrative staff of the Department of Electrical and Electronic Engineering and the Melbourne School of Engineering for their continued support throughout my candidature.

I had a lovely bunch of friends who made my time in Melbourne a memorable one. Charitha Gamlath, Nilanka Ekanayake, Sachinthani Karunarathna, Bhagya Yatipanthalawa, Sachini Pathirana, Chaminga Dissanayake, Manula Rathnayake, I am forever grateful for the good times and the delicious food I shared with you.

Finally, I would like to express my heartfelt gratitude for my family for always being there for me. Their understanding and encouragement have helped me achieve great feats in life.

To my family and Lihini

Contents

List of Figures

List of Tables

Acronyms

5G	5th generation.
AIFS	arbitration interframe spacing.
AP	access point.
BER	bit error rate.
CO	central office.
CP	control plane.
CSK	colour-shift keying.
CSMA/CA	carrier sense multiple access with collision avoidance.
DCF	distributed coordination function.
DIFS	DCF interframe spacing.
DP	data plane.
EDCF	enhanced distributed coordination function.
ETSI	European Telecommunications Standards Institute.
FLOWN	full-duplex split-plane optical wireless network.
FSO	free space optics.
IEEE	Institute of Electrical and Electronic Engineers.
IM/DD	intensity modulation direct detection.
IrDA	Infrared Data Association.
LED	light emitting diode.
LOS	line-of-sight.
MAC	medium access control.

MEMS	micro-electro-mechanical systems.
ns-3	Network Simulator-3.
OFDM	orthogonal frequency division multiplexing.
OFDMA	orthogonal frequency division multiple access.
OOK	on-off keying.
OWC	optical wireless communication.
PCF	point coordination function.
RoF	radio over fibre.
RTT	round trip time.
SIFS	short interframe spacing.
SNR	signal-to-noise ratio.
VAP	virtual access point.
VLC	visible light communication.
VPP	variable pulse position.
WDMA	wavelength division multiple access.
WLAN	wireless local area network.
WPAN	wireless personal area network.

Chapter 1
Introduction

WIRELESS connectivity has been an integral part of our lives for a long time and the connectivity requirements have always been on the rise. Cellular networks and wireless local area networks (WLANs), being the two major wireless networks, have evolved in an outstanding order in the last few decades. Cellular networks usually cover a large geographical area with acceptable data rates, though, the recent 5th generation (5G) cellular network developments are pushing towards smaller cells and higher data rates. On the contrary, WLANs are typically deployed in indoor spaces to cover a comparatively smaller area with much higher data rates. For instance, the Wi-Fi networks found in office spaces and homes are capable of establishing wireless links in the order of hundreds of megabits per second. With such capacity, WLANs are used to cater diverse indoor applications from web browsing to 4k video streaming.

Yet the continuous upgrades of the user applications pose a never-ending pressure on the WLANs to improve the capacity and quality-of-service (QoS). For instance, the virtual reality/augmented reality devices, 8k/16k/360°/uncompressed video streaming applications require data rates beyond the capacity of currently provisioned WLANs [1, 2].

To cater for these emerging user-centric and machine-centric applications, number of WLAN solutions have emerged within the well-established radio frequency techniques as well as from the optical technologies. The introduction of millimetre-waves to the IEEE 802.11 suite opened up a sizeable 2.16 GHz bandwidth in the 60 GHz range [3]. Though the wide market adoption is yet to occur, the 60 GHz Wi-Fi devices are able to handle data rates around 6.7 Gbps. The main challenges the millimetre-wave technologies experience in indoor spaces are the directionality of the beams and blockage [4], which limits the reach of the signals.

With the large-scale penetration of the light emitting diode (LED) illumination infrastructure, visible light communication (VLC) has become an attractive alternative in the optical range [5]. Due to the limited electrical modulation bandwidth of the LEDs, the achievable data rate greatly depends on the other modulation techniques in place [6]. The current IEEE VLC standard caps at 96 Mbps data rate [7] due to the use of simple modulation schemes, however, the upcoming revised version of the standard is expected to reach beyond 10 Gbps using multi-carrier modulation schemes [8].

On the other hand, optical wireless communication (OWC) operates in the infrared region of the optical spectrum and utilises matured laser diodes and photodiodes to generate and detect signals [9]. By incorporating mechanisms like wavelength division multiplexing, OWC can establish point-to-point wireless links in the order of hundreds of gigabits per second [10, 11]. While it is a good insight to the capacity of OWC networks, there are practical challenges in implementing WLANs with OWC. For instance, WLANs prefer wide beams that can cover multiple users, WLANs user tend to be mobile. Therefore, more practical OWC links operate in the range of a few gigabits per second to tens-of-gigabits per second [9, 12]. Emanating from the fibre optics background, OWC links are inclined to use simple modulation schemes such as on-off keying (OOK) as opposed to multi-carrier modulation techniques. In spite of everything, the physical layer of OWC is developing fast and the capabilities will be even broader in a short period of time.

1.1 Motivation of the Thesis

The development of the OWC physical layer brings unprecedented capabilities as well as unique challenges to the WLAN domain. The new transceiver characteristics/operations, channel characteristics, and massive data rates call for novel network layer protocols and architectures. Further, as stated earlier, OWC systems use simple modulation schemes such as OOK as the bandwidth available in the optical region is enormous. Hence, the intent of this thesis is to identify the challenges in multi-gigabit OWC networks and provide solutions to respond to such challenges and realise the full potential of the OWC physical layer.

The high data rates of the OWC links are going to cause bottlenecks in the distribution network. Typically, Ethernet is used as the distribution network in WLAN deployments, which is not ready to cater a large number of OWC access points that operate in multi-gigabit data rates. To this end, we propose a novel network architecture in this thesis, which addresses the distribution network bottleneck. Further, the proposed architecture addresses the distributed control and management issues, such as interference in dense deployments due to overlapping frequency bands, by centralising the network resource allocations and network controlling functionalities.

MAC protocols play a key role in the performance of the WLANs as they control the multi-user access to the transmission medium. The Wi-Fi networks are equipped with both contention-based and contention-free MAC protocols, though, the contention-based mode is widely implemented. It is an open question whether to adopt contention-based or contention-free MAC protocols for the upcoming multi-gigabit WLANs. Most of the upcoming standards tend to adopt both modes in their MAC protocols. Therefore, we have investigated suitable MAC protocols for OWC networks that can cater for the QoS requirements of upcoming end-user applications. First we evaluate the contention-based MAC protocol used in Wi-Fi networks in an OWC setting and propose modifications to improve its performance. Later in the thesis we introduce a novel contention-free MAC protocol to reach the maximum resource utilisation in OWC networks.

Furthermore, we have observed that there is a significant gap in the research tools which can be used to implement and evaluate upper layer protocols and architectures for multi-gigabit OWC networks. Therefore, we developed a simulation module from the ground up for OWC in the Network Simulator-3 [13] project. We have modelled the physical layer transceivers, channels as well as upper layer protocols. Since Network Simulator-3 is an open-source free software, this module can be used by wide community of researchers to implement, evaluate and validate upper layer protocols for OWC networks.

1.2 Outline of the Thesis and Original Contributions

This thesis is organised into seven chapters including the current Introduction chapter. The Introduction chapter sets the context of the thesis, presents the motivation for the work carried out, outlines the contents of each chapter and lists the publication outputs of the thesis. The literature review is compiled into the Chapter 2. Chapters 3-6 are contribution chapters where the main work is presented. The thesis is concluded with the conclusions and future directions presented in the Chapter 7. The following sections outline the work carried out in each chapter and the original contributions.

Chapter 2: Literature Review

In the literature review, we have presented the evolution of the WLAN technologies over the last 20 years. We discuss the emergence of complementary technologies such as 60 GHz Wi-Fi, visible light communication and optical wireless communication, specifically focusing on what led to the development of these technologies and how they address those particular challenges. Finally, we narrow it down to the optical wireless communication and discuss the recent developments in the physical layer and network layer of optical wireless communication to give the reader an understanding of the state-of-the-art of optical wireless communication.

Chapter 3: Contention-based MAC Protocol for OWC Networks

In the Chapter 3, we discuss the application of the contention-based MAC protocol of Wi-Fi to OWC networks. This particular MAC protocol is based on the carrier sense multiple access with collision avoidance (CSMA/CA) mechanism. The CSMA/CA mechanism demonstrates serious performance degradations when applied in OWC networks. Therefore, in this chapter we propose an improved version of the CSMA/CA with novel QoS mechanisms to be used in multi-gigabit OWC networks.

The original contributions of this chapter are as follows,

- Proposed a dynamic contention window tuning mechanism to improve the performance of the CSMA/CA protocol under multi-gigabit conditions.

- Proposed a service differentiation mechanism considering the upcoming traffic types.
- Modified the ns-3 Wi-Fi module to operate in 10 Gbps OOK mode to evaluate the CSMA/CA protocol under multi-gigabit OWC conditions.
- Compared the performance of the proposed CSMA/CA-based protocol with the original CSMA/CA protocol and another dynamic contention window mechanism.
- Demonstrated the performance improvement under increasing load and a real-life network scenario.

Chapter 4: Network Architecture for Multi-gigabit WLANs

Considering the multi-gigabit access points anticipated for the OWC networks as well as other features such as full duplex operation, we have introduced the Full-duplex split-plane optical wireless network (FLOWN) architecture for OWC networks. However, a closer look at the upcoming Wi-Fi and other WLANs reveals that a similar architecture is vital for their future-proof deployment as well. Therefore, in this chapter, we have introduced a generalised version of the FLOWN architecture that can be used for the upcoming WLAN in homogeneous or heterogeneous settings.

The original contributions of this chapter are as follows,

- Proposed the FLOWN architecture that has a fibre optic distribution network and a centralised software and hardware resource pool.
- Discussed the application of the generalised FLOWN architecture to OWC, VLC, Wi-Fi 6 and 60 GHz Wi-Fi networks.
- Evaluated the performance of the generalised FLOWN architecture with an OWC network.

Chapter 5: Design of ns-3 Module for OWC Networks

With the upper layer research on OWC networks getting traction, there is a need to introduce simulation tools to implement and evaluate protocols, algorithms and architectures for OWC networks. Therefore, in this chapter, we introduced a simulation module for OWC in Network Simulator-3 (ns-3) project. ns-3 is an open source project which is extensively tested by researchers worldwide. Therefore, ns-3 simulations are quite close to the real-life performance of network devices. On the other hand, when there is a unified simulation tool like ns-3 for OWC, researchers can implement and generate simulation results in a coherent manner.

The original contributions of this chapter are as follows,

- Modelled the physical layer and channel characteristics of OWC in the ns-3 module.
- Implemented the upper layer protocols such as MAC protocol and scheduling algorithms.
- Integrated the implemented module into the ns-3.29 version of the simulator.
- Demonstrated several features of the implemented module that are not demonstrated in other chapters.

Chapter 6: Contention-free MAC Protocol for OWC Networks

The final contribution chapter introduces a contention-free MAC protocol for OWC networks. Contention-based MAC protocols such as CSMA/CA always lead to some inefficiencies despite the improvements. These inefficiencies are highly pronounced in multi-gigabit networks. Therefore, in order to achieve maximal channel utilisation and to guarantee the stringent latency requirements of upcoming end-user applications, we introduced a contention-free MAC protocol in Chapter 6.

The original contributions of this chapter are as follows,

- Proposed the superframe structure, packet structures and headers for the contention-free MAC protocol.

- Introduced an adaptive beacon interval mechanism and derived the closed-form expressions for the beacon interval based on the user delay requirements.
- Proposed a novel resource allocation mechanism for the delay-sensitive users to achieve guaranteed performance.
- Performance of the proposed MAC protocol was evaluated using extensive simulation studies.

Chapter 7: Conclusions and Future Directions

We present the summary of the thesis in this chapter with potential future directions for furthering the research in optical wireless communication networks.

1.3 Publications

Conference Publications

1. Edirisinghe, S., Lim, C., Nirmalathas, A., Wong, E., Wang, K. and Alameh, K., 2018, March. Dynamic tuning of contention window for optical wireless networks. In *Optical Fiber Communication Conference* (pp. M2K-8). Optical Society of America.

2. Nirmalathas, A., Liang, T., Edirisinghe, S., Lim, C., Wong, E., Wang, K. and Alameh, K., 2018, July. High-speed optical wireless communications for local area networks. In *2018 23rd Opto-Electronics and Communications Conference (OECC)* (pp. 1-2). IEEE.

3. Edirisinghe, S., Ranaweera, C., Wong, E., Lim, C. and Nirmalathas, A., 2019, June. A novel network architecture for indoor optical wireless communication. In *2019 Global LIFI Congress (GLC)* (pp. 1-6). IEEE.

4. Edirisinghe, S., Ranaweera, C., Wong, E., Lim, C. and Nirmalathas, A., 2019, June. ns-3 Module for Optical Wireless Communication. In *2019 Workshop on ns-3 (WNS-3)*.

5. Nirmalathas, T.A., Song, T., Edirisinghe, S., Tian, L., Lim, C., Wong, E., Wang, K., Ranaweera, C. and Alameh, K., 2020, March. Gigabit/s Optical Wireless Access and Indoor Networks. In *Optical Fiber Communication Conference* (pp. M2H-5). Optical Society of America.

Journal Publications

1. Edirisinghe, S., Lim, C., Nirmalathas, A., Wong, E., Ranaweera, C., Wang, K. and Alameh, K., 2019. MAC protocol for indoor optical wireless networks. *IET Communications, 13*(19), pp.3158-3167.

2. Edirisinghe, S., Ranaweera, C., Wong, E., Lim, C. and Nirmalathas, A., July, 2020. Unified Optical Network Architecture for Future Wireless LANs. Submitted to *IEEE Open Journal of the Communications Society.*

Chapter 2
Literature Review

IN the first chapter we presented a brief introduction to optical wireless communication and the original contributions of this thesis. In this chapter, we will discuss more broadly about the development of wireless LAN communication technologies, emerging new technologies in the WLAN space, and how and where optical wireless communication fits in this ecosystem.

2.1 Wireless LAN Communication and Recent Trends

The ALOHAnet wireless network established in 1971 is believed to be the world's first wireless local area communication network that connected a couple of islands in Hawaii [14]. While there have been many prototypes and products by proprietary and amateur communication groups during that time, widely accepted industry-standard products became a norm only after the standardisation efforts of Institute of Electrical and Electronic Engineers (IEEE) and European Telecommunications Standards Institute (ETSI).

In that regard, ETSI introduced the HiperLAN/1 (high-performance radio local area network) in 1996 with physical and MAC layer specifications that can reach 23 Mbps [15]. Soon after that, IEEE introduced IEEE 802.11 [16], which can only reach 2 Mbps. Counterintuitively, IEEE 802.11 quickly penetrated the market due to its simplicity and ease of implementation. HiperLAN/2 was introduced around 2000 with 54 Mbps data rate, yet failed to compete with already popular IEEE 802.11 devices [17].

Since the inception, the IEEE 802.11 standard has been evolving and dominating the WLAN market for more than 20 years to date. However, with the limitations in the bandwidth in radio frequency domain and ever-growing user demands, competitors started to appear in millimetre-waves and optical ranges. Though we call it a competition, these technologies are complementary to Wi-Fi and strengthens WLANs where Wi-Fi has shortfalls. Wireless personal area networks (WPANs) [18], optical wireless communication [9] and visible light communication [5] are a few viable examples that have gained attention in the recent years. 5G cellular networks are also seen as a recent competitor, however, there are fundamental differences between WLANs and cellular networks. The next few subsections are dedicated to present the evolution of the IEEE 802.11 networks, VLC, WPANs and OWC in detail whilst considering the differences between WLANs and cellular networks.

2.1.1 IEEE 802.11 Suite and Wi-Fi

With the introduction of the first IEEE 802.11 standard in 1997, an alliance of industry partners, called the Wi-Fi Alliance, was formed to certify the interoperability of IEEE 802.11 compliant devices. Henceforth, the certified devices were given the Wi-Fi logo. We will use terms IEEE 802.11 devices and Wi-Fi devices interchangeably in the upcoming text, though an IEEE 802.11 device does not necessarily need to be a certified Wi-Fi device.

The initial IEEE 802.11 standard was introduced in 1997 with two modulation schemes; direct-sequence spread spectrum (DSSS) and frequency-hopping spread spectrum (FHSS) with differential quadrature phase-shift keying (DQPSK). These modulation schemes are fairly outdated and only used in very specific applications at present. This standard was designed to achieve a maximum data rate of 2 Mbps with 20 MHz bandwidth. However, the introduction of orthogonal frequency division multiplexing (OFDM) in IEEE 802.11a after two years boosted the data rate to 54 Mbps with the same bandwidth. Note that IEEE 802.11a is in the 5 GHz range whereas the initial version was in 2.4 GHz range. The successor of the 2.4 GHz version, IEEE 802.11b, was able to achieve 11 Mbps and maintained the backward compatibility to older devices. With the IEEE 802.11g version in 2003, 2.4 GHz range was also converted to OFDM and it was able to achieve 54 Mbps.

Many important updates were introduced in 2009 with the IEEE 802.11n version where the limits were pushed along every possible dimension. The bandwidth was dou-

Table 2.1: Evolution of the IEEE 802.11 Standard.

Standard	Year	Frequency	Bandwidth	Max data rate	Antennas	Modulation
802.11	1997	2.4 GHz	22 MHz	2 Mbps	1	DSSS, FHSS DPQPSK
802.11a	1999	5 GHz	20 MHz	54 Mbps	1	OFDM 64QAM, 3/4
802.11b	1999	2.4 GHz	22 MHz	11 Mbps	1	DSSS
802.11g	2003	2.4 GHz	20 MHz	54 Mbps	1	OFDM 64QAM, 3/4
802.11n	2009	2.4/5 GHz	20/40 MHz	600 Mbps	4	OFDM 64QAM, 5/6
802.11ac	2013	5 GHz	20/40/80/ 160 MHz	6.8 Gbps	8	OFDM 256QAM, 5/6
802.11ax	2019	2.4/5/6 GHz	20/40/80/ 160 MHz	9.6 Gbps	8	OFDM 1024QAM, 5/6
802.11ad	2012	60 GHz	2.16 GHz	6.7 Gbps	1	OFDM
802.11ay	2020	60 GHz	8 GHz	20 Gbps	4	OFDM

bled. The number of spatial streams was increased to 4 and the modulation and coding rates were increased. With these improvements, the IEEE 802.11n version was able to reach 600 Mbps of data rate. The introduction of packet aggregation in the MAC layer also contributed to the performance improvement by cutting down a lot of transmission overhead. IEEE 802.11n included a mode called the Greenfield mode that allowed the networks to operate as if there are no IEEE 802.11a/b/g devices connected. This mode was abandoned in the later versions since it did not improve the performance as expected and deployment complexities [19].

After 4 years, the first multi-gigabit sub-6 GHz IEEE 802.11 version was introduced as IEEE 802.11ac. It operated only at 5 GHz range, but supported a maximum bandwidth of 160 MHz. Number of spatial streams was doubled to 8 and downlink multi-user multiple-input multiple-output (MU-MIMO) was introduced. The MU-MIMO capability allows the access point to serve multiple users simultaneously. In addition, the modulation order can now go up to 256-QAM with 5/6 coding rate. This standard was able to achieve a staggering 6.8 Gbps of data rate. Many devices we find nowadays support the IEEE 802.11ac version. Fig. 2.1 shows the improvements of IEEE 802.11ac compared to

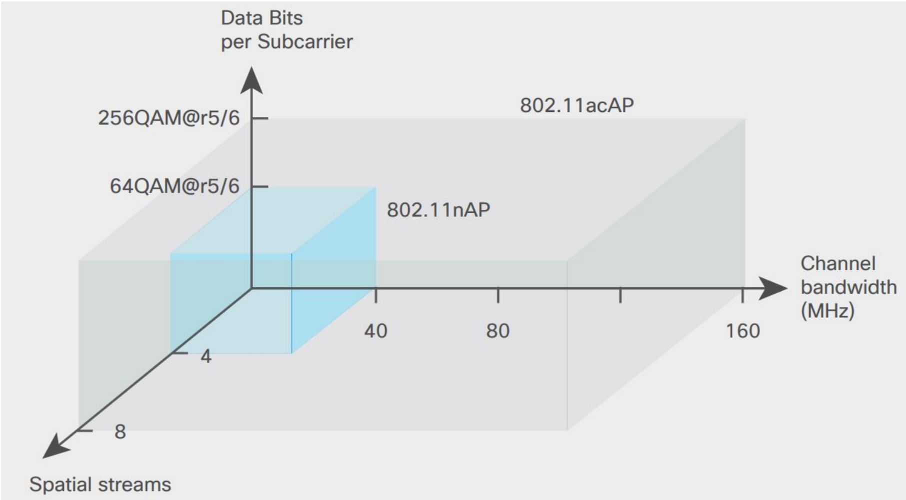

Figure 2.1: Comparison of IEEE 802.11n and IEEE 802.11ac standards in three main dimensions.

the IEEE 802.11n [20].

The most recent IEEE 802.11ax version mainly depends on the modulation schemes (1024-QAM) to improve the data rate while keeping the other parameters unchanged. However, it is worth noting that the task group ax (TGax) was focusing on high-efficiency WLANs rather than merely boosting the data rate. Therefore, several mechanisms such as dynamic power control were added to battle interference in dense deployments [21]. One of the remarkable additions in the IEEE 802.11ax is the orthogonal frequency division multiple access (OFDMA). With OFDMA, the access points are able to allocate spectrum more effectively considering the channel impairments and user demand [22]. In addition, MU-MIMO is now available in the uplink direction as well [23]. It will allow the access points to receive data from multiple users simultaneously. These amendments around the main parameters (spatial streams, bandwidth and modulation order) help the IEEE 802.11ax to be more efficient in dense deployments. Very recently the 6 GHz range was also added under the Wi-Fi 6 as Wi-Fi 6E with regulatory approval pending in different countries. Qualcomm has already developed products in the 6 GHz range that supports over 10 Gbps of data rate [24, 25].

The evolution of the Wi-Fi standards gives good insights into the dimensions along which WLANs grow. For instance, modulation schemes play a key role in the data rate of the network. The upper limit for the modulation schemes depends on the receiver signal-to-noise ratio (SNR) because higher order modulation schemes are more sensitive to noise. On the other hand, number of spatial streams can easily multiply the data rate. However, it is also limited by different factors such as physical dimensions of the device and frequency of operation. Finally, the bandwidth is the most important parameter of all, because once all the other dimensions are exhausted, bandwidth needs to be increased to push the capacity of the network any further. However, wireless communication in the radio frequency spectrum is highly restricted due to regulatory limitations. Therefore, with the increasing demand for wireless connectivity, it is imperative to harness more bandwidth for WLANs. Furthermore, upper layer protocols such as packet aggregation go hand in hand with the physical layer to ensure the physical layer improvements are fully utilised.

One initiative to address the bandwidth scarcity was the 60 GHz front of the 802.11 suite. The IEEE 802.11ad standard proposed in 2012 gained access to a massive 2.16 GHz bandwidth with which it was able to reach 6.7 Gbps data rate [3]. Even though the market has not fully adopted the 60 GHz devices yet, an amendment is being worked out as IEEE 802.11ay which is expected to reach beyond 20 Gbps [26]. Another comparatively smaller but similar body of work was carried out under the IEEE 802.15 work group. The IEEE 802.15.3c standard which was finalised in 2009 operates in the 57-64 GHz range. The main difference from the IEEE 802.11 60 GHz standards is the target applications and the WLAN ecosystem [27]. The IEEE 802.15.3c was developed as a WPAN standard which can be used to establish short-range links compared to Wi-Fi such as kiosks, uncompressed video transmissions and networked storage [18].

Wi-Fi is the most widely used WLAN today with 13 billion devices worldwide. Numerous industry and academic partners were involved in the development of this standard. One clear lesson from the evolution of this standard is that the bandwidth is getting scarce every day with more and more wireless devices connecting to the network. Therefore, it is vital to explore other areas of the electromagnetic spectrum to harvest bandwidth for wireless local area network communications.

2.1.2 Visible Light Communication (VLC)

While the wireless communication using light dates back to the days of Graham Bell [28], the use of light to establish WLANs started in the 21st century [29,30]. The basic idea of VLC is to use the illumination infrastructure to provide wireless connectivity in indoor spaces such as offices and houses. This is fuelled by the wide availability of LED lighting and the spectrum crunch in the sub-6 GHz range that we discussed in the earlier section [31].

Visible light communication consortium (VLCC) in Japan is the first organisation to standardise VLC [32]. Later on in 2011, IEEE also initiated a task group under the 802.15 WPAN work group to standardise VLC. The IEEE 802.15.7 was introduced as a result of that. This standard employ simple modulation schemes such as OOK, variable pulse position (VPP) and colour-shift keying (CSK) as shown in Table 2.2. The maximum data rate is 96 Mbps which can be achieved by using both OOK and CSK [33].

However, the rapid developments in VLC quickly outdated the IEEE 802.15.7 standard. For instance, there were many works around that time that achieved beyond 96 Mbps data rates using OOK modulation [34, 35]. Furthermore, the research community did not limit to the use of simple modulation schemes. Complex modulation schemes such as OFDM were tested for VLC systems to gain better performance [36–38].

With the rapid development in the physical layer research on VLC, IEEE started to update the standard which resulted in two different standards. The first standard, IEEE 802.15.7m continued to operate at lower speeds with the focus of optical camera communications (OCC) [39]. This standard will encompass areas like communication with signage screens, LCD displays and vehicular communications. The second standard is still under development with the IEEE 802.15.13 task group. It is supposed to cover a wide range of data rates with the use of simple modulation schemes to high-speed OFDM. The proposed OFDM 'High Bandwidth PHY' is expected to reach 10 Gbps [40]. It is noteworthy that there is a task group (TG) under 802.11 work group called the light communication TG which also targets VLC [41]. This work is supposed to integrate VLC into the 802.11 MAC and achieve around 5 Gbps at the MAC data service access point.

As we can see from the development of the VLC research, it is possible and beneficial

Table 2.2: Data rates of the IEEE 802.15.7 standard.

Modulation	Optical Clock / MHz	Data rate / Mbps
VPPM	3.75	1.25 - 2
	7.5	2.5 - 5
OOK	15	6 - 9.6
	30	12 - 19.2
	60	24 - 38.4
	120	48 - 96
CSK	12	12 - 18
	24	24 - 96

to implement WLANs in high frequency ranges. The available bandwidth in the visible light region in the electromagnetic spectrum is virtually unlimited. Nonetheless, VLC comes with its own challenges such as limited reach, blockage and uplink. These challenges were addressed in different methods like hybrid VLC networks [42–44]. Hence, VLC networks coupled with existing radio frequency systems can be used to build high capacity heterogeneous WLANs.

2.1.3 Optical Wireless Communication (OWC)

Optical wireless communication has a long history that dates back to early 1990s. The Infrared Data Association (IrDA) first standardised OWC for point-to-point links and later extended to WLANs. Interestingly, the first IEEE 802.11 standard also included an infrared physical layer [16]. However, it was not developed afterwards due to the convenience use of radio frequency signals.

With the recent developments in the physical layer that can exceed 10 Gbps of data rates, OWC has attracted the attention again. OWC is also equipped with a huge bandwidth which can be used to serve multitude of upcoming high data rate applications with its invisible beams. The detailed discussion of OWC is presented in the Section 2.2.

2.1.4 Cellular Communication

The activities in the 5G cellular domain has sparked the discussion on the place of WLANs in the future. Even though the network specifications are becoming more and more comparable, there are a few fundamental differences that we have to consider when understanding this problem.

The access methods of the two networks are very different. The 5G cellular networks are heavily restricted networks which need registration with the service provider, or even insertion of a SIM card to the device that needs connectivity. It is mainly due to the licensed spectrum that costs millions of dollars to the service providers. On the contrary, the WLANs are private, local, and unlicensed networks in which the user can simply connect as many devices as necessary. Therefore, the scaling of the network is easy and low cost with WLANs. Due to the limited bandwidth of the cellular networks, WLANs with wired access network are still and most likely will be the preferred choice for bandwidth-hungry applications such as 4k video streaming and virtual reality whereas 5G cellular networks are useful in outdoor, long range applications [45].

Similarly, integration of on-site facilities such as data servers, network attached storages (NAS) are straightforward and simple in WLANs. These capabilities are more important in enterprise deployments. However, when the WLAN grows to enterprise scale the pure WLAN access, load balancing and authentication mechanisms become impractical. That is the reason behind enterprise network being much closer to cellular networks with restricted access and increased centralisation.

Further, the power consumption of the devices is a key difference between the two networks. WLANs are essentially located a few meters away from the user while the cellular towers could be located a few hundred meters away.

Another much invisible trait is that the development and innovation in these two spaces are fuelled by different motives. The cellular networks are governed by the industry bodies such as 3GPP with a lot of influence from the governments and service providers whereas the WLANs are typically standardised by entities like IEEE and ETSI [46]. The product design and deployments are decoupled from the standardisation entities.

Hence, it is reasonable to expect that the two networks will complement each other rather than competing in the future. Both networks are developing fast and will bring quite attractive features to the users.

2.2 Optical Wireless Communication

Optical wireless communication (OWC) has undergone radical changes since the early market appearances. While most of the research work is in the physical layer, there is an increasing amount of works presented in the last couple of years that address the upper layer challenges as well. The next two subsections will detail the recent developments and challenges in physical layer and upper layers.

2.2.1 Physical Layer and Recent Advancements

OWC operates in the infrared region of the electromagnetic spectrum. The infrared region is a vast range that expands from 700 nm to 1 mm wavelengths. OWC systems that are discussed in this thesis are usually operated in the 780 nm to 950 nm, 1310 nm or 1550 nm ranges, which creates roughly 180 THz of bandwidth [47–49]. For comparison, sub-6 GHz Wi-Fi systems operate with a maximum of 160 MHz of bandwidth while the 60 GHz Wi-Fi systems have access to around 2 GHz of bandwidth. The relative positions of OWC, VLC and microwave techniques in the electromagnetic spectrum are shown in Fig. 2.2 [50]. Due to the close proximity of VLC and OWC, they share similarities in the channel models and propagation characteristics.

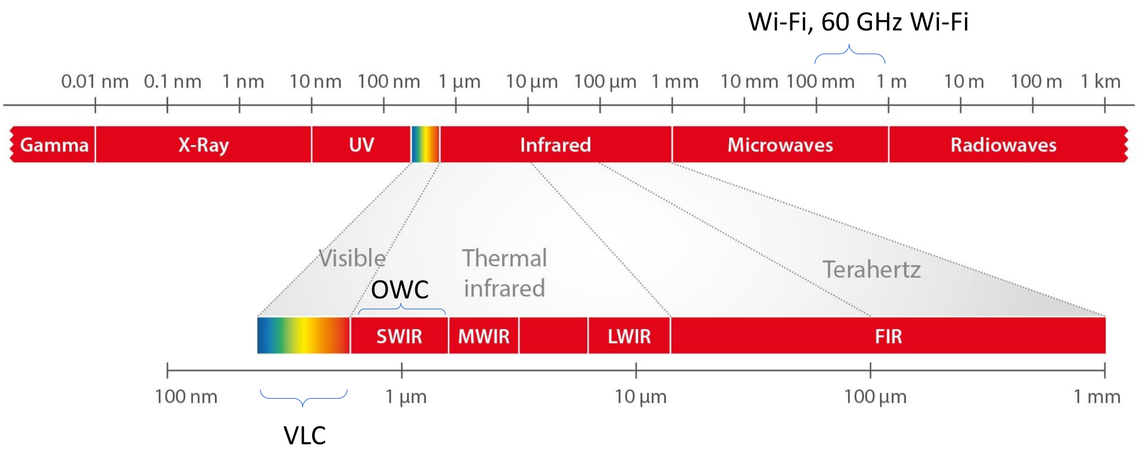

Figure 2.2: Electromagnetic spectrum.

The block diagram of a basic optical wireless system is given in Fig. 2.3. As in any communication system, OWC systems have a transmitter, propagation channel and a

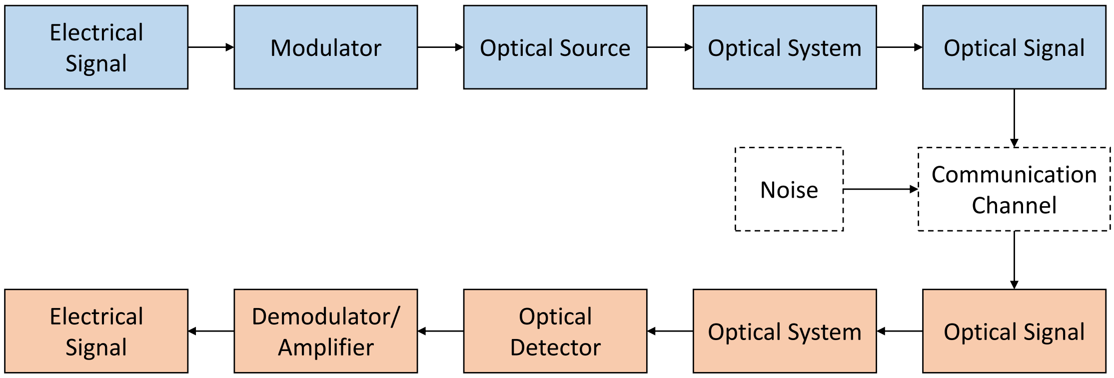

Figure 2.3: Basic components of an optical wireless network.

receiver. Laser diodes or LEDs are used as the optical source in the transmitter. Laser diodes are preferred due to their high modulation bandwidth. The optical system in the transmitter could comprise multiple devices from lenses to micro-electro-mechanical systems (MEMS) for beam-steering. Propagation channel will add noise to the signal during the propagation and depending on the link configuration, multipath effects and attenuation will take place. Receivers usually use filters and concentrators to condition the incident signal. Optical-to-electrical conversion is carried out by a photodetector unit.

Most of the physical layer research stem from the blocks shown in the Fig. 2.3. They can be listed into following categories.

- Modulation and coding techniques
- Laser diodes, LEDs and photodetectors
- Optical systems for signal transmission and reception. For instance, lenses, beam-steering mechanisms, concentrators and filters.
- Multiple access techniques

OWC systems are typically operated as intensity modulation direct detection (IM/DD) systems where the transmit signal is modulated to the instantaneous optical intensity. The frequency and phase information are not used in these modes. Therefore, most of the systems employ OOK or VPP for lower to multi-gigabit data rates [11,51]. The IEEE

802.11-1997 specifically used 16-PPM and 4-PPM schemes [16]. The IM/DD systems have the advantage of simplicity in the signal processing domain compared to radio frequency systems such as Wi-Fi.

On the other hand, coherent modulation schemes such as OFDM are also trialled. The main advantage of OFDM systems is the resilience to multipath effects. The IM/DD systems work well for the line-of-sight (LOS) links. However, when the link is non-LOS (NLOS), the multipath effects come into play causing inter-symbol interference (ISI) [52]. OFDM OWC systems are fairly robust against the multipath effects and the spectrum utilisation is also better compared to IM/DD systems. Nonetheless, they come with the cost of complex signal processing requirements. In addition, for OFDM implementations, unipolar OFDM implementations are required due to the non-negative nature of the optical signals.

The recent OWC developments have an optical fibre heritage as opposed to the earlier systems [53, 54]. Therefore, the recent developments are biased to use laser diode transmitters than LED transmitters. LEDs provide a good diffusion of the signal, however, the modulation bandwidth is far too limited to implement anything near gigabit range. Therefore, laser diodes, with their well established fibre optic techniques have taken the place of transmitters. Receivers are built using photodiodes that are suitable for the operating wavelength. Optical concentrators and filters are mounted to enhance the quality of the incident signal at the photodiode.

One of the physical layer aspects that is of particular interest for this thesis is the beam-steering operation. Since the OWC links are very narrow beams, it is necessary to steer them towards the users to have a useful SNR value. Further, using narrow beam widths and precision beam-steering, it is possible operate multiple overlapping channels in the same coverage area without causing interference. The beam-steering mechanisms can be broadly categorised to two groups; active and passive mechanisms [53].

In the active beam-steering mechanisms, there are active devices such as micro-electro-mechanical systems that actively move the mirrors, lenses or any other components of the beam-steering arrangement. These mechanisms often result in wide steering angles with high resolution. For instance, authors in [55] present an OWC link of 3 Gbps with

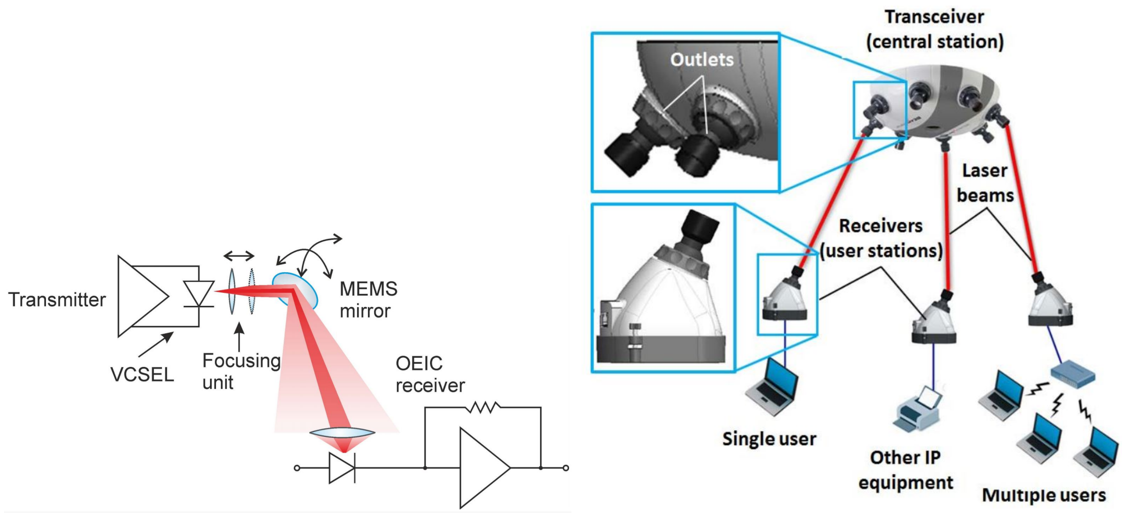

(a) (b)

Figure 2.4: Beam-steering arrangements from (a) Brandl et al. and (b) Glushko et al.

MEMS-based beam-steering. The adaptive focus capability allows them to start with a wider beam and gradually narrow the beam when alignment is achieved. The arrangement of the mirror and lenses are shown in the Fig. 2.4a. A similar system, shown in Fig. 2.4b, is proposed in [56] with multiple transmitter support. This particular system also includes an energy maximisation search algorithm for robust tracking of the users under varying conditions. Although the active beam-steering arrangements have attractive traits to them, the low speed movement and the complex mechanical arrangements have led people to explore passive mechanisms for beam-steering.

One of the most popular passive beam-steering mechanisms presented in the literature are the diffraction grating based beam-steering systems. These mechanisms do not have moving parts nor do they need local processing or power. Diffraction grating based systems steer the beam by changing the wavelength of the data signal. Since the wavelength tuning times of the tunable lasers are small, these beam-steering mechanisms achieve high speeds. Authors in [49,57] have introduced diffraction grating based beam-steering mechanisms that achieve different tuning angles.

Multiple access techniques allow number of users to share the channel. Typically, communication systems implement multiple access mechanisms in the physical layer as well as the MAC layer. In fact, the MAC layer usually controls the resource allocations of the physical layer multiple access mechanisms.

The following multiple access techniques are applicable in OWC with its unique physical layer characteristics [58].

- wavelength division multiple access (WDMA)
- Space division multiple access (SDMA)/Beam-steering

WDMA is somewhat similar to frequency division multiplexing used in radio frequency techniques. However, the immense bandwidth and optical components make it easier to divide the bandwidth into number of independent channels. Authors in [10] reports a very exciting system which reaches above 400 Gbps with WDMA. They have used 14 WDMA channels with coherent modulation schemes. Similarly, authors in [59] also use WDMA to reach around 50 Gbps capacity. On the other hand, SDMA uses beam steering to enable multiple access. Some research groups widely use SDMA with beam steering in their OWC architecture to enable higher network capacity [49]. It involves allocating a separate beam for a user or a collection of users if there is another multiple access stage in the MAC protocol.

In addition to that, there are a few multiple access mechanisms that operates in the upper layers [48, 60].

- Time division multiple access (TDMA)
- Frequency division multiple access (FDMA)
- Code division multiple access (CDMA)
- Non-orthogonal multiple access (NOMA)

TDMA systems allocate a dedicated time slot for every user depending on their traffic demand. TDMA is usually implemented higher in the MAC layer since it is quite transparent to the actual physical layer. Similarly, FDMA allocates frequencies for different users. However, OFDMA is the more popular version of FDMA techniques due to its high efficiency [38]. CDMA uses optical orthogonal codes (OOC) in the transmitting end to enable multiple simultaneous transmissions. The receiver correlates with the designated OOC to extract the expected transmission [61]. Since CDMA allows transmission at overlapping times and wavelengths, it is possible to develop hybrid systems like WDMA/CDMA or TDMA/CDMA [62]. NOMA has recently attracted the attention from many fields of communication. The basic idea is to differentiate signals in the power domain. NOMA techniques have been demonstrated for VLC systems in combination with other techniques such as OFDM [63].

Hence, it can be seen that OWC is progressing as a viable WLAN technology that can address some of pressing issues the radio frequency systems face today. For instance, the high density deployments, increasing interference and spectrum crunch in the low frequencies are easily addressable using OWC systems. When coupled with radio frequency systems, the heterogeneous deployment of OWC and RF systems can enable high-capacity WLANs that the upcoming applications demand.

2.2.2 Network Layer

As mentioned in the previous subsection, there have been two principal standardisation activities for optical wireless communication. IrDA led activities mainly focused on point-to-point links even though subsequently they started developing multi-user systems. The IEEE 802.11 standard had the optical wireless physical layer from the very beginning and the flexible MAC design was able to cater both radio frequency and infrared physical layers.

IrDA MAC Layer

IrDA introduced the Advanced Infrared (AIr) standard to establish indoor WLANs with non-directed wide-angle transceivers ($\pm 60^{\circ}$). This particular standard was able to achieve data rates in the range of 250 kbps to 4 Mbps using 4PPM with variable repetition encoding (4PPM/VR). VR encoding was supported to improve the SNR when the link quality degrades. Doubling the repetition rate improves the SNR by 3 dB. The MAC protocol proposed for this standard was called the AIr-MAC which was based on the CSMA/CA mechanism. This MAC protocol supported both reliable and unreliable modes of trans-

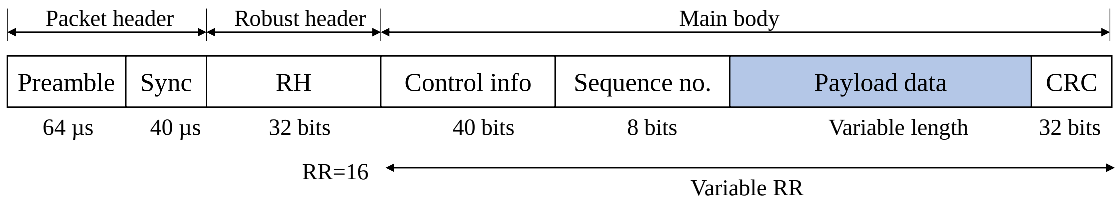

Figure 2.5: AIr-MAC frame format.

missions [64].

Frame structure of the AIr-MAC is shown in Fig. 2.5. The preamble is used for carrier sensing and synchronisation. Robust header (RH) is used to convey the physical and MAC layer management information. Therefore, RH is always transmitted at the highest repetition rate (RR=16). The rest of the frame contains other control information and the data payload with a CRC at the end [65].

AIr has four modes of packet transmission based on the reliability and channel reservation. These transmission modes are illustrated in Fig 2.6. Fig. 2.6(a) depicts the unreserved and unreliable packet (UDATA) transmission. In this mode of operation, request-to-send/clear-to-send (RTS/CTS) handshake is not used and the sender does not get an acknowledgement (ACK). This method is only used for multicast or broadcast services. All the other three modes are reserved modes where an RTS/CTS handshake reserves the channel before packet transmission.

Fig. 2.6(b) shows the reserved unreliable mode that does not acknowledge the packets. After the last packet the sender transmits the end-of-burst (EOB) packet and the receiver terminates the channel reservation with an end-of-burst-confirm (EOBC) packet. Fig. 2.6(c) and Fig. 2.6(d) show the reliable reserved modes where the receiver acknowledges packets. In the first case, each packet is acknowledged (ADATA) soon after reception while the second case shows the sequential packet (SDATA) transfer with aggregated acknowledgement at the end of the channel reservation [64, 65].

As stated earlier, the AIr-MAC protocol implements the CSMA/CA mechanism. Therefore, the users have to contend for the channel access when they have data to transfer. Fig. 2.7 shows the operation of the reserved sequenced mode (Fig. 2.6(d)). A user should pick a random number z from the contention window $(0, W-1)$ where W is the current

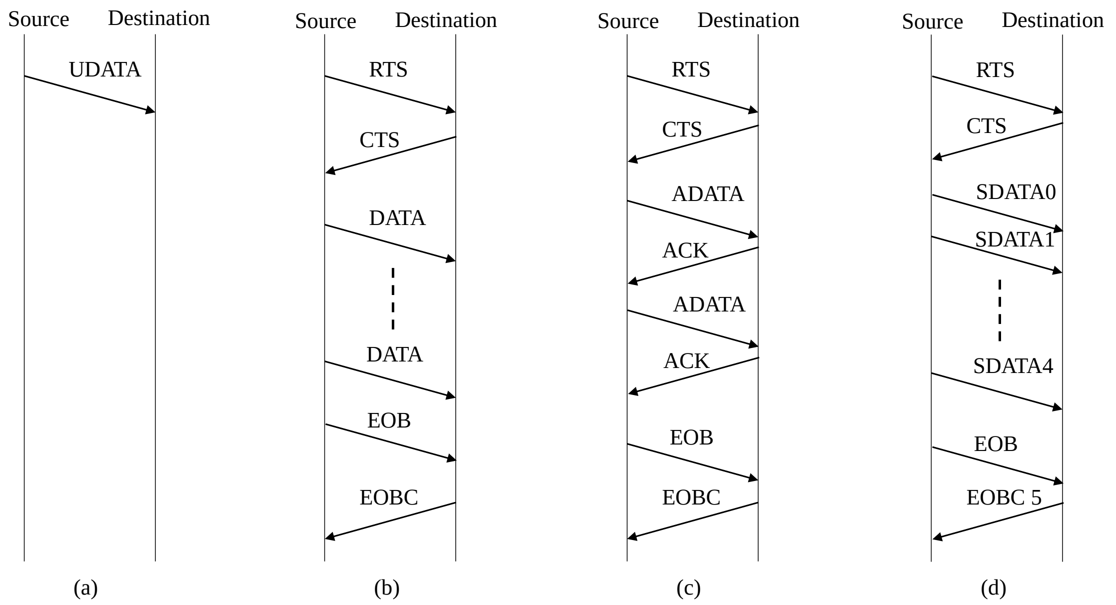

Figure 2.6: AIr transfer modes. (a) Unreserved mode transfer (UDATA frame). (b) Reserved mode transfer with no acknowledgement (DATA frame). (c) Reserved mode transfer with frame acknowledgement (ADATA frame). (d) Reserved mode Sequenced transfer (SDATA frame).

contention window size. Then the user waits z contention-avoidance-slots (CAS). If it senses a transmission during this period, it will freeze the timer until the transmission is finished. Once the timer is expired, the user transmits the RTS frame. Receiver responds with a CTS frame after a turn-around-time (TAT) such that the transmitter's receive circuitry has time to recover. If a user ends up in a collision, they will increase contention window. The increment is linear as oppose to the binary exponential increase used in the IEEE 802.11 standard.

The transmitter starts the data transmission after a TAT delay and requests an end-of-burst confirmation by sending an end-of-burst frame. The burst includes packets per burst (ppb) number of packets. Once the burst is finished the EXIT1 and EXIT2 timers are used to bring all the stations to synchronisation and ready for the contending again.

The IrDA AIr standard was not developed actively after around 2012. Some of the last research evaluates its potential to operate underwater specifically targeting swimmers' body-worn devices [66]. On the other hand, authors in [67] proposed modifications to

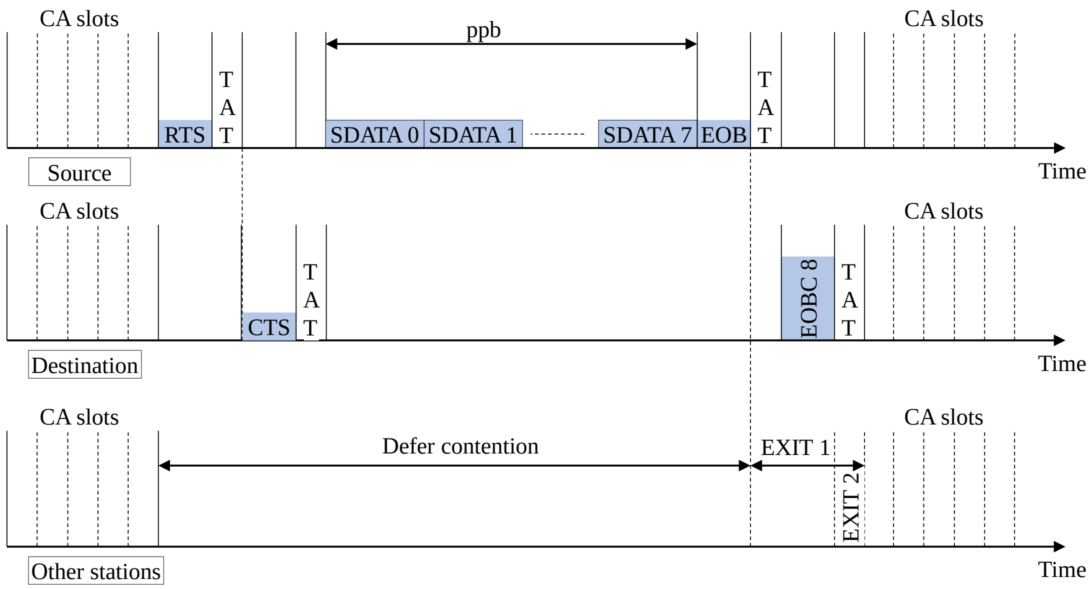

Figure 2.7: IrDA CSMA/CA operation: reserved access scheme with sequenced mode transfer.

IrDA-AIr standard to improve the performance under multi-user conditions. They proposed to remove the carrier sensing operation and replace it with RTS scheme effectively removing the collisions.

IEEE 802.11 MAC Layer

This subsection will briefly explain the MAC protocol of the IEEE 802.11-1997 standard, which was expected to operate with the OWC physical layer. The IEEE 802.11 MAC protocol had a major revision in the IEEE 802.11e 2005 amendment for the inclusion of different access categories. The enhanced version is outlined in the Chapter 3 as our work presented Chapter 3 is based on the enhanced version.

The IEEE 802.11 standard has two channel access methods. The first one is the distributed coordination function (DCF) which is based on the CSMA/CA mechanism similar to the AIr-MAC. On the contrary, the point coordination function (PCF) is a polling MAC protocol in which the access point acts as the central coordinator. PCF is optional for IEEE 802.11 and it is not widely used due to inefficiencies [68].

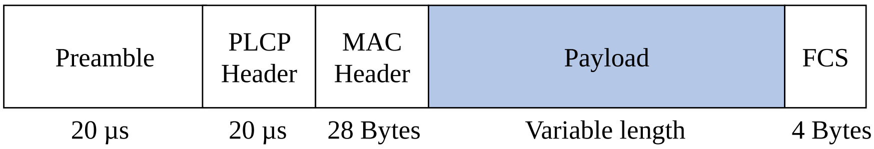

Figure 2.8: IEEE 802.11 packet format.

Another key difference between the IEEE 802.11 and IrDA-AIr is the binary exponential back-off in CSMA/CA. When a user experiences a packet collision the contention window is increased before rescheduling the transmission. AIr-MAC uses a linear increment while IEEE 802.11 uses a binary exponential increase.

The basic frame format of the IEEE 802.11 consists of the preamble, physical layer header, MAC header and payload. Unlike in IrDA, preamble and header fields can get different forms depending on the modulation schemes in use. The size and the structure of the payload can vary depending on the aggregation type in use. Figure 2.8 shows a basic frame format of IEEE 802.11.

There are two packet transmission modes in IEEE 802.11 that are shown in Fig. 2.9. The first mode does not reserve the channel. A successful transmission finishes with the ACK packet from the receiver. Second mode reserves the channel using a RTS/CTS handshake. This mode is only used for the packets that are larger than a user-defined threshold [69]. Unlike in AIr-MAC, all the packet transmissions in the IEEE 802.11 are acknowledged.

The fundamental CSMA/CA operation of IEEE 802.11 is similar to that of the AIr-MAC standard. Nonetheless, there are some differences in the implementation. A user who needs to transmit a packet has to wait a DCF interframe spacing (DIFS) duration and pick a random number z from $[0, CW]$ where CW is the current contention window. After that, the user waits z time slots before transmitting the packet. If the channel gets busy during the back-off, the countdown will be frozen until the channel is free again. Once the countdown is finished the packet will be transmitted. Receiver will send an ACK packet if the reception was successful. If the packet got collided with another packet, the transmission will be rescheduled with a larger contention window. As shown in Figure 2.10 users wait a DIFS duration before initiating a packet transmission. In this case

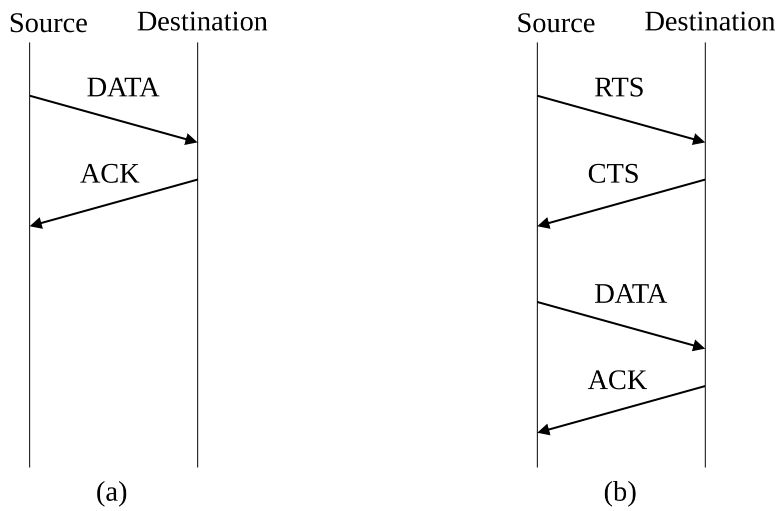

Figure 2.9: IEEE 802.11 packet transfer modes.

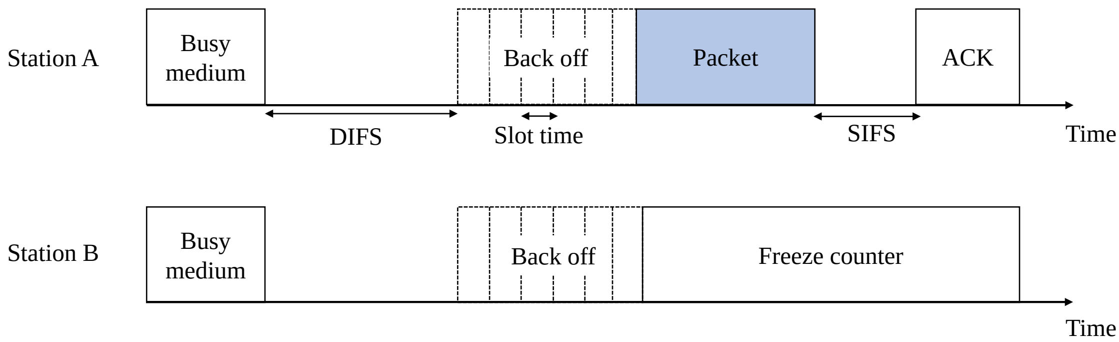

Figure 2.10: IEEE 802.11 CSMA/CA operation.

Station A wins the contention due to the shorter back-off period. Management frames like ACK packets wait only a short interframe spacing (SIFS) duration thereby gaining higher priority over the normal data packets [16, 69].

Contention-free operation or the PCF does not employ the CSMA/CA mechanism. Users who need guaranteed access will make a request to the point coordinator (PC) stating the traffic requirements. PC will include the user terminal in polling list.

IEEE 802.11ad MAC Layer

A brief introduction to the IEEE 802.11ad MAC layer is presented in this subsection since it features scheduled access periods. As discussed earlier, scheduled access periods are essential in providing guaranteed access to the delay-sensitive users.

Similar to the other protocols in the IEEE 802.11 suite, the 60 GHz variation also divides the time into beacon intervals (BI). However, with the transceiver directionality, scheduled access periods and other complexities, the beacon transmission becomes more complicated in IEEE 802.11ad. The transmission of beacons are now associated with two more operations that help with the beamform training and channel access scheduling. As shown in the 2.11, these three operations are bundled into the beacon header interval (BHI). During the first part, in beacon transmission interval (BTI), AP transmits beacons in all the directions announcing network management information [70].

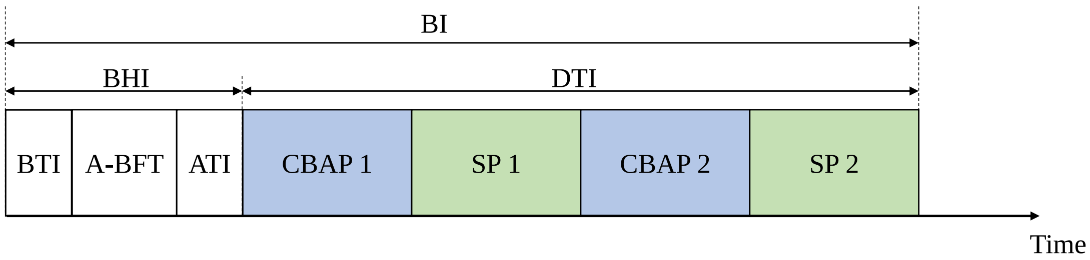

Figure 2.11: IEEE 802.11ad beacon interval.

The association beamform training (A-BFT) period is used by the users that are willing to join the network to train their beams with the AP. This period is slotted so that multiple users can do the beamforming with the AP concurrently. During the announcement time interval (ATI), the AP and users exchange requests and responses/allocations regarding the data transfer interval (DTI). It is worth noting that the transmissions in BTI and A-BFT happens in lowest order modulation scheme to maximise reliability [4].

The DTI is divided into multiple contention-based access periods (CBAP) and scheduled periods (SP) to support different levels of service. The data transmissions during CBPAs follow a modified 802.11 contention-based access mechanism to fine tune for directional transmissions. On the other hand, the transmission in SPs are scheduled for particular users [70]. Various scheduling algorithms can be used for the purpose of scheduling different types of traffic to the SPs.

IEEE 802.15.3c MAC Layer

In addition to the IEEE 802.11ad MAC layer, the IEEE 802.15.3c MAC layer also features a scheduled access period. IEEE 802.15.3c uses a piconet architecture where a set of independent devices can communicate with each other through a piconect coordinator (PNC) [27].

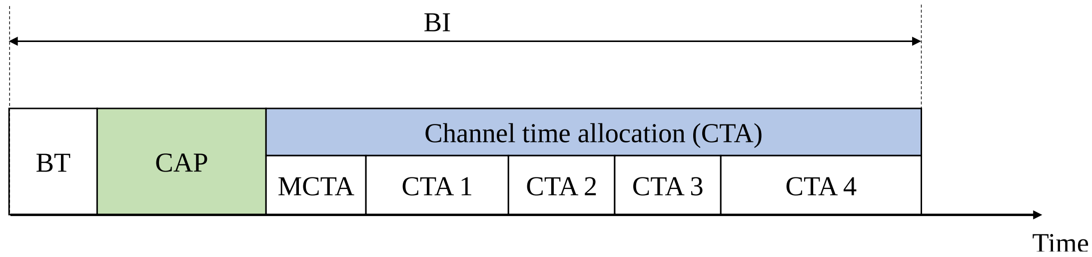

Figure 2.12: IEEE 802.15.3c beacon interval.

Similar to the MAC protocols discussed above, IEEE 802.15.3c also use beacon intervals to perform its data transmission. In here, the BI starts with a beacon transmission (BT). The contention access period (CAP) is optional in the IEEE 802.15.3c standard and operates on the CSMA/CA mechanism. The operation of the IEEE 802.15.3c MAC protocol is depicted in Fig 2.12. As shown, the rest of the time is allocated on the basis of time division multiple access (TDMA) and the management CTA (MCTA) is used for the management of those allocations [71]. Allocation of CTA slots are decided by the scheduling algorithms implemented in the device.

Other Recent Developments

Without proper standardisation yet, most of the upper layer research done on OWC have taken independent directions. The closest recent standardisation activities are the IEEE 802.15.7 and IEEE 802.15.13. While the latter is still under development, the former proposes network protocols that are very similar to IEEE 802.11 [7].

One of the comprehensive piece of work on OWC upper layers can be found under the OMEGA-Home Gigabit Access Project [72]. This project has introduced a technology-independent MAC layer, shown in Fig. 2.13, that can be transparently used for any multi-gigabit WLAN technology. This MAC layer is called Inter-MAC and it paves the way to heterogeneous WLANs with radio frequency and optical technologies. The Inter-MAC architecture has a split plane architecture where the data plane is directly interfacing the transmission technologies while the control and management planes are transparent to the underlying physical layer characteristics. A practical demonstration involving the Inter-MAC and OWC techniques are shown in [73] with high data rate VR headsets.

Authors in [74] discussed the challenges of heterogeneous WLANs with multiple technologies such as network management, load balancing, network flexibility and security. They proposed to use software defined network (SDN) architecture to tackle these challenges. SDN architectures decouple the control plane from the data forwarding plane and treat it as a centralised entity. The benefit of these kind of approaches is the use of standardised protocols and mechanisms such as OpenFlow [75].

Though these works introduce MAC architectures, there is a lack of understanding of the specific MAC protocols to use. For instance, MAC protocols can be broadly categorised into two; contention-based and contention-free. Therefore, further work is necessary to develop suitable MAC protocols for OWC networks.

Centralised architectures are considered for both OWC and VLC in many places [57, 76,77]. In particular, the authors in [76] uses a Central Communication Controller (CCC) to house the tunable laser sources. This architecture makes it easier to control and scale the network. With the help of an optical cross-connect switch, authors were able to dynamically allocate the laser sources to different transmitters on demand. Each of these beams are expected to have a capacity around 10 Gbps. Therefore, the authors further emphasise the importance of a high capacity fibre distribution network.

Centralised architectures are preferred in most of the high-capacity sophisticated deployments such as enterprise Wi-Fi networks. The research on OWC centralised network architectures need further studies to the develop the exact functional blocks and evaluate the performance with different deployment scenarios.

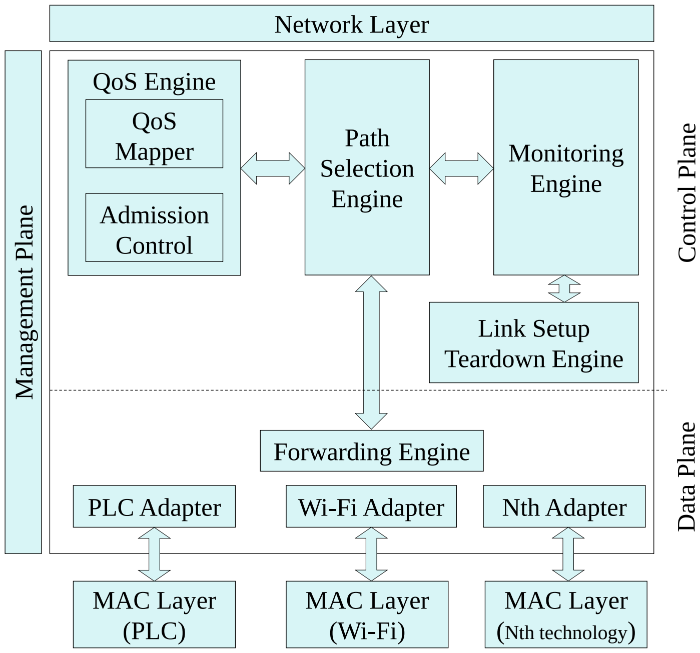

Figure 2.13: Inter-MAC architecture.

2.3 Conclusion

In this chapter, we have reviewed the current and emerging wireless LAN technologies. We have discussed the evolution of Wi-Fi technology over the last 20 years and in which directions it has evolved. Further, the emergence of different complementary WLAN technologies such as millimetre-wave Wi-Fi, visible light communication and optical wireless communication was discussed. Finally, we explored the recent developments in the optical wireless physical layer with special attention to modulation schemes, beam-steering and multiple access mechanisms. The discussion on the upper layers starts with the earlier Wi-Fi standard to the most recent optical wireless architectures. We have identified that the MAC protocols and network architectures need further investigations to support guaranteed services to upcoming delay-sensitive high data rate users and to support complex network coordination functions such as handovers and beam-steering. Therefore, this background will serve as a foundation for the upcoming chapters.

Chapter 3

Contention-based MAC Protocol for OWC Networks

3.1 Introduction

THE medium access control (MAC) protocol of a WLAN plays a key role across all the performance metrics of the system. Primarily, the MAC protocol defines how multiple users share the communication medium. However, often it spans across the quality-of-service, service differentiation, beamforming/beam-steering, and handover mechanisms as well. Even though OWC physical layer can support multi-gigabit communication, OWC does not have a standardised MAC protocol yet to gain all the benefits that its physical layer can offer. Therefore, as the first step of developing a MAC protocol for OWC, we try to adopt the IEEE 802.11ac [78] MAC protocol to OWC to operate at multi-gigabit data rates. Recent OWC implementations such as [79] uses the IEEE 802.11 MAC protocol in their OWC systems. First we evaluate the performance of the IEEE 802.11 MAC protocol in its original form in the multi-gigabit range and propose modifications to improve the performance with the increased data rates to suit the OWC networks.

The IEEE 802.11 MAC protocol is one of the most successful MAC protocols used in WLANs which has been evolving since its introduction in 1997. The IEEE 802.11 MAC protocol supports both contention-based and hybrid (contention-based plus contention-free) modes of operation. However, the contention-based mode, which is explained in the next section, is far more common due to its simplicity [80]. Correspondingly, visible light communication standard, IEEE 802.15.7, has a similar contention-based MAC protocol

[7]. Both standards use the CSMA/CA mechanism in the MAC protocol. CSMA/CA is a distributed mechanism where users decide the channel access on their own with little to no information about the channel status [81]. Although distributed MAC protocols perform at a reasonable efficiency at low data rates, they become prohibitively inefficient at the multi-gigabit data rates as shown later in this chapter. Therefore, in this work, we embed some features of centralised MAC protocols to the CSMA/CA based IEEE 802.11 MAC protocol and thereby overcome the adverse effects of distributed control.

In particular, the contributions of the work presented in this chapter are twofold.

- Firstly, we proposed a service differentiation mechanism that is different from IEEE 802.11 MAC protocol, to suit optical wireless networks and the associated diverse types of next generation traffic such as virtual reality (VR) and augmented reality (AR). Originally, IEEE 802.11 standard supports voice, video, best effort and background traffic types, which cannot support a proper differentiation for the predicted next-generation traffic profiles. Cisco has estimated that Internet traffic will comprise 82% video by 2021 and accordingly, future WLANs should be able to differentiate different video types [82].

- Secondly, we propose a heuristic dynamic contention window (DCW) tuning algorithm that adjusts the contention window based on the congestion levels of the optical wireless network to enhance the efficient use of resources and the quality-of-services [83]. This algorithm ensures the best possible performance under diverse network conditions by mitigating the conventional use of static contention window size. It is worth noting that with minor modifications the proposed mechanisms are applicable to other WLANs that are based on different physical layer technologies.

The rest of the chapter is organised as follows. Section 3.2 explains the operation of the IEEE 802.11ac MAC protocol. Section 3.3 explains the proposed service differentiation mechanism. Dynamic contention window tuning algorithm is introduced in Section 3.4. Performance analysis and the results are presented in Section 3.5. Finally, Section 3.6 concludes the chapter.

3.2 IEEE 802.11 MAC Protocol

The contention-based access mode of the IEEE 802.11 standard is called the enhanced distributed coordination function (EDCF). Under the EDCF, a user who wishes to access the channel has to wait until the channel is free for an arbitration interframe spacing (AIFS) duration. Once that condition is satisfied, the user will pick a random number, z, from the range called the contention window $[0, CW]$ where CW is the current contention window size. The user then waits z time slots as the back-off countdown and transmit the packet at the end of the countdown. This operation is depicted in Fig. 3.1. However, if the user detects any transmissions from other users during back-off, it freezes the countdown and resumes once the other transmission is finished. A transmitted packet is considered successful if it was acknowledged by the receiver within an SIFS duration. The CSMA/CA mechanism relies on random numbers to avoid collisions. Therefore, if two or more users pick the same random number, their packets will be lost due to collision. In the case of a collision, users reschedule their transmissions with a larger contention window, which in turn reduces the probability of collisions.

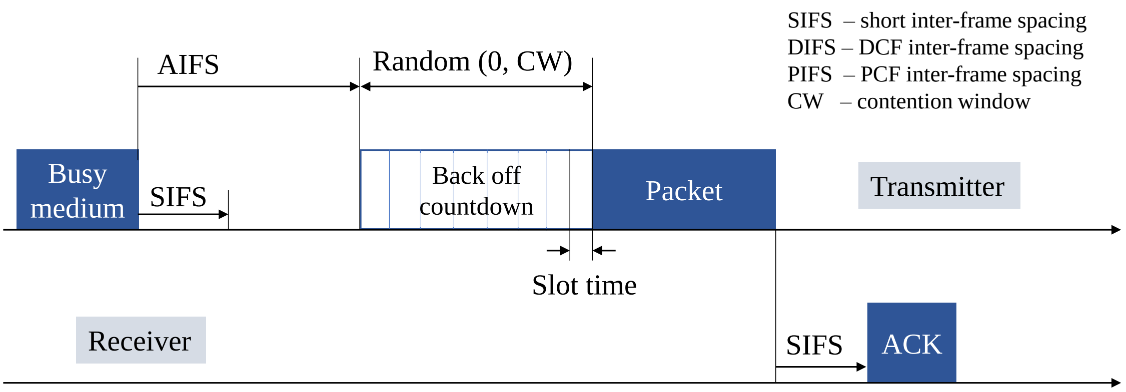

Figure 3.1: EDCF operation in IEEE 802.11 MAC protocol.

Service differentiation in the IEEE 802.11 MAC protocol is implemented using the AIFS and CW values [84]. As stated earlier, IEEE 802.11 defines four types of traffic called access categories (AC), namely, voice, video, best effort and background. The AIFS duration is calculated according to Eq. 3.1 depending on the priority of the traffic. The smaller AIFS means higher priority and quicker channel access.

$$AIFS = SIFS + AIFSN \times timeslot \tag{3.1}$$

The AIFSN (AIFS number) for each AC are listed in Table 3.1. SIFS is a delay that depends on hardware. Similarly, timeslot also depends on hardware and both SIFS and timeslot are fundamental delays in the IEEE 802.11 MAC protocol. All the other delay values are derived based on SIFS and timeslot. Eq. 3.2 and Eq. 3.3 show how SIFS and timeslot are calculated and the values for IEEE 802.11ac are 16 μs and 9 μs, respectively [78].

$$SIFS = RX - RF\ delay + RX\ PLC\ delay + RX - TX\ turnaround + MAC\ processing \tag{3.2}$$

$$Timeslot = channel\ assessment + RX - TX\ turnaround + propagation\ time + MAC\ processing \tag{3.3}$$

Similarly, CW values are also set depending on the traffic priority. High priority traffic is assigned smaller CW ranges such that they have a high probability to get channel access prior to the low priority traffic. IEEE 802.11 MAC protocol always starts with the CW_{min} and doubles the values up to CW_{max} each time there is a packet collision. This behaviour is explained in detail in Section 3.4.

Table 3.1: MAC protocol parameters of the IEEE 802.11ac standard.

Access Category	CW_{min}	CW_{max}	AIFSN	AIFS
Voice	3	7	2	34 μs
Video	7	15	2	34 μs
Best Effort	15	1023	3	43 μs
Background	15	1023	7	79 μs

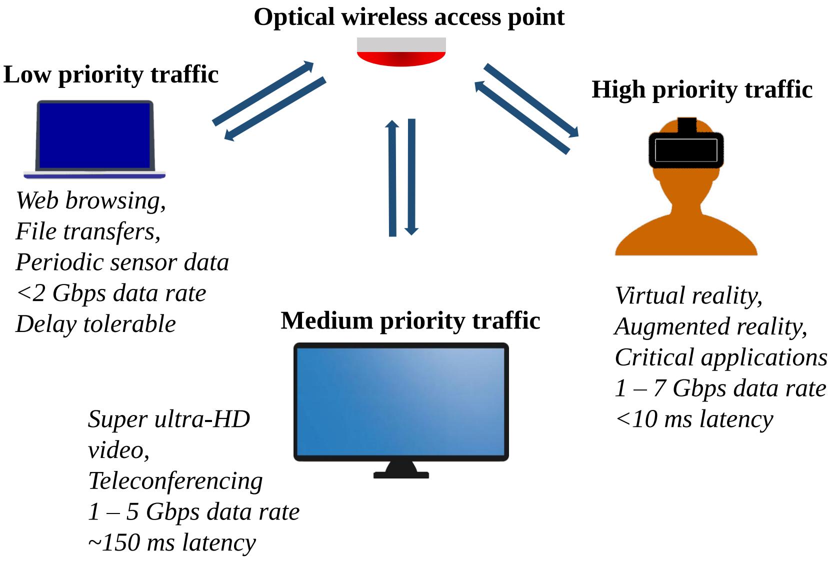

Figure 3.2: Typical use cases of indoor optical wireless networks.

3.3 Proposed Service Differentiation Mechanism

A closer look at the upcoming traffic and the network deployment scenarios of the indoor optical wireless networks reveals that the IEEE 802.11 service differentiation is not suitable for optical wireless networks. For example, traffic types, such as VR, poses more stringent demands than voice traffic and are not open for bandwidth reductions like video streaming [4, 85]. Therefore, it is essential for the future WLANs to have a suitable service differentiation structure to better support diverse types of traffic. In this work, we have proposed three types of traffic, where the first priority is assigned to the highest priority traffic, and the second type for medium priority traffic. Example applications and their requirements of each type of priority class are shown in Fig. 3.2.

First, we carry out simulation analyses to identify the most suitable values for the contention window and AIFSN for each type of traffic categories. Simulations are carried out using ns-3 platform [13]. For these simulations, the physical layer is assumed to be an ideal 10 Gbps OOK channel without impairments as we are evaluating the performance of the upper layer protocols. We have modified and reused the IEEE 802.11 module of the ns-3 project in order to implement and compare our algorithms. Repository of our implementation could be found in [86].

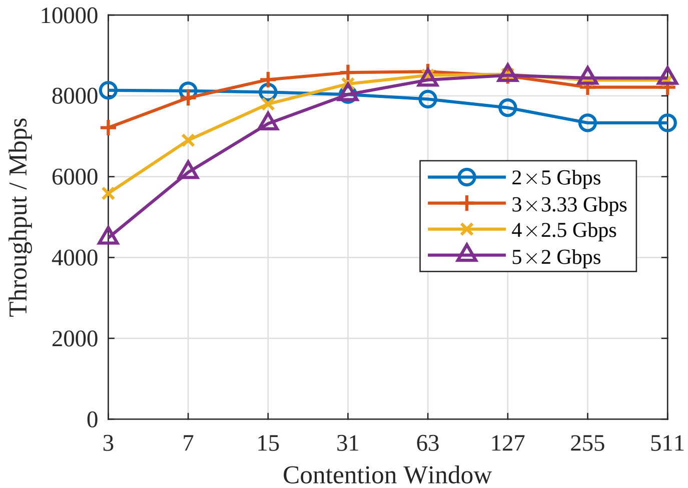

Figure 3.3: Throughput variation of the high priority traffic with varying contention window.

3.3.1 High Priority Traffic

As discussed, the high priority access category is expected to serve applications such as VR and AR, which have strict throughput and delay requirements. For the simulations, we assume that the maximum number of devices that have high priority traffic in the optical wireless network is five. Simulations are carried out by varying the number of high priority users from 2 to 5, all sharing 10 Gbps of data rate. We use constant bit rate (CBR) on-off traffic distribution to simulate the high priority traffic with a 1500 bytes packet size and 10 ms interval considering the large packets generated by video applications at high frames-per-second (fps) rates [1]. On-off traffic is used to imitate the packet arrival of bandwidth hungry applications such as VR.

The results shown in Fig. 3.3 and Fig. 3.4 depict how the network performs with different contention window values for the high priority category. In particular, Fig. 3.3 shows the variation of the throughput of the high priority users under each network scenario as a function of the contention window size of the high priority traffic. It can be observed that, in order to enhance the network throughput, larger contention windows are needed when the network has high number of high priority users. For example, for a maximum number of users (5), we need to implement a contention window size of 127. However, for two high priority users, a contention window size of 127 is too large and

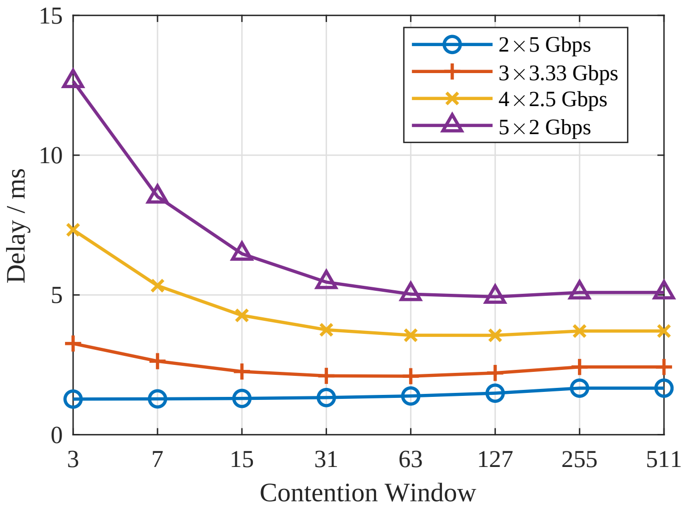

Figure 3.4: Delay variation of the high priority traffic with varying contention window.

results in throughput degradation.

Figure. 3.4 shows the variation of delay of the high priority traffic type as a function of contention window size. Figure. 3.4 clearly illustrates how the correct contention window could reduce the packet delay. For example, when we increase the contention window, the delay drops approximately 50% when the network has higher number of users. The high priority traffic shows constant delay irrespective of the size of the contention window when the network has a low number of active users. The results suggest that there is an optimum contention window size for a given number of users and since we expect to have only five users in the high priority category at a given time, we can select the contention window size that ranges from 3 to 127. This would enable the use of an appropriately selected contention window size based on the number of users accessing the optical wireless network.

3.3.2 Medium Priority Traffic

Medium priority traffic will include services such as ultra-HD video and teleconferencing. These services can tolerate the network congestion up to some extent by adjusting the quality-of-service, such as video quality. For the simulation, we assume medium priority traffic could emerge from a maximum of 10 users in the network. Since this category

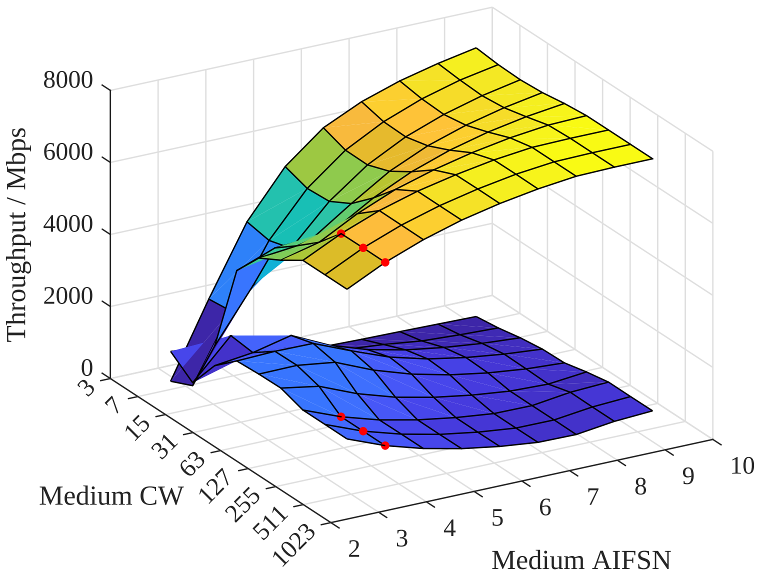

Figure 3.5: Throughput variation of medium priority traffic with varying contention window and AIFSN of the medium priority traffic.

is below the high priority traffic, both contention window and AIFS affects the prioritisation of this category. Therefore, we have carried out a series of simulations with both the contention window and AIFSN as variables. Further, we have to consider a mixture of high and medium priority traffic for the simulations. Therefore, we use a ratio of 4:1 based on the Cisco VNI forecast [82], which works out to be 8 Gbps of high traffic and 2 Gbps medium traffic. Packet size and on-off interval are chosen as 1280 byte and 20 ms for the medium traffic. We simulate the worst-case scenario for medium priority traffic where there are 5 high priority users each offering 1.6 Gbps data to the network and 2 Gbps of medium traffic offered by 10 medium users.

Fig. 3.5 shows the throughput of the high and medium traffic versus the contention window and AIFSN of medium priority traffic. As expected, increasing these parameters result in more transmission opportunities for the high priority traffic while medium priority traffic starves of bandwidth. We can observe that the plateaus of two surfaces do not overlap, indicating it is not possible to find a parameter set where the throughput of both traffic categories are maximised. Therefore, there is a trade-off between how much priority should be given to each category. The points marked by the red dots results in reasonable throughputs for both categories. For instance, a contention window size of 255

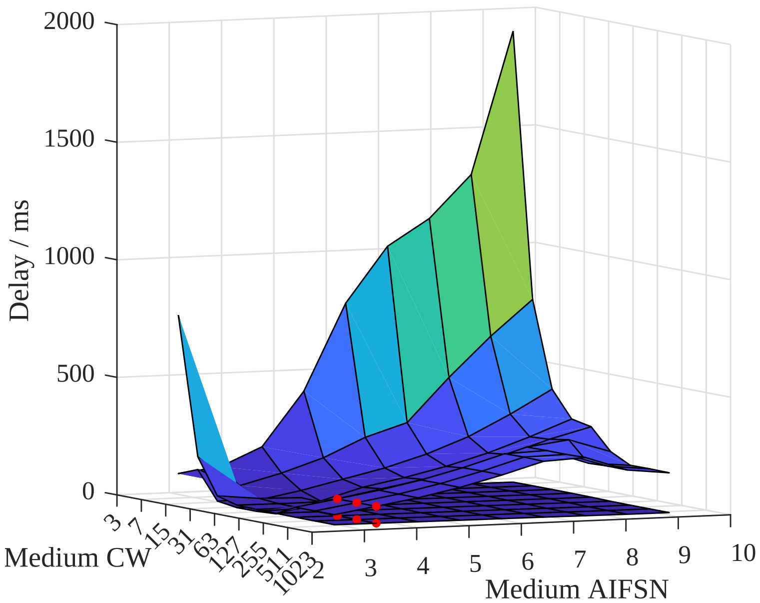

Figure 3.6: Delay variation of medium priority traffic with varying contention window and AIFSN of the medium priority traffic.

and AIFSN of 3 for medium priority traffic result in over 6.3 Gbps and 1.2 Gbps throughput for high and medium traffic categories, respectively. Fig. 3.6 shows how the delay of the two traffic categories vary with the medium priority traffic parameters. High priority traffic does not experience any notable variation whilst the medium priority packets increase delay with the AIFSN. Further, medium priority delay becomes worse if the contention window is too small as well. As shown in Fig. 3.6, the delay of the high priority traffic in the selected region is close to 7.5 ms and that of the medium priority traffic is around 80 ms, which falls within the expected performance range of these traffic types.

3.3.3 Low Priority Traffic

Finally, we analyse how these parameters affect the low priority traffic category, which is responsible for carrying delay-tolerant, non-critical traffic in a best effort fashion. The applications fall under low priority category do not have strict throughput or delay requirements. Depending on the availability of channel bandwidth, it is possible to offload these traffic to other networks such as Wi-Fi networks. Similar to the medium priority traffic, we assume a maximum of 10 user applications accessing the optical wireless net-

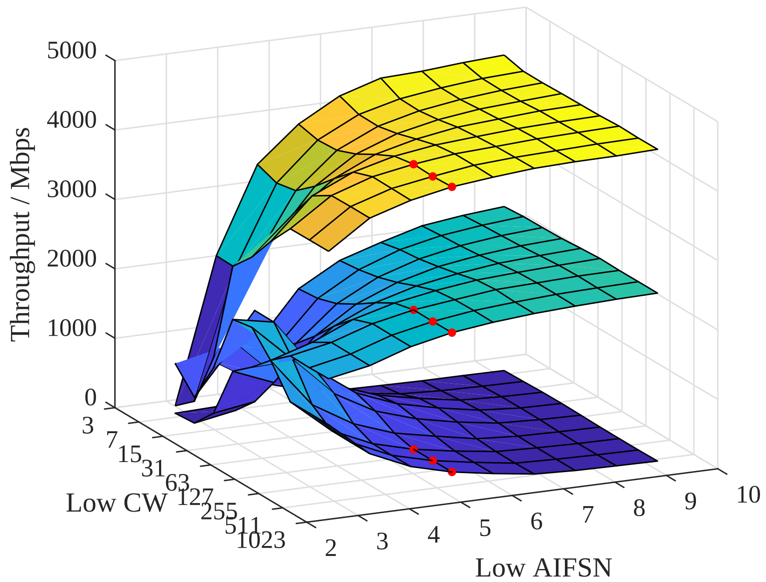

Figure 3.7: Throughput variation of low priority traffic with varying parameters of low priority traffic.

work simultaneously. However, unlike the case of higher priority categories, we enforce a throughput limit of 2 Gbps for all the low priority traffic applications. Simulations were carried out with 5 high priority users, 10 medium priority users and 10 low priority users offering 5 Gbps, 3 Gbps and 2 Gbps, respectively. Note that the low priority traffic streams consist of 1500 bytes packets with a 20 ms interval while the other traffic streams are fixed at their previous values.

Fig. 3.7 depicts the throughput of high, medium and low priority traffic whilst Fig. 3.8 shows the delay variation of the low priority traffic. In this particular case, increasing the AIFSN and contention window size of low priority traffic results in more transmission opportunities for both high and medium priority users. The red dots mark reasonable points of operation where the throughputs of high, medium and low priority traffic are 4.3 Gbps, 2.2 Gbps and 250 Mbps, respectively whilst the delays are 10 ms, 40 ms and 500 ms, respectively. As mentioned earlier, it is possible to select a different trade-off point depending on the traffic requirements. For instance, the AIFSN can be increased since the low priority traffic category can tolerate delay in the range of seconds for most of the cases.

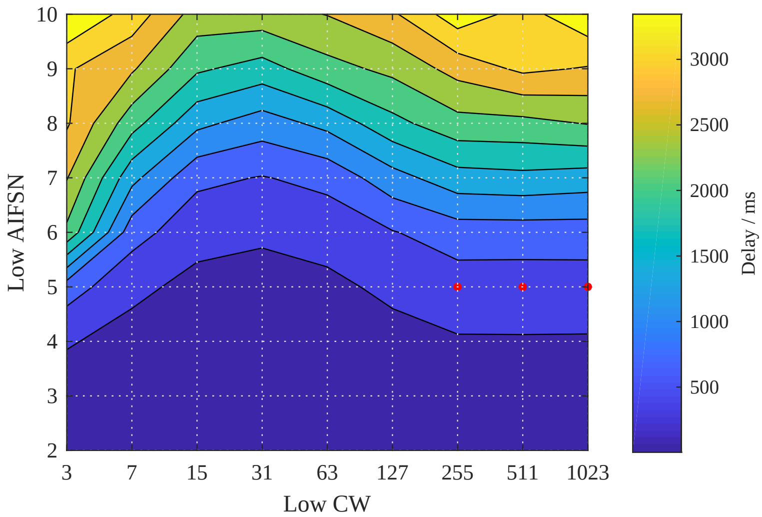

Figure 3.8: Delay variation of low priority traffic with varying parameters of low priority traffic.

3.4 Proposed Dynamic Contention Window Tuning Mechanism

As described in the earlier section, the size of the contention window has a significant effect on the service differentiation of the optical wireless network and a fixed contention window size could not perform well for each network condition [69, 87]. To recall, IEEE 802.11 schedules transmissions by picking a random number from the range $[0, CW]$ where CW is the current contention window value. Moreover, contention window is set to CW_{min} at the start of each transmission and doubled each time a collision occurs until it reaches CW_{max} as shown in Fig. 3.9 [88]. In this particular case shown in Fig. 3.9, the $CW_{min} = 31$ and $CW_{max} = 1023$. In a congested network, it is highly likely that each packet has to go through this process. An efficient way would be to set the contention window according to the congestion level of the network. A too small contention window causes many collisions, while an unnecessarily large contention window will result in high delays and low channel utilisation.

There have been several proposed dynamic contention window mechanisms for the IEEE 802.11 standard. A few of them operate heuristically by observing the network status, while the rest follow a theoretical path to calculate the desired contention window size. Collision rate has been a popular metric in determining the network status. For example, authors in [89] have proposed the first dynamic contention window mechanism based on collision rate. In their mechanism, contention windows are adjusted by a factor calculated based on collision rate after each transmission attempt. However, IEEE 802.11 standard later limited the adjustment of contention window to doubling or halving. Authors in [90] have introduced another collision rate based mechanism that has a set of collision rate threshold values. In their mechanism the contention windows are adjusted either by doubling or halving depending on the current collision rate. One of the common challenges in this approach is determining the threshold values. Further, in [87, 91], dynamic contention window mechanisms have been proposed using different adaptation methods. Even though collision rate is a very elegant metric to evaluate network status, in Section 3.5.2, we show that it cannot unambiguously represent the network status, which results in adversities in decision making.

On the other hand, there have been mechanisms that predominantly use theoretical models with minimal real-time inputs. For example, [92] estimates the number of active

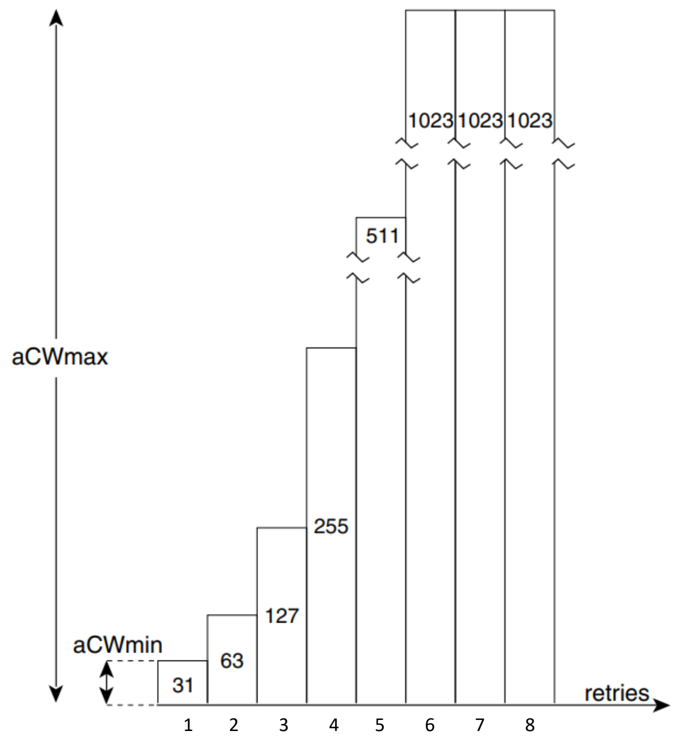

Figure 3.9: Growth in contention window with retries.

users and determines the optimal contention window size based on theoretical models. Another similar model is given in [93] where the collision probability is determined theoretically and is used for adjustment of contention window. There have been many other approaches such as Markov models to derive deterministic equations for the dynamic contention window tuning [94]. However, most of the theoretical models use assumptions that are not valid in real network operations, such as the usage of fixed packet sizes.

In this work, considering the variability and diversity of the traffic types and also to provide an enhanced user and network performance, we have proposed a heuristic algorithm that monitors network metrics such as throughput and delay in addition to collision rate. The algorithm tunes the contention window sizes of all the traffic categories in order to reduce the packet collisions. Thus, the network can dynamically adjust itself to the current traffic load.

3.4.1 Operation of the proposed DCW mechanism

The proposed DCW mechanism has three main steps in operation. Firstly, user terminals inform the optical wireless access point (AP) of the required throughput and delay limits for each access category using small management packets. The AP maintains a table consisting of all access categories versus the required throughput, delay, and collision rate. Secondly, the AP monitors the throughput, delay and the collision rate of the network in real-time and passes the values to the algorithm running in each AP. Finally, the algorithm informs the AP whether to adjust the contention window or not. The AP announces all contention window changes in the beacon frames. This process is repeated every T_u seconds, where T_u is the update interval. Upon disassociation or finishing a significant transmission, user terminals inform the AP to update the table. In here, we use three equations to calculate four important network metrics.

$$S[AC] = \sum_{n=1}^{N} S_n \tag{3.4}$$

$$D[AC] = \frac{\sum_{n=1}^{N} D_n}{\sum_{n=1}^{N} M_n} \tag{3.5}$$

Table 3.2: Threshold values of the DCW algorithm.

Access Category	Throughput threshold/%	Delay threshold/ms	Lower collision threshold	Higher collision threshold
High	90%	10	0.05	0.5
Medium	90%	150	0.05	0.5
Low	90%	2000	0.1	0.9

$$f[AC] = \frac{\sum_{n=1}^{N} f_n}{\sum_{n=1}^{N} M_n} \tag{3.6}$$

where N is the number of users, M_n is the number of data packets the n^{th} user received. Eq. 3.4 calculates the throughput (S) of each traffic/access category by summing the throughput of all users in each category. The throughput calculation only includes the data packets carrying useful information. Eq. 3.5 calculates the per-packet delay (D) for each access category by taking the ratio between the total packet delay and total number of packets in each category. Similarly, Eq. 3.6 calculates the per-packet collisions (f) for each AC. All these metrics go through an exponentially weighted moving average filter before being fed to the algorithm.

Upon receiving the latest network metrics, the algorithm compares the throughput against the value in the table. If the network throughput is above 90% of the expected value, it checks the collision rate of the network. If the collisions are below a certain lower threshold, it considers halving the contention window. On the other hand, if the collision rate is above a higher threshold and the delay of the network is also high, the algorithm doubles the contention window. If the network has a throughput below 90% of the expected value, the contention window will be doubled. Threshold values of the network metrics are listed in the Table 3.2. These values are set based on observations taken when the network operates with suitable contention window sizes which could be used to tune the algorithm. For example, reducing the lower threshold results in lower collisions in the network. The complete pseudo code of the algorithm is given in Algorithm 1.

In this section we also present the results of a specific case to demonstrate the operation of the DCW algorithm while more generalised and comparative results are presented

Algorithm 1 DCW Algorithm

Input: Instantaneous throughput, delay, collision rate
Output: Contention window adjustment

```
Initialization:
while true do
    Retrieve throughput, delay and collision rate
    if (throughput is high) then
        check collision rate
        if (collision rate is high) then
            check delay
            if (delay is high) then
                double contention window
            end if
        else if (collision rate is low) then
            halve contention window
        end if
    end if
    if (throughput is low) then
        double contention window
    end if
end while
```

in the performance evaluation section. Consider a situation where two high priority users are transmitting 2.5 Gbps each in the uplink and two medium priority users transmitting 300 Mbps each. We have observed the network performance with the MAC protocol settings given in the Table 3.3. For the conventional network, the CW values are fixed as shown in Table 3.3 while for the DCW network, the values can be varied within the given range.

Figure 3.10 shows the throughput and the delay of the network for 30 seconds. As shown in the Fig. 3.10a, the throughput of the high priority traffic is hardly affected by the packet collisions. However, the medium priority traffic is severely affected due to

Table 3.3: MAC Protocol Parameters.

	Access Category	CW_{min}	CW_{max}
Conventional	High	3	127
	Medium	7	255
DCW	High	3-127	7-127
	Medium	7-255	15-255

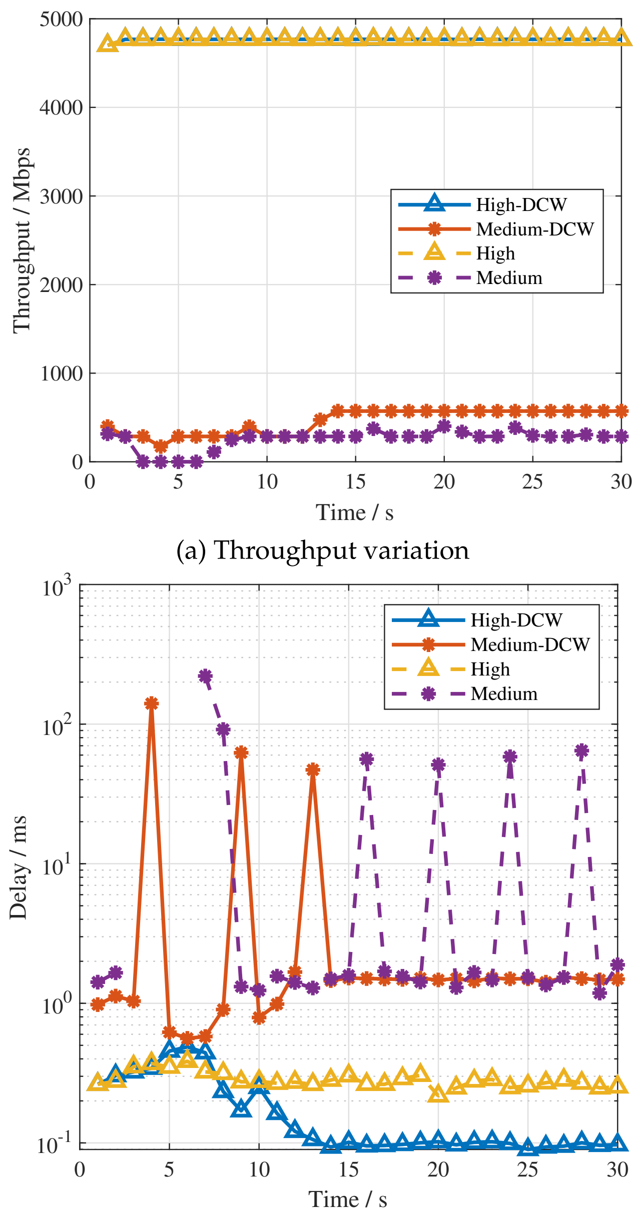

(a) Throughput variation

(b) Delay variation

Figure 3.10: Throughput and delay variation of the network with and without DCW algorithm for 30 seconds.

collisions. There is a drop of 200 Mbps in the average throughput of the medium priority traffic. These adverse effects are more visible in the delay of the medium traffic shown in Fig. 3.10b, where the discontinuity is caused because there were no packets received during that period. It is possible to shed some light into this behaviour by looking at the

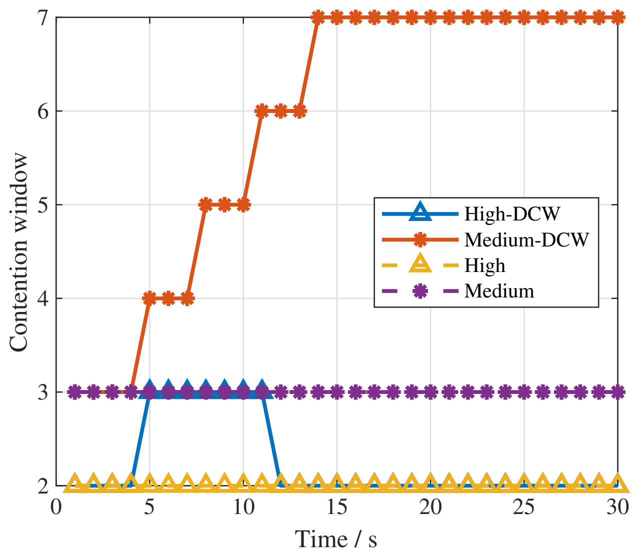

Figure 3.11: Tuning of the contention windows using the DCW algorithm.

CW values picked for each transmission.

Fig. 3.12a and Fig. 3.12b show the CW values picked by a high priority user and a medium priority user for each of their transmissions. The high priority CW_{min} is set to 3 and depending on the congestion of the network it can go up to 127. Observe that majority of the transmissions are concentrated between 0-20 range while there is a considerable number of dots beyond 20 as well. The downside of this behaviour is that it creates a big overlap with the medium priority traffic CW range which is 7-255. Therefore, with the massive number of high priority packets invading into the medium priority region, medium priority traffic finds it hard to access the channel. As a result, medium priority traffic ends up rescheduling with large CW values. It is worth noting that, if there was no congestion, the CW values should lie inside $[0, CW_{min}]$ for both high and medium priority traffic. However, we can observe that both types of users experience a lot of retries for packet transmissions.

On the other hand, Fig. 3.12c and Fig. 3.12d show the CW traces when the CW_{min} are adjusted dynamically. For the high priority traffic, the CW_{min} is set to 3 and temporarily it increases to 7 while the algorithm is stabilising. After that, the CW_{min} values stay within [0, 3] range. Note that, the CW values go to 7 because of retries. When the CW_{min} is 3, CW_{max} is the next stage which is 7. Therefore, everything above 3 is a retry. The high

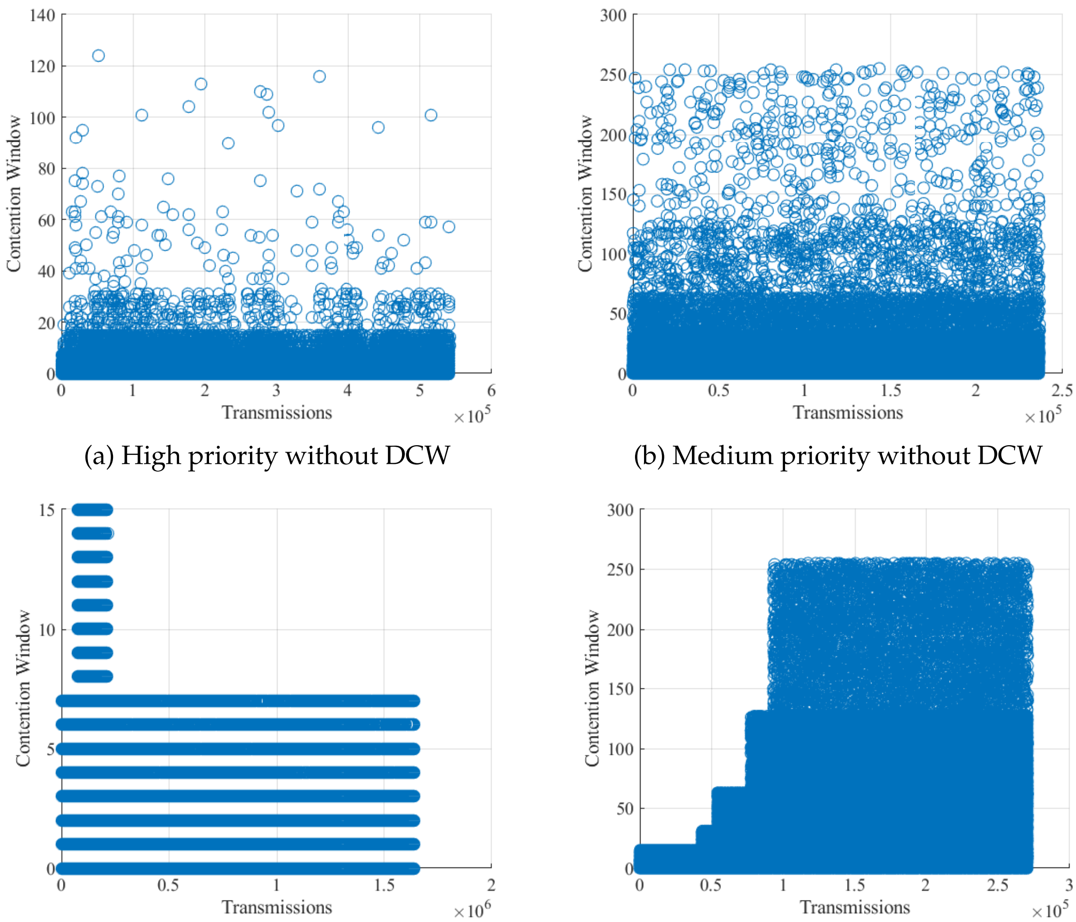

(a) High priority without DCW

(b) Medium priority without DCW

(c) High priority with DCW

(d) Medium priority with DCW

Figure 3.12: Traces of contention window sizes used by the conventional and DCW MAC protocols.

priority users experience considerable amount of retries, however, they are limited to [0, 7] range now. The CW_{min} of the medium traffic is increased up to 127. We can see that the CW trace of medium traffic which is shown in Fig. 3.12d has a more uniform density. That means the almost all the transmissions consider picking a CW value from the [0, 127] range at the first try, without trying a smaller range first. This eases the congestion of the network. The performance improvement is visible in the Fig. 3.10. Throughput of the medium priority users stabilises around 571 Mbps and the delay stabilises around 1.5 ms. The execution of the DCW algorithm can be seen in Fig. 3.11, which shows how the CW values are tuned.

3.4.2 Implication of the parameters on the performance

There are three parameters that define the dynamics of the algorithm. The first parameter is the update interval (T_u), which is the interval at which metrics are calculated and the contention windows are updated. Once the contention windows are adjusted, the algorithm will leave some time for the network metrics to stabilise without changing the contention window again. This stabilising time, which is the second parameter, is referred to as waiting time (T_w). The third parameter is the smoothing factor, α, of the averaging filter, which also plays a key role in the dynamics of the algorithm.

We evaluate the implications of these three parameters on the performance using a step response analysis. Fig. 3.13a and Fig. 3.13b show the implication of the update interval by adding 5 users simultaneously offering a total of 8 Gbps of high priority data to the system as a step. Here, we use contention window size of 31. As can be seen from Fig. 3.13a, smaller update intervals result in faster settling time in the throughput. However, there are a few factors that affect the lower limit of the update interval. Firstly, there is an associated computational power cost on the access point to calculate all required metrics. Secondly, the calculated contention window sizes have to be communicated to the users via beacon frames. Reducing the beacon interval will cost some of the system throughput as control overhead. Finally, smaller update intervals will result in an algorithm that is more sensitive to sudden changes, which is not a subject of interest for this work. For instance, as shown in Fig. 3.13a, we also simulate a throughput dip of 1.6 Gbps at 15s for a 500 ms period. Both $Tu = 200\ ms$ and $Tu = 500\ ms$ update intervals responded to this by increasing the contention window as shown in Fig. 3.13b. However, $T_u = 1\ s$ did not respond and the system naturally comes back to normal. Therefore, once the sensitivities for the various traffic categories have been set, we can adjust the update interval so that the proposed algorithm responds accordingly.

The second parameter, the waiting period (T_w) allows the system to come to steady state after a contention window size change has been applied. Fig. 3.13c and Fig. 3.13d show the dynamics of the algorithm for waiting periods 1, 3 and 5 seconds. As depicted in Fig. 3.13d, when the waiting period is 1 s, the algorithm adjusts the contention window size again in the next instance if the throughput has not reached the desired value. This

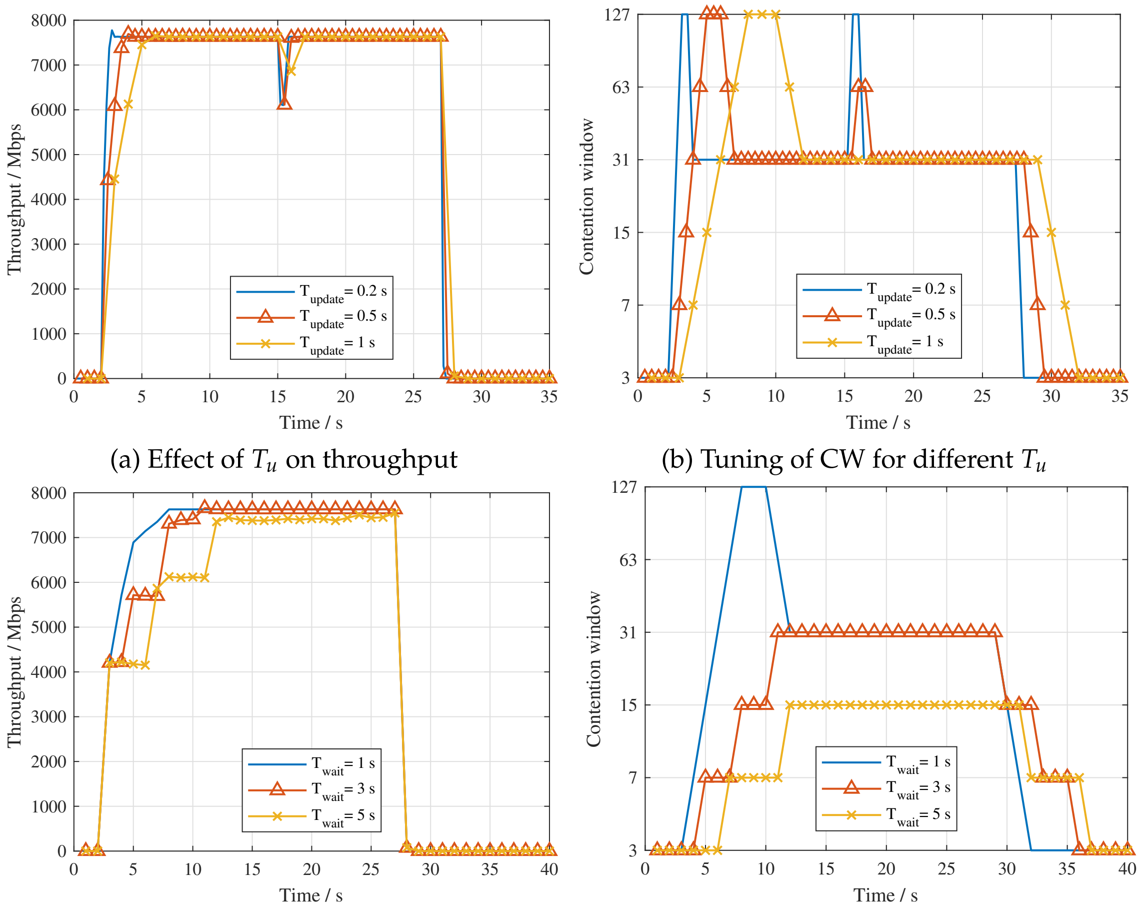

(a) Effect of T_u on throughput
(b) Tuning of CW for different T_u
(c) Effect of T_w on throughput
(d) Tuning of CW for different T_w

Figure 3.13: Effect of different parameters of DCW algorithm and the tuning of the contention window.

is an aggressive behaviour and causes overshoots, as shown in Fig. 3.13d. However, this behaviour stabilises the throughput faster. This can also cause one traffic category to interfere with a lower priority category due to unnecessarily large contention window values. Larger waiting times (e.g. 5 s), could cause slower response, but they might settle down for a smaller contention window than the other waiting times, and this is helpful for system stability. For example, the target throughout at this setting is 7.2 Gbps (90% of 8 Gbps), which is achievable by both 15 and 31 contention window sizes. Smaller waiting times would rush into the larger contention window size, while a bit longer waiting time would steadily reach the smaller contention window.

Finally, the third parameter, the effect of the smoothing factor (α) on the performance

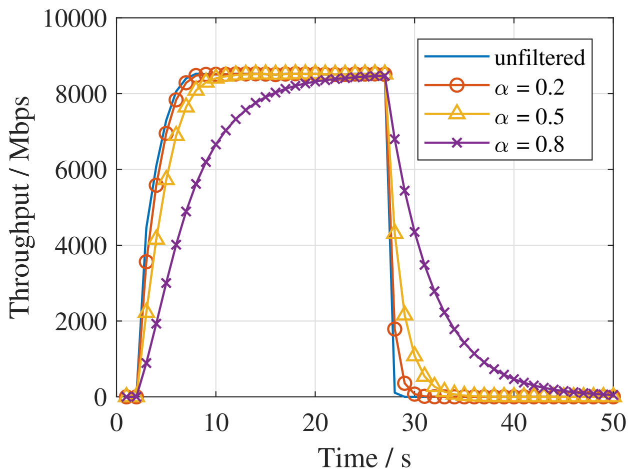

Figure 3.14: Effect of α on the network metrics.

is shown in Fig. 3.14. α, helps to reduce the sudden dips and spikes in the metrics, which is due to the randomness of the traffic. A smaller α biases the metrics to the latest observation and makes the algorithm sensitive to sudden changes while a larger α biases the metrics to older values and smoothen the response.

All these parameters can be manipulated to suits the conditions of each access category to obtain the desired dynamics of the algorithm such as very quick response for the high priority traffic while a moderate response for low priority traffic.

3.5 Performance Analysis

We have compared the performance of the proposed DCW algorithm with the existing IEEE 802.11 CSMA/CA protocol and the contention window adaptation (CWA) algorithm proposed in [90]. Further, we have demonstrated the effectiveness of the proposed algorithm under a real-life network scenario.

3.5.1 Comparison with CSMA/CA algorithm

For the comparison with the CSMA/CA protocol, we have used diverse network loads. The offered network load is increased by adding more users to the network instead of increasing the data rate of a fixed number of users. In this approach, the effects of user collisions are clearly demonstrated. The ratio of number of users in each loading condition is maintained as 1:2:2 for high, medium and low access categories, respectively. The data rate of a high priority user is set to 1 Gbps whilst the medium and low priority users offer 300 Mbps and 200 Mbps, respectively. Network configuration at each loading condition is given in the Table 3.4.

Fig. 3.15a shows the improvement in the throughput with the DCW algorithm. The high priority users observe an increasing throughput degradation with more users accessing the channel. The DCW algorithm was able to reduce the number of collisions in the network and reclaim the throughput. At the highest offered load, there is a notable improvement of around 1 Gbps in the throughput. Similarly, both medium and low traffic categories undergo severe throughput degradation if the original MAC protocol was in place and the network fails to support more than 10 users offering 4 Gbps. However, once the proposed DCW algorithm is in place where the contention windows are adjusted based on the offered load, both medium and low traffic categories gain around 1 Gbps throughput before being suppressed by the high priority traffic when the offered load is increased to 10 Gbps.

Delay comparison of the two MAC protocols are depicted in Fig. 3.15b. First loading condition observes delays in the order of microseconds as the collisions are very minute. With 10 users in the next offered load of 4 Gbps, the delays surge to the milliseconds range. Nonetheless, high priority traffic is able to remain below 10 ms with the DCW algorithm until the 10 Gbps loading condition where the network is loaded beyond its capacity. Even without the DCW algorithm high priority traffic is able to maintain a constant delay around 40 ms.

Table 3.4: Simulation parameters for the comparison with CSMA/CA protocol.

	Total Offered load	2 Gbps	4 Gbps	6 Gbps	8 Gbps	10 Gbps
No. of users	High	1	2	3	4	5
	Medium	2	4	6	8	10
	Low	2	4	6	8	10
Offered load / Mbps	High	1000	2000	3000	4000	5000
	Medium	600	1200	1800	2400	3000
	Low	400	800	1200	1600	2000

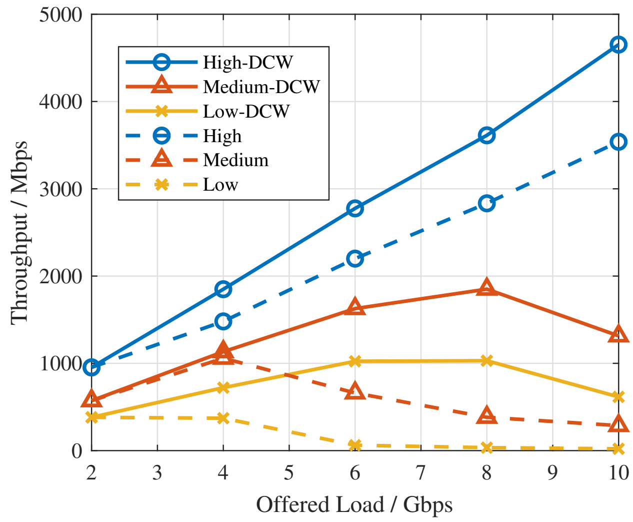

(a) Throughput improvement

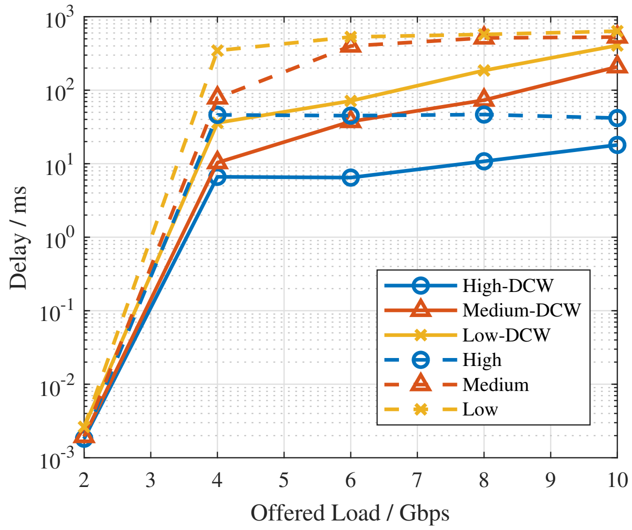

(b) Delay improvement

Figure 3.15: Throughput and delay of the network with conventional CSMA/CA MAC protocol and the improved DCW MAC protocol.

In contrast, the medium and low priority traffic show a persistent increase in the delay with offered load. Yet the DCW algorithm significantly reduces the delay of medium and low priority traffic categories and maintains them below the tolerable margins in comparison to current MAC protocol.

3.5.2 Comparison with CWA algorithm

We have compared our DCW algorithm with the CWA algorithm proposed in [90] to emphasise the importance of using end-user performance metrics such as throughput and delay in addition to the collision rate as inputs in the decision process. Many of the heuristic algorithms are solely based on the collision rate of the network for the decision making. In this comparison, we have used two network configurations that allow us to highlight that collision rate does not fully represent the status of the network and the end-user performance could be drastically different.

The first network configuration we have considered has a 16 kB maximum aggregated packet length. To further elaborate, the largest packet that this network can form is 16 kB. In contrast, the second network has a maximum aggregated packet length of 64 kB, which allows the second network to form larger packets and reduce the number of transmissions. The maximum aggregated packet length is adopted from the IEEE 802.11n standard. We have configured both networks to offer 5 Gbps of traffic using 10 medium priority users. Due to the different maximum aggregate packet lengths, the two network configurations show different dynamics despite the same traffic load.

We have applied both DCW and CWA algorithms to the two network configurations. The resulted throughput, collision rate, and contention window adaptation are shown in Fig. 3.16. The throughput of the two network configurations shown in Fig. 3.16a and Fig. 3.16b are improved under the DCW algorithm since it detects the drop in throughput and takes countermeasures. In contrast, the CWA algorithm fails to detect the throughput drop since it only monitors the collision rates shown in Fig. 3.16c and Fig. 3.16d. As it can be seen from these figures, the collision rates of both network configurations are the same. As a result, if the threshold collision rate is set based on the 64 kB network, CWA algorithm will not trigger for the 16 kB network. The contention window adaptations are depicted in Fig. 3.16e and Fig. 3.16f. This is an inevitable problem with observing only one network metric, because the real network scenarios tend to deviate from the values we set based on limited observations. Therefore, it is better to observe the metrics that directly relates to user experience and devise algorithms to adjust the network parameters accordingly.

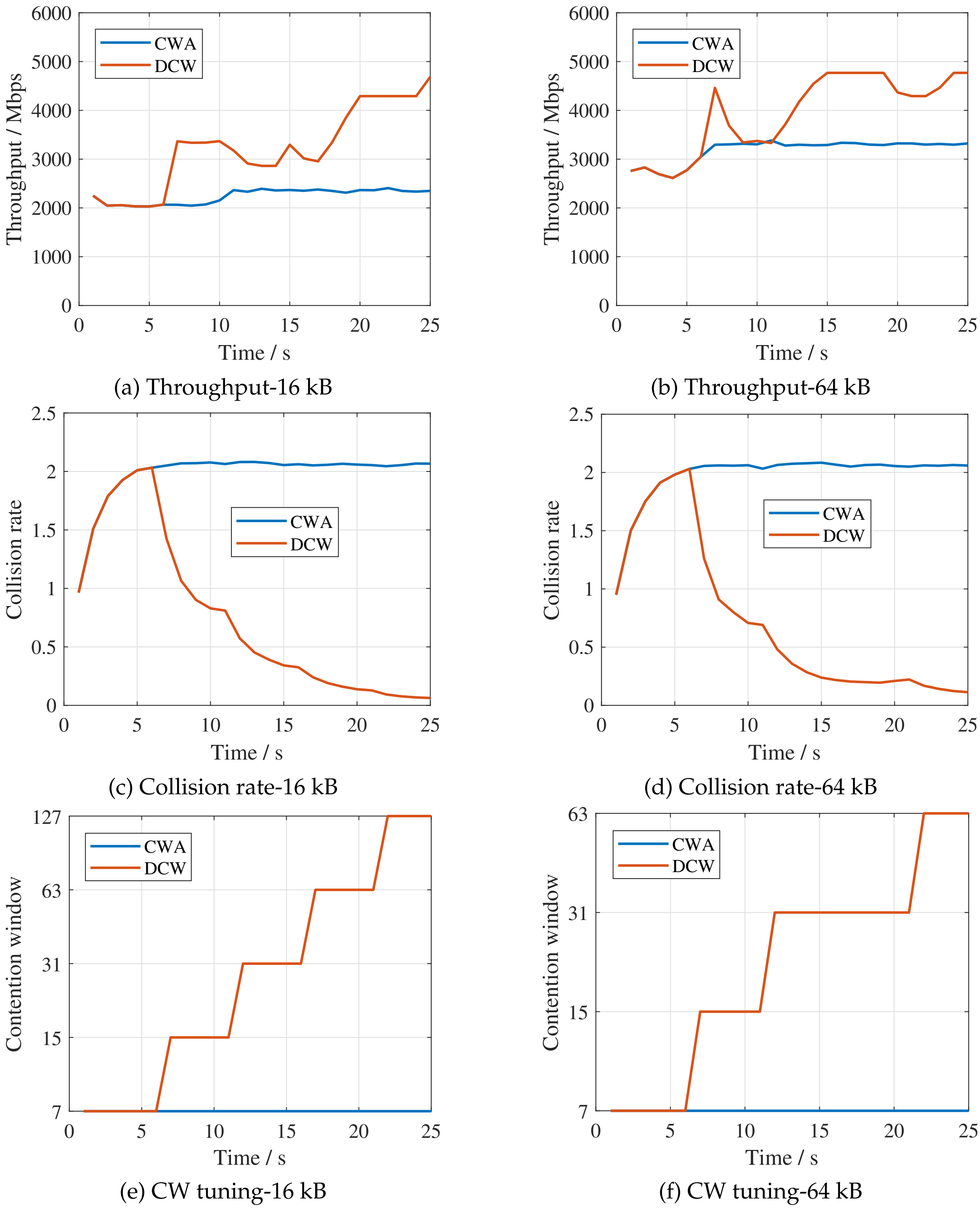

Figure 3.16: Performance comparison of DCW and CWA algorithms.

3.5.3 Performance in a real-life scenario

To further demonstrate the effectiveness of our DCW tuning algorithm in a real-life situation, we replicated a real network scenario in our simulations. In this analysis, users from different traffic categories were added and removed within the 100 seconds period. We considered 10 low priority users, and the number of low priority users remained constant throughout the entire simulation period. Then, 6 medium priority and 2 high priority users were added and removed at different times to evaluate performance of the algorithm for dynamic network scenarios. Table 3.5 lists the simulation parameters used for this analysis. Fig. 3.17 depicts the results under the considered network condition and performance improvement when the proposed DCW algorithm and conventional CSMA/CA algorithm are in place.

The variation of the throughput of the system shown in Fig. 3.17a is heavily affected when the contention windows were static. However, when the network is operated under our proposed algorithm, the contention windows are adjusted according to the congestion and each traffic category is received a fair portion of the bandwidth. The throughput of the medium priority traffic was dropped during 40-60s mark because more low priority traffic accessed the network. Based on the contention window and AIFS values, it is possible to adjust the bandwidth proportion each traffic category achieved.

The dynamic tuning of the contention window for each traffic category shown in Fig. 3.17b explains how the throughput of the system improved with the DCW algorithm. Both medium and low traffic categories increase their contention window size several times to cope with the collisions in the network. In addition, the high priority traffic category is also able to reach the expected throughput faster with an increased contention window.

Table 3.5: Simulation parameters of the real-life scenario.

Access category	Offered Load/Mbps	Start time/s	End time/s
High	2×5000	40	60
Medium	6×500	20	80
Load	10×200	0	100

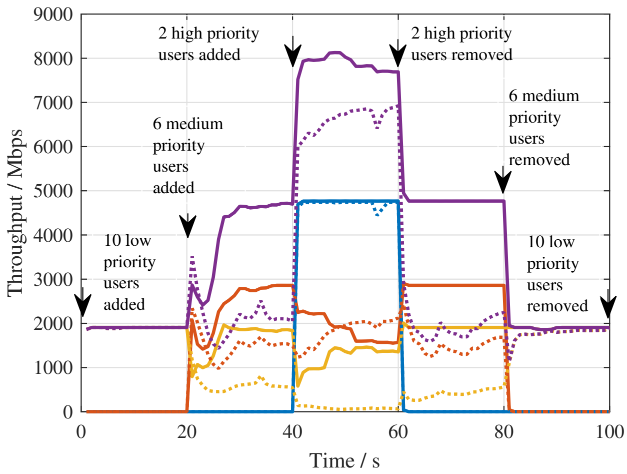

(a) Throughput

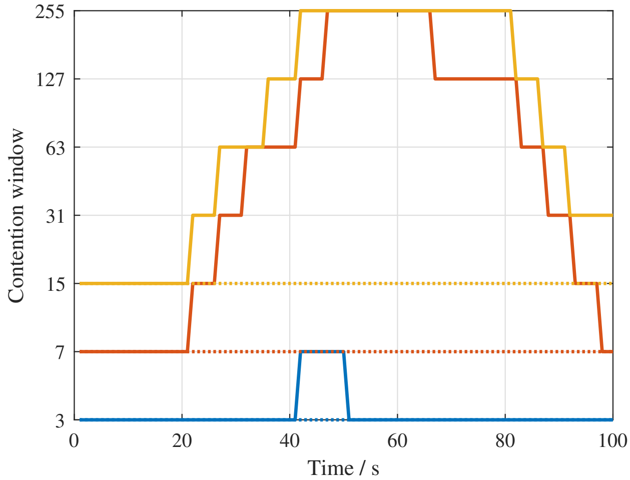

(b) Tuning of contention window

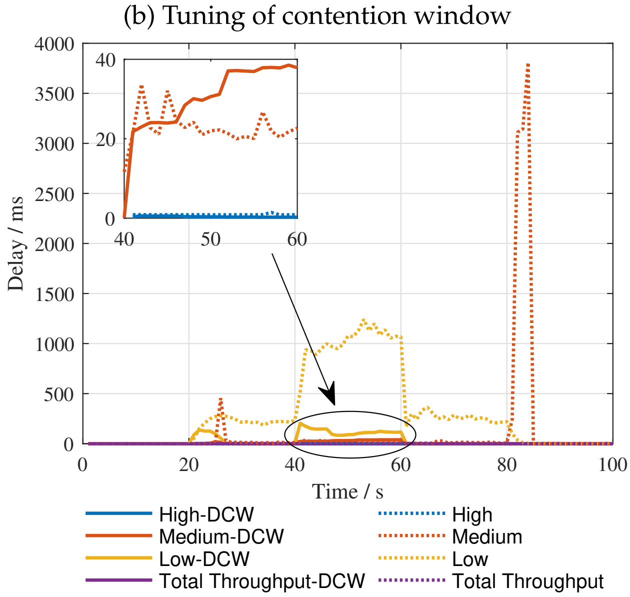

(c) Delay

Figure 3.17: Performance of the network with dynamic loads.

The delay variation of the network under the considered network scenario is shown in Fig. 3.17c. As shown, the delay of the low priority traffic is reduced from seconds to milliseconds range when employing DCW algorithm. The delay of the medium priority traffic is always maintained within the required limit when the DCW algorithm is in place and shows significant improvement in comparison to the conventional algorithm. The delay of the high priority traffic is also maintained well below the required limit by the DCW algorithm.

It is clear from these results that the proposed DCW algorithm along with the service differentiation mechanism improved the network performance and could guarantee the data rate and delay requirements of diverse next-generation applications.

3.6 Conclusion

Optical wireless communication needs suitable upper layer protocols to perform at their full potential under multi-gigabit multi-user environments. Therefore, in this chapter, we proposed a contention-based MAC protocol for indoor optical wireless networks that can be used to efficiently handle diverse services instigated from multiple users simultaneously in a multi-gigabit network environment. In particular, we have proposed a service differentiation mechanism with three traffic categories to effectively handle the anticipated traffic types of future high data rate wireless networks. Service differentiation is realised by manipulating contention window and AIFS values of the three traffic types defined for strict bound, medium, and low priority traffic. We have also proposed a contention-based algorithm for uplink operation, which can heuristically adjust the contention window based on the congestion level of the network since the conventional use of static contention window sizes does not typically perform well under diverse network conditions. We have demonstrated that the proposed dynamic contention window algorithm finely adjusts the contention window so that the packet collisions are minimised, and network performance is maximised. Furthermore, we have shown that the novel use of end user metrics such as throughput and delay in heuristic algorithms can ensure guaranteed performance. Finally, our results signify that the proposed mechanism is able to facilitate required quality of service to next-generation services whilst significantly enhancing the throughput and delay performance of the network compared to when the conventional WLAN MAC protocol in place.

Chapter 4

Network Architecture for Multi-gigabit WLANs

4.1 Introduction

OPTICAL wireless communication operates at multi-gigabit data rates. Hence, depending on the capacity provisions, OWC APs are expected to handle network traffic in the order of tens-of-gigabits per second. Typical WLAN APs are connected to Ethernet distribution networks which are not designed to support network traffic of this magnitude. Therefore, a future-proof OWC deployment would require a network architecture with a high capacity distribution network.

Furthermore, OWC networks use quite narrow beams which require precision beam-steering, user tracking, and feedback. Also, considering the fact that OWC networks will be femto cells, a centralised controller is required to enable smooth operation throughout the deployment with frequent handovers of multi-gigabit links. A centralised controller could monitor the network status and execute beam-steering and handovers more effectively than isolated APs carrying out handovers themselves.

Therefore, we have introduced the FLOWN (Full-duplex split-plane optical wireless network) architecture in [95] as a viable architecture for OWC networks. The FLOWN architecture has a full-duplex data plane, which is assisted by a separate control plane. It includes a central office with the active devices, which is connected to individual APs in the coverage areas via optical fibre links. Coupled with advanced features including network function virtualisation, FLOWN architecture could realise future-oriented high-capacity optical wireless networks to support diverse next-generation mobile applications.

Considering the upcoming WLANs as well as the trends in the telecommunications space, it is evident that next generation networks exhibit key features including massive scale of cell densification and high capacity APs [96]. Despite the frequency/wavelength ranges, these deployments need a strict management and control capability and a high capacity distribution network to operate smoothly without interference or bottlenecks. Therefore, in this chapter, we introduce a generalised FLOWN architecture that can be used for radio frequency, optical range or heterogeneous networks to enable multi-gigabit WLANs. We consider visible light communication, Wi-Fi and 60 GHz Wi-Fi for the generalised architecture since they have demonstrated viability in future WLAN landscape.

Visible light communication, which uses the LED illumination infrastructure to provide wireless connectivity has been proven to be a promising solution in WLANs [97]. VLC was first standardised as IEEE 802.15.7 [7]. However, with the rapid development, this standard is being revised as IEEE 802.15.13 [8] focusing on delivering beyond 10 Gbps. While the existing low data rate commercial products and deployments tend to use Ethernet as the distribution network, high data rate VLC implementations demand optical fibre distribution networks [77].

On the other hand, conventional Wi-Fi networks have always been under continued development to meet ever-growing consumer demand. Latest Wi-Fi 6 standard aims at 9.6 Gbps data rate with much more emphasis on dense deployments. Moreover, the 60 GHz front of the IEEE 802.11 standards suite is also under development to reach beyond 10 Gbps soon. Therefore, the need for a high-capacity distribution network is a common factor across all the future-oriented WLANs. Centralised architectures are not peculiar to Wi-Fi networks. They always had centrally controlled deployment options for community Wi-Fi networks, campuses, organisations, etc. Hence, an improved centralised architecture would advance the future Wi-Fi deployments in a multitude of directions with the new features introduced in Wi-Fi 6.

We make the following three main contributions in this chapter.

- Firstly, we introduce the novel network architecture for upcoming WLANs. This is a generalised version our FLOWN architecture proposed in [95].

- Secondly, we discuss the application of the proposed architecture in OWC networks, VLC networks, and Wi-Fi networks.
- Finally, we carry out detailed performance analysis of the proposed architecture using an OWC network and a Wi-Fi network.

The rest of the chapter is organised as follows. Section 4.2 introduces the generalised FLOWN architecture. Next, the Section 4.3 provides a discussion on the application of the generalised FLOWN architecture to VLC, Wi-Fi and OWC. Performance of the proposed architecture is presented in Section 4.4. Finally, Section 4.5 concludes the chapter.

4.2 Generalised FLOWN Architecture for Multi-gigabit WLANs

An overview of the proposed architecture in a deployment is shown in the Fig. 4.1. Coverage areas are divided into smaller cells and each cell is served by an AP. Each AP has a couple of beams to carry the data plane (DP) operation and the control plane (CP) operation of the network. On the other hand, the central office (CO) consists of transceivers and processing power to execute upper layer processing functions of the network. Optical fibre links are used to connect the APs to the central office, conceivably avoiding any capacity bottlenecks with growing demand.

4.2.1 Access Points (AP)

APs typically use a couple of narrow, directional beams to transport the DP. High frequency signals, which are used in upcoming WLANs are inherently directional and provide the best performance under well-aligned transceiver conditions. These directional beams are represented as sectors of the AP and operate independent from each other, allowing concurrent transmissions. The number of sectors depends on the user density and the geometry of the cell. It is possible to dynamically change the number of sectors with adjustable transceivers. For example, if the demand of an AP is increasing, the area can be divided into more sectors creating spatial reuse and distribute the load. The use of two distinct frequencies for upstream and downstream in a sector enables full-duplex

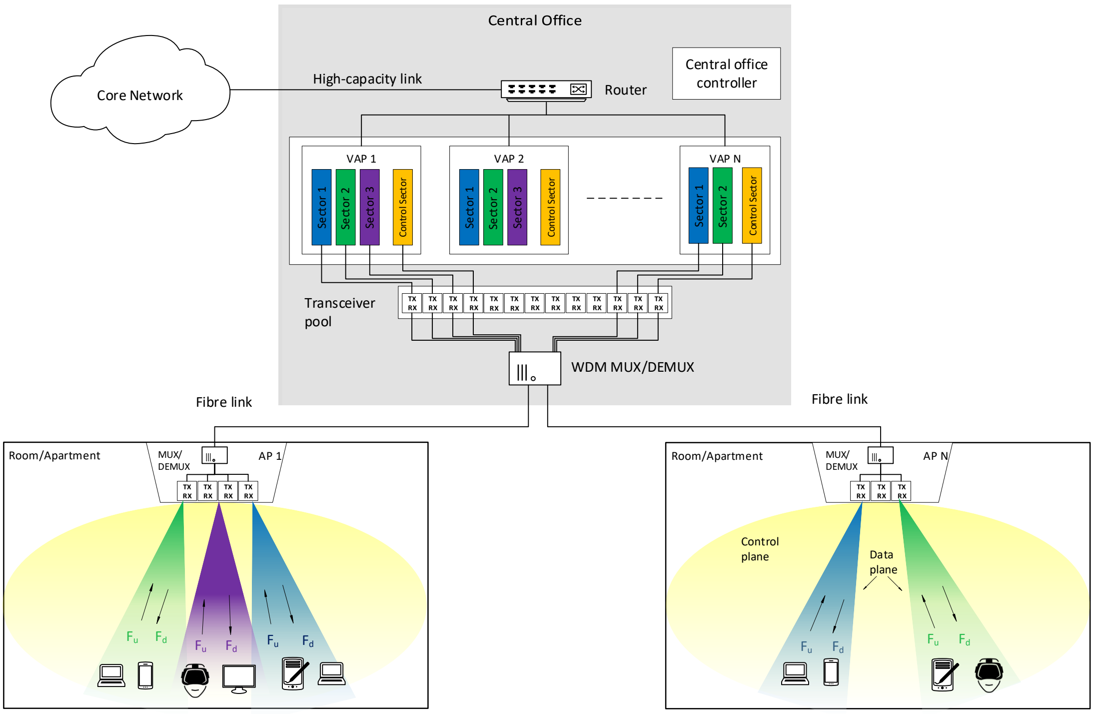

Figure 4.1: Generalised FLOWN architecture.

operation. Furthermore, inter-sector interference can be mitigated through careful planning and allocation of frequencies through the CO controller. DP operates at higher order modulation schemes to cater the high throughput demand.

On the other hand, each AP has a wider beam that overlooks the whole coverage area. This beam is used to carry the CP signalling of the network. However, CP can also be used to carry both DP and CP data if the high frequency directional beams are temporarily unavailable. Wider beam increases the visibility of the control channel, thus, allowing the users to communicate the control information despite their location and/or transceiver orientation. Typically, users discover the existence of the network by the beacons sent in the CP. If a user wishes to join the network, initial handshake also happens through the CP. It operates at lower order modulation schemes so that even a user with low received signal strength (RSS) can successfully decode control packets.

APs are equipped with radio or optical transceivers depending on the type of WLAN. Front-end of the transceivers communicate with the users through radio or optical wireless interface, while the back-end of the transceivers are connected to the WDM MUX/DEMUX (Wavelength division multiplexed multiplexer/demultiplexer). Therefore, back-end of the transceivers send and receive signals in optical fibres. WDM MUX/DEMUX connects the AP to the central office via highspeed optical fibre links.

4.2.2 Central Office (CO)

The CO houses a pool of transceivers and computational resources. Depending on the coverage area it could be in a basement of a building or in a separate infrastructure. Due to the flexible resource provisioning in the proposed architecture, it is possible to upgrade the CO capacity by adding more hardware and updating the current allocations through software.

As shown in Fig. 4.1, the fibre links from the APs connect to the WDM MUX/DEMUX in the CO, which aggregates/de-aggregates the WDM signals and routes them to the relevant transceivers in the transceiver pool. Each AP is represented inside the CO as a virtual access point (VAP) that carries out the upper layer network operations of each AP. VAPs are abstractions of computational resources allocated for each AP depending on their requirements. As shown in the Fig. 4.1, an AP will have parallel threads running for each sector since the sectors operate independent of each other. Mapping between the sectors and the transceivers is carried out during the resource allocation phase by the CO controller. The router in CO has the knowledge to forward packets directly to the relevant sectors without another switching stage inside the VAPs.

The next two subsections will explain the operation of VAPs and user devices with the aid of Fig. 4.2. At the bottom of Fig. 4.2 it depicts a VAP with N sectors and a control sector. Let us denote that M user devices are connected to this VAP through the AP in the top-left corner which is physically located in the coverage area such as in a room/a hallway. At the top of Fig. 4.2 it depicts the functional blocks of a user device.

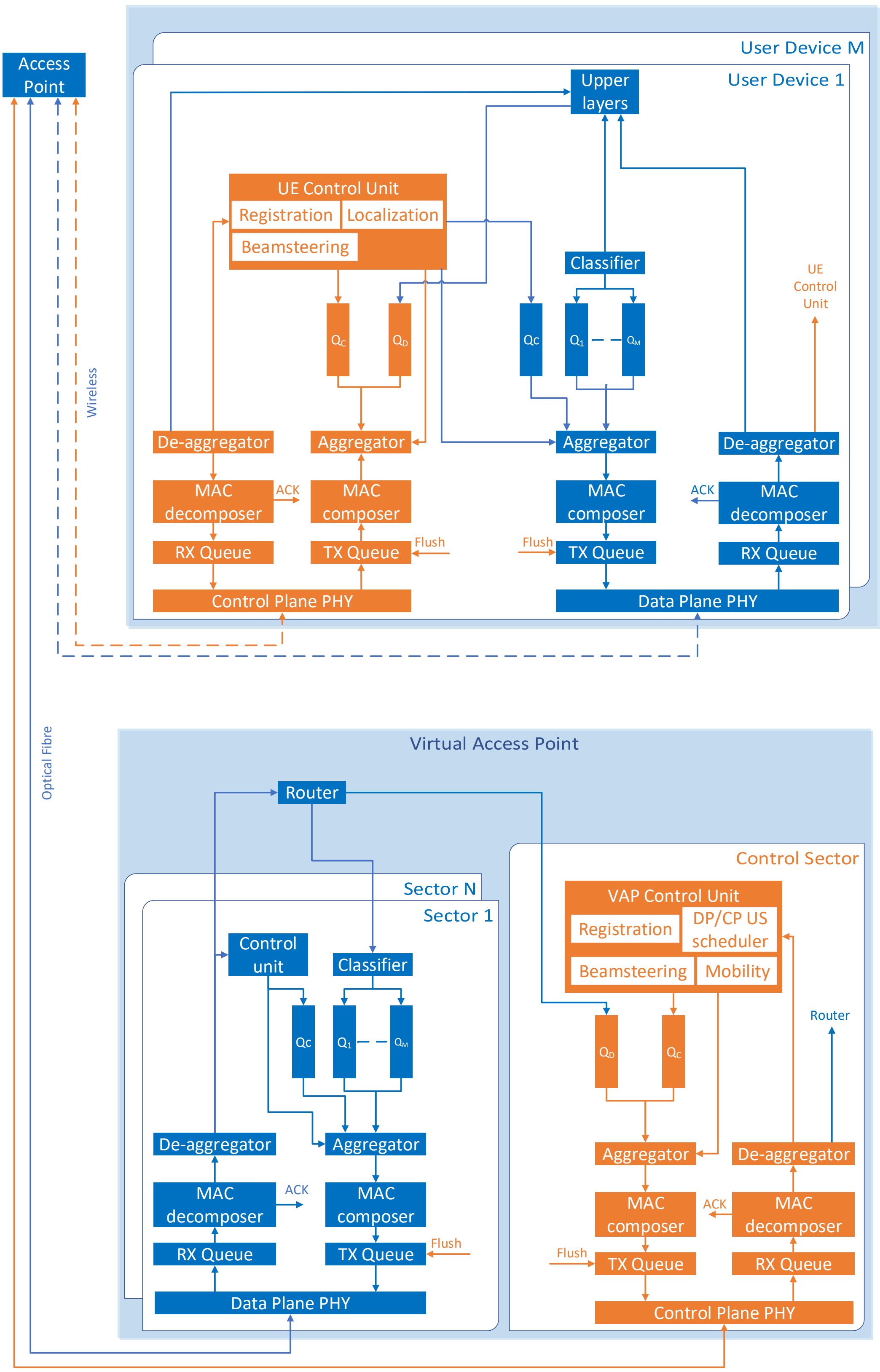

Figure 4.2: Functional block diagram of a VAP and a user device.

4.2.3 Virtual Access Point (VAP)

A VAP is comprised of several sectors working in parallel and a control sector. Once a packet is forwarded to a sector by the router, it will first go through a classifier which will read the Internet Protocol (IP) header of the packet and extract the Type of Service (TOS) field. Based on the TOS field, the packet will be put into one of the packet queues. The number of packet queues can be varied for different situations to achieve desired performance. For instance, an office environment could be benefited from a set of packet queues to differentiate various traffic types. That makes it easier to impose network policies such as limiting video streaming. In contrast, a virtual reality escape room only need a minimum number of packet queues since the data flows are quite bounded. Hence, the central office controller can efficiently allocate the resources to match the individual requirements of APs. Control packets generated by the control unit will be placed in a separate queue that is dedicated for control packets.

The sector control unit regularly monitors the packet queues and decides a composition of an aggregated packet based on the scheduling algorithm. Next, the aggregator will dequeue the packets and compose the aggregated packet with subframe headers or delimiters. Finally, the MAC composer will carry out the encryption, add the MAC header and cyclic redundancy check (CRC) sequence to the aggregated packet. The aggregated packet will be placed in the transmit queue until it is transmitted and acknowledged. Control packets also go through the same process except the aggregation and encryption in some instances. As it can be seen from Fig. 4.2, data packets can be routed via the control sector as well. It is useful if the DP loses the link temporarily. The VAP control unit has to update the routing table of the router in order to forward the packets to itself. It is worth noting that the control sector cannot always guarantee availability for high data rates or low latency DP plane packets that will be transmitted through CP since control sector might be involved in another transmission and control packets get priority over data packets. While there is no mechanism in the proposed architecture to communicate the congestion to the upper layers, most upper layer protocols such as TCP can sense the congestion and will automatically reduce the data rate.

On the reception path of VAP, the physical layer will add the incoming packets to the receive queue. The MAC decomposer will process each packet by checking the MAC headers and the CRC. The packets that make it through the MAC decomposer will be de-aggregated at the de-aggregator and passed to the router as IP packets.

A VAP has a control unit for the control and management functionalities of the AP. These include sending beacons, association/disassociation requests, and beam-steering messages. For most of the control and management functionalities, the VAP control unit seek updates and status from the sectors such as acknowledgements and queues statuses. The control unit has its own packet queue to buffer the control packets. In addition, as mentioned earlier, there is another queue for data packets that are for users who lost the DP temporarily.

The control sector only uses one frequency for both upstream and downstream giving rise to time division duplexed operation. It is reasonable given the low number of transmissions in the control sector. In addition, the transmissions in the control sector are tightly controlled by the VAP control unit.

4.2.4 User Device

User devices will have different transceivers depending on the technologies they support. Wi-Fi radio chip-sets are quite common in almost all the consumer devices today. OWC and VLC transceivers will come in different shapes and forms based on the device and capabilities such as beam-steering and lenses.

Regarding the upper layer operations, as it can be seen from Fig. 4.2, the DP of a user device is similar to that of a sector, except for the fact that the upstream scheduling is done at the VAP. Users receive the upstream schedule from the VAP via grant messages. A notable difference here in the user device is that the CP is now integrated with the DP as there is only one DP. Yet the CP and DP operate in parallel to each other. User devices typically have applications that generate and consume data rather than a router. Therefore, the IP packets inside the user device are either generated or consumed by applications such as video players or web browsers.

The proposed architecture shares some similarities and dissimilarities to 5G architectures. For instance, the CO and fibre distribution network fundamentally carry out the same tasks in both 5G and WLANs. However, the specific implementations and resources are quite different from one another. Indeed, with proper planning, it is possible to house both technologies in the same physical infrastructure and even execute vertical handovers between 5G and WLANs.

4.3 Application to Next-Generation WLANs

This section is dedicated to the discussion of how to apply the proposed architecture to the WLANs. We discuss the advantages and challenges in using the FLOWN architecture for OWC, VLC, Wi-Fi and, 60 GHz Wi-Fi networks.

4.3.1 Application to OWC

OWC uses infrared beams to establish indoor WLANs. They demonstrate superior performance and higher flexibility compared to VLC links. Invisible radiation has the advantage of less ambient noise, which significantly improves receiver performance. A basic form of OWC was included in the first IEEE 802.11 standard in 1997 [16]. However, it was not developed thereafter. Recent developments in the OWC domain are quite advanced and promising. Transceivers are now capable of reaching beyond 10 Gbps using simple modulation schemes like OOK [98]. Robustness of the links are further improved by beam-steering techniques that can follow users and maintain connectivity under mobile or blocking scenarios. With such improvements, OWC networks are also demonstrating data rates well beyond 10 Gbps for the mobile users.

OWC networks are often operated in wavelength division multiplexed (WDM) mode and allows the allocation of wavelengths to different users and/or planes. Therefore, it is relatively easy to implement full-duplex or split-plane architectures in optical wireless networks. Such fine wavelength allocations require centralised management. Therefore, most of the gigabit optical wireless systems are centralised. For example, authors in [99] demonstrated an optical wireless communication system which centrally tunes the wavelengths to steer the beams.

Application of the proposed architecture to the OWC networks will enhance the overall performance of the OWC networks given the high capacity and heavy processing involved in the networks. Without having rigorous standardisation yet, it is a quite open area for optical wireless networks to evaluate the applicability of diverse network architectures.

4.3.2 Application to VLC

VLC is also rapidly developing as a WLAN technology. VLC aims to utilise the illumination infrastructure to provide wireless connectivity in indoor environments. It was first standardised in IEEE 802.15.7 [7]. However, the fast developments quickly outdated this standard. Therefore, a revision of this standard, IEEE 802.15.13 [8], is underway at the moment. This standard targets data rates up to 10 Gbps as oppose to 96 Mbps in the first version.

Current standards and commercial products of VLC often design the APs to work as standalone devices. That means one light fixture acts as a standalone AP connected to the backbone data network. However, with the density and short range of VLC APs, there has to be many APs in a given environment which have given rise to many complications in the management and coordination of the overall network. Therefore, centralised architectures are proposed to VLC networks to improve the efficiency and performance of the networks.

For instance, authors in [100] has proposed C-LiAN (centralised light access network), which centralises the AP operations to a central controller and deploy the luminaire as dummy transceivers. This enables centralised processing and collaborative signal transmission which are helpful in number of aspects such as coordinated decision making, load balancing, and resource provisioning. Further, centralising the processing power reduces the cost of each AP and greatly benefits the scalability of the network as well.

Furthermore, authors in [77] suggests a network architecture similar to PON for VLC networks. The authors pointed out that the VLC APs are likely to operate around 10 Gbps data rates, which calculates up to around 100 Gbps in the backbone network. Only a fibre network can handle that capacity efficiently. Therefore, an architecture like PON is suitable for high data rate VLC deployments considering the data rates and latency requirements of the upcoming traffic types.

With the concept of heterogeneous access, VLC networks are usually deployed as hybrid networks with radio frequency (RF) systems augmenting the coverage. As mentioned earlier, VLC APs inherently have a spatially limited coverage and does not support beamforming. Therefore, Wi-Fi networks, for example, are used as a fall-back network and a coordination layer. This is analogous to the control sector proposed in our architecture which can carry the data plane for temporary outages. Such a system is proposed in [101] with detailed analysis on throughput and outage performance. The authors proposed to use a central unit which monitors the VLC link performance and carry out the handover to RF if the performance degrades below acceptable limits. Authors in [43] also introduced a hybrid VLC/RF system that has a Wi-Fi network as a back-channel. This allows the users to maintain connectivity even the VLC link is blocked or out of range.

With similar approaches, VLC systems are further extended to operate in full-duplex mode as well. Most straightforward approach is to use different technologies in the uplink and downlink. For instance, authors in [102] use infrared in the uplink to differ it from visible light. Similarly, [103] introduces a 60 GHz for the uplink effectively avoiding self-interference.

It is clear that VLC networks, especially those that target gigabit data rates, can highly benefit from a centralised architecture that support split-plane and full-duplex networks. Therefore, it is evident that the proposed architecture is suitable for high data rate VLC networks.

4.3.3 Application to Wi-Fi

Wi-Fi networks were initially designed to setup basic WLANs as extensions to local area networks (LAN). However, they quickly became an integral part of the access networks due to the appealing untethered connectivity. Since then, Wi-Fi networks were aggressively deployed to cater the increasing user demands. At present, this success itself has started causing performance degradation in Wi-Fi networks. Highly dense Wi-Fi deployments we encounter in apartment buildings, organisations, major cities are often degraded by severe interference. Most of the time, APs are not coordinated nor optimised to work in a dense scenario. As a result, APs operating at closer bands will cause interference to each other and ultimately degrades the user quality-of-service.

Thus, the latest Wi-Fi standardisation task group, TGax, is focused on high-efficiency WLANs (HEW) to improve the efficiency of dense deployments [22]. Number of techniques are proposed to battle the inefficiencies in dense Wi-Fi networks. The introduction of orthogonal frequency division multiplexed access (OFDMA) opens many doorways to improve the efficiency of dense networks. For instance, data frames in Wi-Fi networks are often small and does not need the whole bandwidth for transmission. Therefore, allocating small set of subcarriers for a user with minimum fading would improve the efficient use of network resources. Furthermore, TGax introduces spatial reuse of frequencies through basic service set (BSS) coloring. The idea behind BSS colouring is to enable the users to identify transmissions from neighbouring APs and neglect them without being interfered. In addition to that TGax also uses uplink and downlink multi-user MIMO to increase the data rate.

All the novel techniques proposed by TGax for the upcoming Wi-Fi 6 standard could be enhanced by a centralised architecture. For example, inter-AP communication is quite straightforward with a centralised architecture. Therefore, allocation of subcarriers and timeslots (a.k.a. resource units) can be easily determined to minimise the interference. Furthermore, allocation of power levels and beamforming is also effective in a centralised architecture where VAPs can exchange information easily. In addition to that, complex protocols used in MU-MIMO call for high processing power in the APs, can also be provided using the central office resources.

In fact, most of the large-scale Wi-Fi networks are deployed as enterprise networks which are essentially centralised. Enterprise networks were introduced by vendors like Cisco and Aruba to manage large-scale deployments such as universities and large organisations [104, 105]. These deployments are often based on the CAPWAP (Control and Provisioning of Wireless Access Points) [106] and/or proprietary protocols which help deploying APs in an enterprise network. Main feature of an enterprise network is the split-MAC which divides the MAC layer functions between the APs and a WLAN controller (WLC). WLC is a high-performance device which can execute MAC operations of a few thousand APs simultaneously with a large number of active users. Due to the small cell inclination in the 5G, networks service providers are also keen in deploying their own citywide Wi-Fi networks to enable heterogeneous networks so that it is possible to offload heavy traffic into Wi-Fi networks.

Adapting 5 GHz Wi-Fi networks to the proposed architecture is quite effortless with the well-established enterprise networks. The central office controller can instantiate Wi-Fi VAPs inside the central office and the Wi-Fi transceivers will generate radio frequency signals. The most efficient way to transport the RF signal in the fibre would be to use radio over fibre (RoF) techniques. On the AP end, the RoF signal will be converted back to RF again. It is worth noting that the enterprise networks will split the MAC functions between the VAP and AP. The local MAC will include time-critical functions such as sending beacons while the VAPs will execute the other MAC functions that are not time-sensitive

Wi-Fi networks, at their basic form, does not support CP and DP separation nor does it support full-duplex operation. Nonetheless, with the introduction of OFDMA in Wi-Fi 6, full-duplex operation is realisable. Similarly, OFDMA paves the way to split-plane architecture as well. So far, most of such implementations were based on multiple radios working on different bands [107, 108]. As it can be seen, our proposed architecture is well-suited for the upcoming Wi-Fi 6 standard and already includes many avenues for future developments

WLANs in 60 GHz range are standardised in IEEE 802.11ad [3] and ECMA-387 [109] standards. They were driven by the high congestion in the low frequency range as well as the huge unlicensed spectrum in the 60 GHz range. One of the main challenges the 60 GHz systems faces is the high directionality of the transceivers. There has been numerous works on addressing the directionality in both physical layer and MAC layer. The basic mechanism used in IEEE 802.11ad standard is beamforming [3]. Specifically, exhaustive beamforming is used to find the optimal pair of antennas for the users to communicate.

With the high directionality of the 60 GHz networks, it is often difficult to establish ubiquitous connectivity. Hence, there has been research investigating the suitability of incorporating a 5 GHz network into 60 GHz networks to improve connectivity [110]. Especially, due to the fast session transfer (FST) feature and tri-band/dual-band commercial products, it makes more sense for the three frequencies to cooperate to deliver the best quality-of-service to users. Since this analogous to the proposed architecture, it is possible to map a whole AP to a VAP inside the central office and treat 5 GHz channel as the control sector.

Evidently, the proposed architecture can be used to implement standalone 5 GHz Wi-Fi networks with or without advanced features such as OFDMA, full-duplex or CP/DP separation. Similarly, standalone 60 GHz networks are also implementable in the proposed architecture, however, heterogeneous schemes such as [110] are more suitable with the propagation characteristics of the 60 GHz bands.

4.4 Performance Evaluation

We have demonstrated the performance of the proposed architecture in comparison to the existing architectures as well as the protocols. First, we observed the round trip time (RTT) from a user device to the closest CO or switch in order to understand the main latency contributors of the architectures. Second, we observed the network performance with and without full-duplex operation as the uplink and downlink of the current networks are getting increasingly symmetrical. Finally, the split-plane operation is demonstrated to highlight the importance of the wider fallback channel.

4.4.1 Round Trip Time

We have compared a typical Wi-Fi network architecture with the proposed architecture for the RTT study. As shown in the Fig. 4.3, a 1 km of fibre adds a delay of 4.67 μs to the link. The rest of the delay is caused by packet serialisation [111]. Packet processing delay is considered to be negligible. Depending on the physical layer modulation, CP and DP result in different serialisation delays, hence, the CP experiences more delay in the link.

On the other hand, Wi-Fi network experiences a delay more than one order of magnitude compared to OWC due to the inherent nature of the MAC protocol. Furthermore, OFDM modulated Wi-Fi packets are temporally quite large compared to OOK modulated

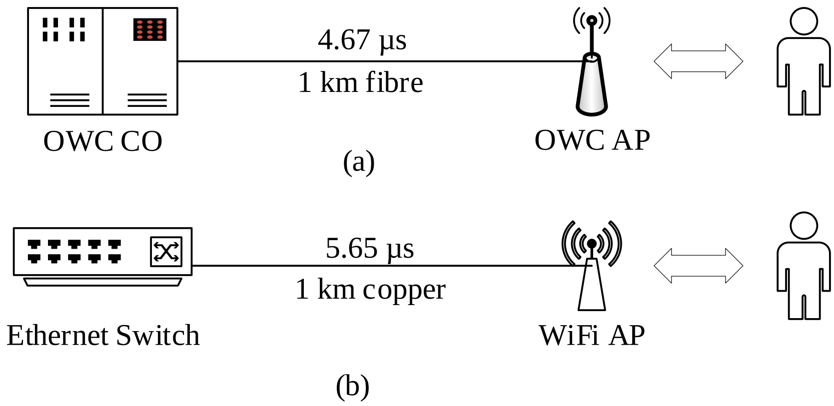

Network	RTT/µs
Wi-Fi 6	370
Data plane (10 Gbps)	11.69
Control plane (1 Gbps)	26.84

(c)

Figure 4.3: (a) OWC network with 1 km fibre link to the central office. (b) Wi-Fi network with 1 km of copper links to the nearest switch. (c) RTT of the Wi-Fi network, OWC CP, and DP.

OWC packets.

While the difference between copper and fibre is not substantially large, it is worth noting that the difference is significant compared to the 10 Gbps OOK modulated packets. These packets take only a couple of microseconds to serialise. It is similar for other technologies such as VLC which uses OOK modulation.

4.4.2 Full-duplex Operation

Full-duplex operation provides a plain performance gain to WLANs because of the simultaneous uplink and downlink transmissions. There are also indistinct advantages of full-duplex operation in the protocol level which greatly improve and simplify the operations.

We have studied the performance of uplink and downlink of the Wi-Fi and OWC networks with increasing load. The load is increased by adding more users to the network. In the OWC network, a user transmits 1 Gbps of data in the uplink while receiving 1 Gbps

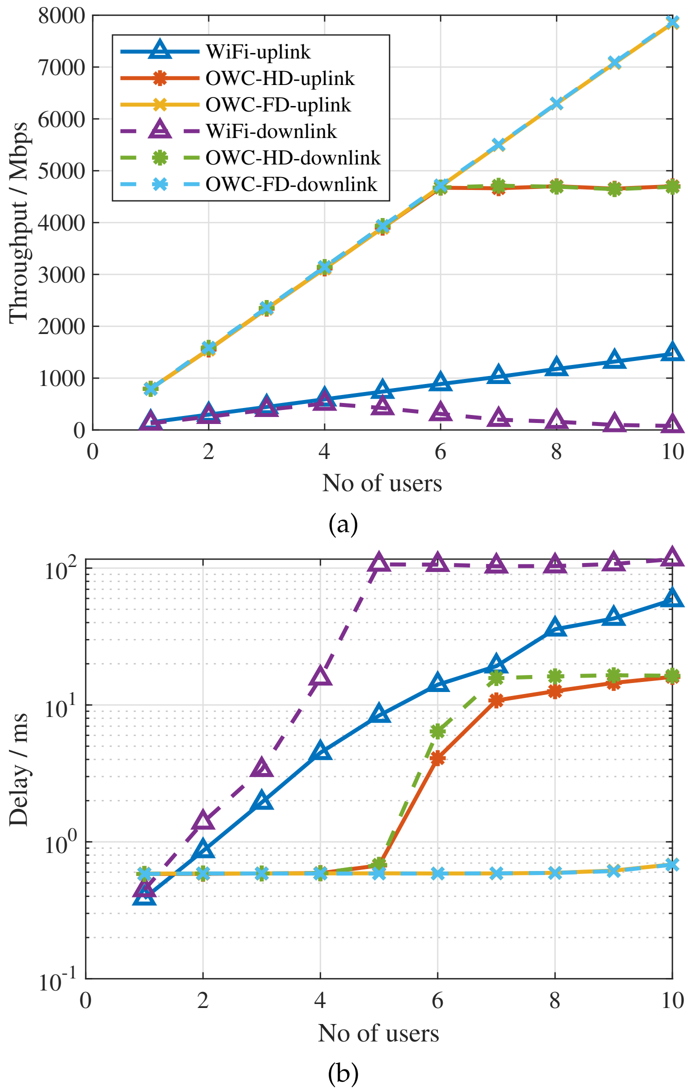

Figure 4.4: (a) Throughput and (b) delay of the Wi-Fi and OWC networks in the uplink and downlink.

of data in the downlink. OWC network can operate in both full-duplex (FD) and half-duplex(HD) mode. Users in the Wi-Fi network offer 150 Mbps in the uplink and receive 150 Mbps in the downlink. Wi-Fi network is configured as an IEEE 802.11ax network with MCS 11 and 4×4 MIMO [112].

One of the key observations in the network throughput, shown in Fig. 4.4a, is the symmetrical performance of the OWC network. Despite being full-duplex or half-duplex, it is capable of ensuring the fairness for uplink and downlink. In addition, as stated earlier, full-duplex operation has caused a plain improvement in the throughput. Full-duplex operation is quite straightforward to implement with WDMA or OFDMA.

On the other hand, Wi-Fi networks do not support full-duplex operation yet though OFDMA was introduced in IEEE 802.11ax standard [22]. Therefore, the simulated Wi-Fi network operates in half-duplex mode with CSMA/CA mechanism. In contrast to the OWC, Wi-Fi network fails to ensure the fairness in the uplink and downlink. With the increasing number of users the downlink is severely affected resulting in around 80 Mbps for the maximum load.

Delays of the networks are shown in the Fig. 4.4b. Note that in this case the delay is obtained from AP to user without the fibre/copper link to the CO/switch. The delay of the OWC networks depend on the mode of operation. Full-duplex network always maintains a delay below 1 ms while the delay of the half-duplex network quickly jumps to around 16 ms with increasing load. Wi-Fi uplink consistently increases the delay with the increased contentions of the network. However, downlink delay is capped around 5 users due to buffer overflowing.

4.4.3 Split-plane Operation

While the concept of control and data plane separation is implemented in various forms from networking to telecommunications, using split-plane operation in WLAN architectures received minimal attention so far. Therefore, in this section we attempt to demonstrate the virtues of split-plane operation using two scenarios.

First, we demonstrate a scenario where a user walks from one end of a 10 m room to the other end at a speed of 1 m/s. This scenario is used to show the network dynamics when the user enters and leaves the two planes of the network. At the start, the user quickly associates with the network once it receives the CP beacons as shown in Fig. 4.5. The user is served by the CP until it reaches the DP. Once the user receives DP beacons it will update its association status and the routing tables will be updated accordingly. Eventually, after walking away from the DP coverage, the user stops receiving the DP beacons, at which point the user again falls-back to the CP.

The traffic flows from the AP to the user at a rate of 1.5 Gbps. The transients of the

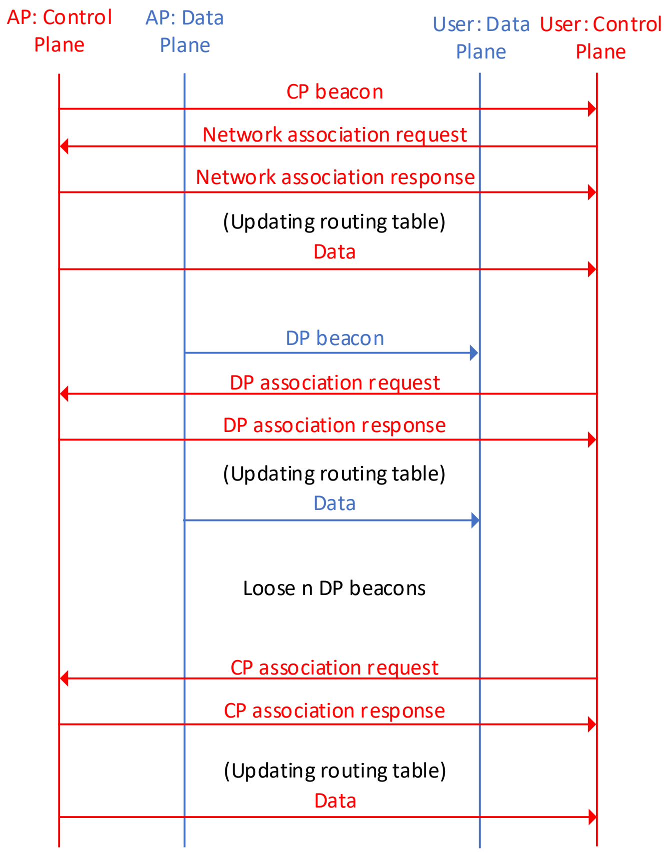

Figure 4.5: Control plane and data plane messages during the network association, data plane association and reassigning to the control plane.

network are shown in the Fig. 4.6. The throughput of the user, shown in Fig. 4.6a, is saturated just below 1 Gbps because the CP queues are overflowing, and the traffic variations are filtered out. However, once the user connects to the DP it receives the data real-time and the bursty nature is visible. In addition, there is a spike at the beginning of DP connection. This is due to the concurrent transmission from CP and DP during that period. The CP continues to transmit the available packets in its queue even after the user is connected and receiving from the DP. Further, Fig. 4.6a also shows the CP utilisation. When the CP is not involved in a data transmission, it is widely available for control and management functions of the users. However, if the CP is used for data transmission, it will not be as available as earlier for control and management functionality. The utilisation can be programmed such that CP does not fail to serve the control or management

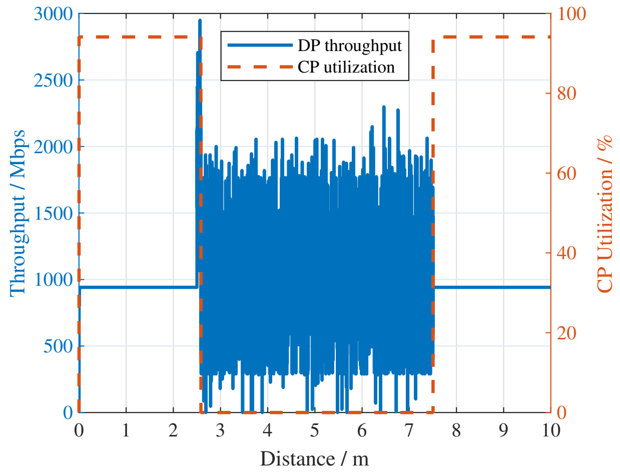

(a)

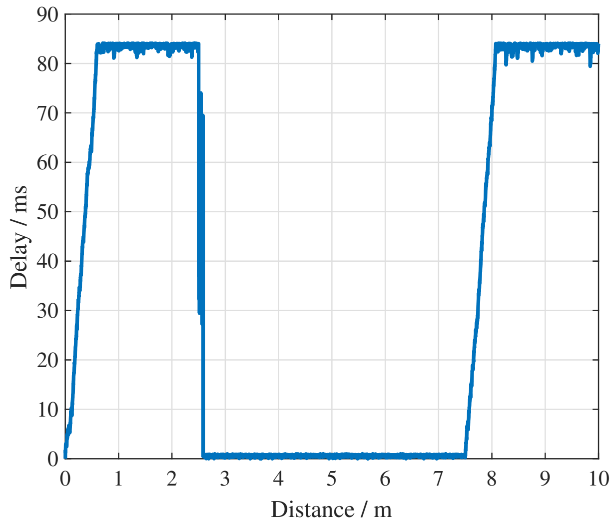

(b)

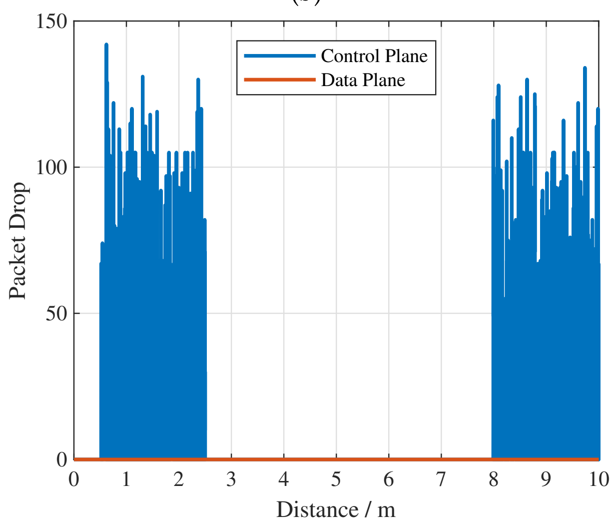

(c)

Figure 4.6: (a) Throughput, (b) delay and (c) packet drop of the network for the split-plane scenario.

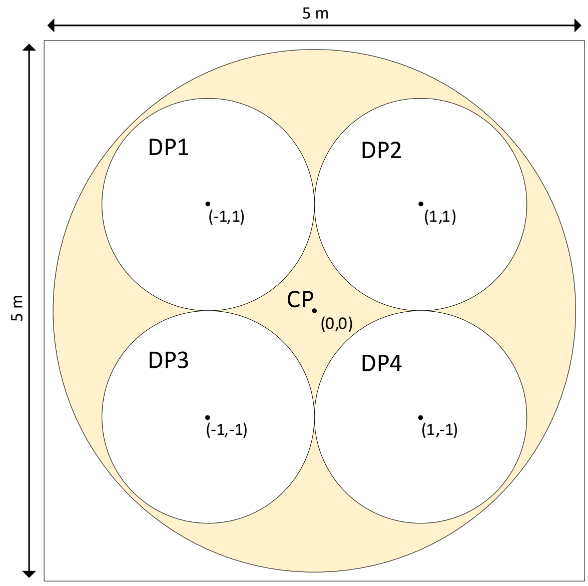

Figure 4.7: Arrangement of the coverage area.

functions of the users.

The packet delay of the network is depicted in Fig. 4.6b. The delay of the network is seen to rise from 1 ms to around 80 ms when the user loses the DP connections. Therefore, even though the CP operates as a fallback option, it is vital to have a thorough coverage from the DP for time-sensitive applications. Similarly, Fig. 4.6c represents the packet drops in the CP and DP where the DP drops are almost zero for the whole duration. CP packet drops could also be reduced by using larger queues, however, it results in higher delays.

Next, we consider a coverage area of 5 $m \times 5$ m with CP beam located at the centre as shown in Fig. 4.7. Considering the centre as the origin, DP beams are located at coordinates of (1,1), (-1,1), (1,-1) and (-1,-1). A DP beam can cover a circular area with 1 m radius with beam-steering. We put a few users into the coverage area and evaluate their capacity without a CP and with a Gaussian CP. This study will give a generalised evaluation of the performance improvement of the fallback CP.

Each user receives 1 Gbps traffic in the downlink. We have modelled the user movement in two different ways. The first model is the random walk (RW) model in which the

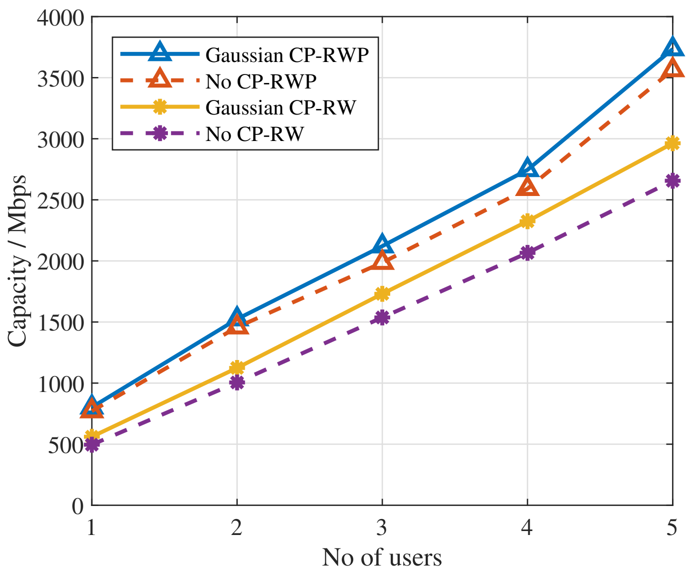

Figure 4.8: Capacity of the random walking users with increasing load for Gaussian CP and no CP cases.

users are always moving in random directions at random speeds. This model resembles the worst-case scenario of the user movements where every user is mobile at all times. Conversely, the random waypoint (RWP) model models rather natural user movements by including pauses in between movements. Depending on the location the user might be connected to either DP or CP.

The capacity of the network for the two models are shown in the Fig. 4.8. As expected, the random walk model achieves low capacity compared to the random waypoint model. With the random walk model, the Gaussian CP improves the network capacity by 12% on average. On the other hand, in the random waypoint model, the improvement introduced by the Gaussian CP is around 5% which is around 100 Mbps. It should be noted that in this case the CP is a 1 Gbps link. It is possible to improve the gain with a higher capacity CP.

4.5 Conclusion

WLANs are evolving fast to keep up with the ever-growing user demands. Recent WLANs have demonstrated their abilities to provide unprecedented data rates in the multi-gigabit range. However, with the increasing capacity and complexity of the upcoming WLAN deployments, it is extremely difficult to ensure the required data rates, control/management, stringent latency requirements and coordination with the use of existing distributed network architecture. Therefore, in this chapter, we introduce a centralised network architecture for WLANs that can facilitate full-duplex and split-plane operation in addition to flexible hardware and software resource allocations. This is a generalised version of our FLOWN architecture, which was introduced for OWC networks. We evaluated the improvement in the latency of the network with the proposed architecture and demonstrated the benefits of the full-duplex and split-plane features with application to a 10 Gbps optical wireless communication network.

Chapter 5

Design of ns-3 Module for OWC Networks

5.1 Introduction

THE physical layer of the OWC networks has been developing fast for the last few years. As we discussed in the previous sections, these developments have introduced unprecedented data rates to WLANs. However, at the same time, OWC networks use complex mechanisms such as beam-steering to establish and maintain the multi-gigabit links. Moreover, data rates of this magnitude push the existing protocols beyond their limits. For instance, in Chapter 3 we showed the inefficiency of the contention-based MAC protocols at multi-gigabit data rates.

Thus, it is vital to have simulation tools to implement and evaluate these new and existing network layer protocols/algorithms/architectures such that they can be tested at the multi-gigabit conditions. Typically, the physical layer simulations are carried out as continuous-event simulations in software packages such as MATLAB [113]. However, it is computationally too intensive to run network layer simulations in continuous-event fashion. Hence, discrete-event simulations are chosen for evaluating network layer implementations. For example, ns-3, OPNET, NetSim and OMNeT++ [13,114–116] are popular discrete-event network simulators.

With the network layer research for multi-gigabit OWC networks getting traction, we decided to develop a simulation module for OWC in ns-3. While there are a few works on VLC simulators in ns-3 [117, 118], they do not target multi-gigabit OWC networks. The earlier attempts in OWC were also in the free space optics (FSO) domain with ns-2

[119]. The decision to use ns-3 was based on a few compelling features of ns-3.

- ns-3 simulator is widely accepted and tested. The modules are easily shareable and integrable. Hence, ns-3 project receives new modules from the community for many upcoming technologies [120–122].
- Simulation results can be repeated exactly using the fixed seed random number generator.
- ns-3 network protocols are directly taken from the Linux kernel. Therefore, the simulations are very close to real-life implementations.
- Emulation support; which allows the simulator to interact with real implementations.
- ns-3 can generate standard outputs such as PCAP, which can be analysed using other industry-standard tools like Wireshark [123].
- ns-3 is an open-source project licensed under the GNU GPLv2 license and it is freely available with a wide community support.

For the best of our knowledge, this is the first OWC ns-3 module that is designed for multi-gigabit data rates. Therefore, this module will fill a gap in the vital research tools that are necessary for the development of the OWC networks.

The rest of the chapter is organised as follows. The Section 5.2 will introduce the architecture of the ns-3 simulator. Next section will present the design and the implementation of our ns-3 module for OWC. Finally, we present some of the features of the proposed module in Section 5.4 and conclude the chapter in Section 5.5.

5.2 Introduction to Network Simulator-3

The ns-3 project was started in 2006 with the aim to introduce a much-improved successor to ns-2 simulator [124]. Therefore, ns-3 was written from scratch without the backward compatibility to ns-2. The first version of ns-3, ns-3.1, was released in 2008. After more than 14 years of evolution, today we have the ns-3.31 version of the ns-3 simulator.

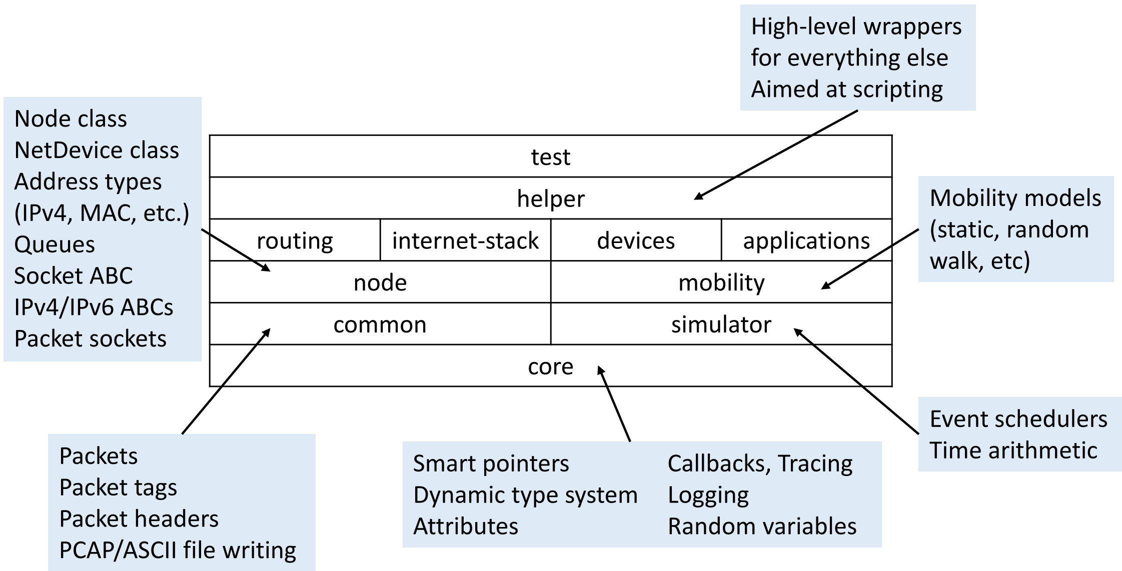

Figure 5.1: Software organisation of ns-3.

ns-3 simulator was written in C++ as a collection of modules which can be combined to build complex network scenarios. This modular architecture makes it quite flexible and the addition of new modules seamless. Though the core of the ns-3 was written in C++, it supports Python using wrappers.

Fig. 5.1 shows the software organisation of the ns-3 project. The bottom most layer is the core of the simulator. The core includes the foundational blocks of the simulator. For instance, the core module includes the attributing system and callbacks, which are vital functionalities of the simulator. The attributing system allows the users to access the internal variables of the modules. Hence, the users can tune parameters of the protocols on-the-fly and observe the network performance. Similarly, the callbacks system is implemented to decouple the modules from each other. Conventionally, different modules interact with each other using known functions, which results in inter-dependency. In contrast, callbacks are implemented using pointers that directs to functions. Further, the core module implements an in-built random variable generator for the ns-3 simulator. Apart from that, as shown in Fig. 5.1, the core module also implements the logging functions, tracing function, smart pointers and type casting mechanisms as well.

The real simulator or the simulation engine in built upon the core module as shown in the Fig. 5.1. The `Simulator` class implements the functions of the simulator such as control the time and execution of events.

The `Node` class is another important class. A `Node` object resembles a physical node in a network like a computer. Similar to a physical node, a `Node` object could contain many different `NetDevice` objects. The `NetDevice` class resembles the network interface card (NIC). Therefore, a node can contain an Ethernet `NetDevice` as well as a Wi-Fi `NetDevice`.

ns-3 has a collection of mobility models that could be used to implement various mobile networking scenarios. From static positioning to random walks can be simulated using these models. We have listed a few common mobility classes implemented in ns-3.

- `ConstantPositionMobilityModel`
- `ConstantVelocityMobilityModel`
- `ConstantAccelerationMobilityModel`
- `RandomWalk2dMobilityModel`
- `WaypointMobilityModel`
- `RandomWalk2dOutdoorMobilityModel`

In order to generate traffic and also to build interacting systems, ns-3 implements a set of applications. These applications can be used to generate different types of traffic by tuning their attributes. For example, the `OnOffApplication` can be used to simulate a saturated traffic source by setting the `OnTime` attribute to 1 and `OffTime` attribute to 0. On the other hand, one can set random variables to the `OnTime` and `OffTime` attributes to generate different types of bursty traffic such as Poisson. ns-3 comes with a `UdpClientServer` and `UdpEcho` applications which are useful in testing UDP connections.

Routing protocols and internet stack of the ns-3 project are taken from the Linux kernel. Hence, they can simulate the behaviors of the protocols quite close to the real-life situations.

Different communication technologies are implemented as devices inside the ns-3 simulator. For instance, Wi-Fi and 4G LTE have different `NetDevice` classes, which enclose all the functionalities of the particular technology. Once we instantiate a certain `NetDevice` object, we have to populate it with the relevant channel model, physical layer and MAC layer objects to finish the implementation. This is a tedious task which can take many lines of code. The solution is the helper classes which are implemented for each module. As an illustration, take a Wi-Fi network. One can instantiate the Wi-Fi `NetDevice` class and starting adding everything from the channel model to the internet stack, which is unnecessarily time consuming. Instead of that, we can use the helper classes to do the hard work. We have to set the attributes of the helper classes, such as the particular Wi-Fi standard we need to use. In fact, almost all the user codes (simulation scripts) in ns-3 are written using helper classes.

ns-3 also comes with a testing framework mainly used to test the robustness of the modules. These tests are usually run by BuildBots. They cover areas like build tests, system tests, and performance tests.

5.3 Proposed ns-3 Module for OWC Networks

The proposed ns-3 module is implemented considering the network architecture proposed in the Chapter 4. Fig. 5.2 illustrates the centralised architecture and the locations of a few important classes. The core network is an IP network which interacts with the central office in the IP layer. The central office itself is modelled as the `OwcCoNetDevice` class. Inside the central office, as shown in Fig. 4.1, there are multiple VAPs. Each VAP will have multiple sectors and a control unit. Note that the Fig. 5.2 only shows a single VAP and a data sector due to space limitations.

MAC operations of the data sectors are governed by the `OwcCoDataMac` class whereas the `OwcCoCtrlMac` is used for the control sector. Physical layer is modelled by the `OwcPhy` class and is common for all the devices. Physical layer is connected to the `OwcChannel` class which models the communication medium. Propagation loss and error models are added to the channel to simulate transmission errors.

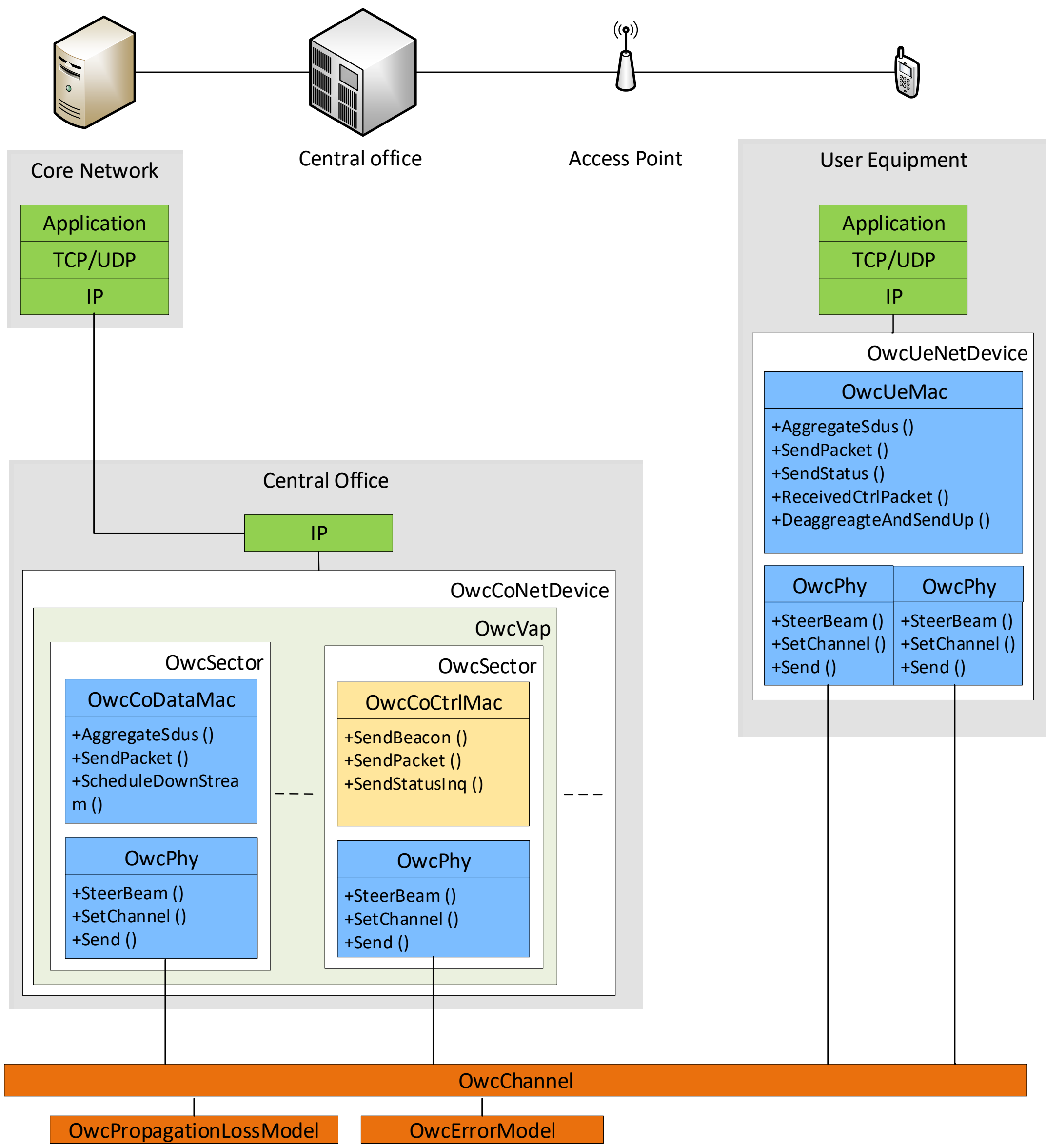

Figure 5.2: Network architecture of the ns-3 module.

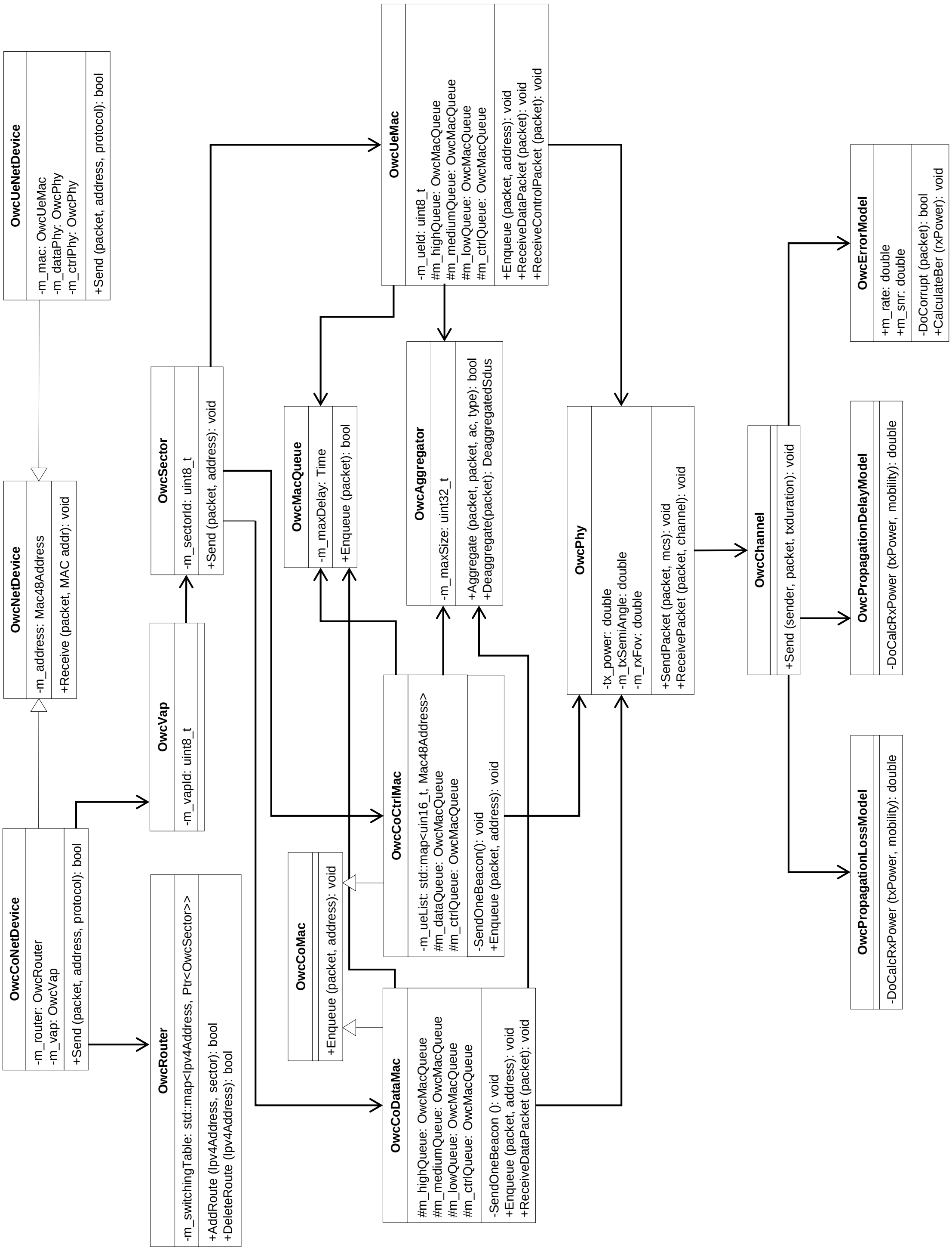

Figure 5.3: Class diagram of the ns-3 module.

On the other side, the user device uses the common physical layer class to connect to the channel. However, the MAC operations are modelled using the `OwcUeMac` class which has integrated the data and control plane operations together. Despite the integrated MAC, the control plane and data plane MAC operations run as parallel threads.

Fig. 5.3 shows the detailed class diagram of the proposed module with the relationships between classes. The complete module includes around 10,000 lines of C++ code. Further, it is worth noting that the proposed module is implemented in ns-3.29 version. Next subsections are dedicated to explaining the implementation of the key classes of the module.

5.3.1 Channel

The proposed module uses the `OwcChannel` class to model the propagation channel behaviour. The propagation channel comprises two mediums. The first section is the fibre between the central office and the AP. This section is modelled as a delay without considering the fibre impairments. Other fibre impairments does not influence the upper layer protocol performance. The second section is the wireless propagation between the AP and user.

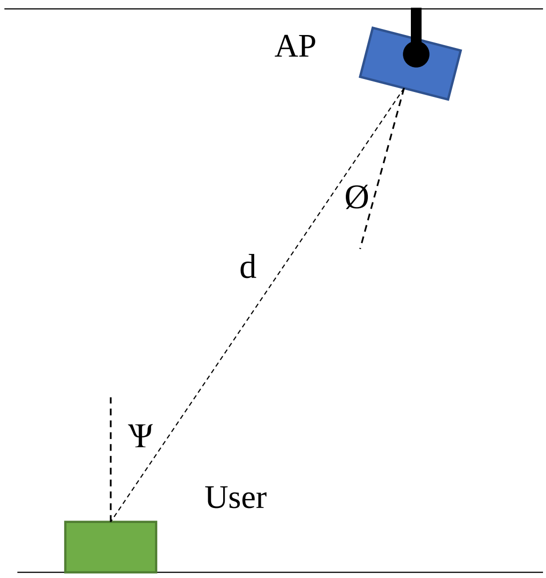

Figure 5.4: Transmitter and receiver geometry.

The wireless section of the channel works as an intensity modulated direct detection system. Since the OWC signals are real and positive, the received signal (P_r) can be expressed using the DC gain of the channel and the transmitted signal (P_t) as follows [125],

$$P_r = H(0)P_t \tag{5.1}$$

In this study we assume the channel to be a directed LOS channel and neglect the non-LOS components. Hence, the DC gain of the channel can be calculated using the generalised Lambertian intensity [47].

$$H(0) = \begin{cases} \frac{(m+1)A}{2\pi d^2} cos^m(\phi) cos(\psi) T_s(\psi) g(\psi), & 0 \leq \psi \leq \psi_c \\ 0, & \psi > \psi_c \end{cases} \tag{5.2}$$

where A is the area of the detector, d is the distance between the transmitter and receiver, ϕ is the angle of irradiance with respect to transmitter axis, ψ is the angle of incidence with respect to receiver axis, ψ_c is the receiver cut-off angle, $T_s(\psi)$ is the gain of the optical filter and $g(\psi)$ is the optical concentrator gain. m is the Lambertian order which is given by,

$$m = \frac{-ln(2)}{ln[cos(\phi_{1/2})]} \tag{5.3}$$

where $\phi_{1/2}$ is the transmitter semi-angle at half power. The gain of the concentrator can be calculated using the following expression [47],

$$g(\psi) = \begin{cases} \frac{n^2}{sin^2(\psi_c)}, & 0 \leq \psi \leq \psi_c \\ 0, & \psi > \psi_c \end{cases} \tag{5.4}$$

n is the internal refractive index.

The `OwcChannel` class uses the mobility objects of the transmitter and receiver to calculate the relevant distances and angles. Further, the `OwcChannel` has a few attributes such as `FiberDelay` to customise the channel parameters.

Table 5.1: Parameter values of the noise calculation.

Symbol	Parameter	Value
R	Photodetector responsivity	0.8 A/W
q	Charge of an electron	1.602×10^{-19} C
B	Bandwidth	10 GHz
I_B	Background current	5 mA
I_2	Noise bandwidth factor	0.562
k	Boltzman constant	1.380×10^{-23} $m^2kgs^{-2}K^{-1}$
T	Absolute temperature	300 K
η	Fixed capacitance of photodetector per unit area	112 pF
G	Open loop voltage gain	10
A	Photodetector area	0.001 m^2
Γ	FET channel noise factor	1.5
g_m	FET transconductance	30 mS
I_3	Noise bandwidth factor	0.0868

5.3.2 Error Model

Simulating the packet drops and errors are offloaded to the `OwcErrorModel` class. It will get the received optical power at the receiver, P_r, from the `OwcChannel` and calculate the SNR as follows,

$$SNR = \frac{(RP_r)^2}{\sigma_n^2} \tag{5.5}$$

R is the responsivity of the detector at the operating wavelength, σ_n^2 is the noise power of the receiver.

There are two main noise sources in OWC receivers. First one is the shot noise σ_{shot}^2 and the second is the thermal noise $\sigma_{thermal}^2$.

$$\sigma_{shot}^2 = 2qRP_rB + 2qI_BI_2B \tag{5.6}$$

$$\sigma_{thermal}^2 = \frac{8\pi TkC_{pd}AI_2B^2}{G_{ol}} + \frac{16\pi^2kTk\Gamma C_{pd}^2A^2I_3B^3}{g_m} \tag{5.7}$$

The parameters values used for the noise calculations are listed in the Table 5.1. We can calculate the bit error rate (BER) of the link using the SNR for the modulation scheme in use. For OOK modulated signals, the BER is calculated as follows [126],

$$BER_{OOK} = Q(\sqrt{SNR}) \tag{5.8}$$

The `CalculateSnr` and `CalculateBer` functions are used for these two calculations. Finally, the `DoCorrupt` function will calculate the packet-error-rate (PER) based on the packet length and BER as follows,

$$PER = 1 - (1 - BER)^{8 \times packet\ length} \tag{5.9}$$

The PER is compared with a random value to make the final decision. The random value is picked from a random variable distribution which can be set using the `RanVar` attribute.

5.3.3 Physical Layer

The physical layer is modelled using the `OwcPhy` class. This class captures the effects of modulation schemes, wavelength allocations, and other physical layer related behaviours. Two of the main functions of the `OwcPhy` class are the `SendPacket` and `ReceivePacket` functions. The `SendPacket` function receives a fully formed MAC frame from the MAC layer and pushes it down to the channel with a physical layer preamble. The physical layer preambles are largely used for receiver synchronisation. This function will calculate the transmission duration using the `CalculateTxDuration` function and bring the channel to `TXING` state to flag the channel is in the middle of a transmission. The `TXING` flag does not prevent other users from accessing the channel, but rather it would cause a collision trigger like in a real channel. A complete list of states is given in the Appendix A.

When the channel pushes a packet up to the `OwcPhy`, it is received by the `ReceivePacket` function, which will check whether it was received properly. Unlike in a real system, all packets are received at the receiver. The `ReceivePacket` will simulate packet drops with the help of the `OwcErrorModel` class. As shown earlier, the `OwcErrorModel` will get the packet length and based on the BER of the link, it will decide whether each packet is successfully received or not.

Moreover, the `OwcPhy` class has a range of functions to execute the beam-steering operation.

`OwcPhy` has two attributes that allow the users to tune its parameters. First one is the `ChannelNumber` which indicates the channel number assigned for the particular `OwcPhy` object. Depending on the wavelength used in the device, this attribute can be changed at the beginning or on-the-fly. Second attribute is the transmitter type; Gaussian or uniform. The Gaussian physical layer creates a Gaussian power distribution in the coverage area. These are the more common types of transmitters. On the other hand, uniform physical layer can establish a uniform power distribution throughout the coverage area. The uniform transmitters are still experimental devices.

Further, `OwcPhy` class provides four trace sources, `PhyTx`, `PhyTxDrop`, `PhyRx`, and `PhyRxDrop` to track the packet transmissions. While the names of the trace sources are quite self-explanatory, further explanations are given in the Appendix A.

5.3.4 Data Plane MAC Layer

The `OwcCoDataMac` class implements the MAC layer of the data plane in the central office side. The overall function of this class is to receive IP packets from the application layer, form MAC frames with/without aggregation, add MAC header and pass it to the physical layer. The reverse operation is carried out for incoming packets. Note that ns-3 do not implement the encryption stages solely to save simulation time.

There are a few trace sources and attributes that are used in this class. `MacRx`, `MacRxDrop`, `MacTx`, and `MacTxDrop` trace sources are implemented to track the packet transactions. Please refer to the Appendix A for detailed explanation. On the other hand, the `DPBI` attribute sets the beacon interval of the data plane. The beacons are sent periodically to establish service intervals, send grants, request buffer statuses, etc. By tuning this parameter, a user can change the beacon interval, which has a significant effect on the MAC layer performance. This aspect analysed in detail in Chapter 6.

The `OwcCoDataMac` class interfaces with the upper layers using the `Enqueue` function. The upper layer class that needs to send a packet will call the `Enqueue` function to add a packet to the queue of the `OwcCoDataMac` class. The `Enqueue` function has an in-built classifier which will read the TOS field of the IP packet and put it to the relevant queue. Note that there will be multiple packets queue to enable differentiated access.

Depending on the downlink scheduling algorithms, the MAC layer will decide the transmission of packets from the queues. The MAC layer will use the `DequeueAndAggregate` function to form aggregated packets for transmission. This function will get packets from the queues and form an aggregated packet, add the headers and pass it to the `SendDataPacket` function. The `SendDataPacket` will write the final header values such as packet size and sequence numbers and push it to the physical layer as a MAC frame.

`ReceiveDataPacket` function is used to handle the incoming packets from the users. This function will filter the data and control packets and direct them to relevant places. The data packets will be deaggregated and the individual packets will be pushed up in the stack while the control packets will be sent to relevant functions such as `UpdateUplinkQueueStat`.

A few more functions including `SendBeacon`, `SendGrant`, `ScheduleDownlinkTransmisssions` are explained in the Appendix A.

5.3.5 Control Plane MAC Layer

Control plane in the central office is implemented in `OwcCoCtrlMac` class. This class is responsible for sending the CP beacons, grants, status inquiries and association messages. Similar to the `OwcCoDataMac`, this class implements trace sources to track the packets. The `OwcCoCtrlMac` class has an attribute called `CPBI` to adjust the CP beacon interval. The default value of `CPBI` is set to 100 ms.

A notable difference from the `OwcCoDataMac` is that `OwcCoCtrlMac` only has two packet queues. One is used for the control messages while the other one is used for data packets if the data plane is not available temporarily. The packet transmission and reception functions are quite similar to those of the `OwcCoDataMac`.

There are a few control functions such as `SendAssociationResponse` and `SendStatusInquiry` to implement the overall control of the VAP. These are explained in the Appendix A.

5.3.6 User Device MAC Layer

The MAC layer of the user device is implemented in the `OwcUeMac` class. This MAC layer has the trace sources to track packets, which are similar to `OwcCoDataMac` and `OwcCoCtrlMac` classes.

The packet generation and reception are also quite similar to the earlier classes. One notable difference is that the `OwcUeMac` has both data and control plane functions included in the same MAC layer. However, it should be noted that the physical layers are separated and the execution is also decoupled. Therefore, essentially the two planes are operating independently.

5.4 Feature Demonstration

The proposed ns-3 module is used in all the simulations carried out in this thesis except in Chapter 3. In this section, we will demonstrate some of its features that were not elaborated in other chapters.

5.4.1 Beam-steering Operation

Beam steering is an important functionality for highly directional optical wireless transceivers serving mobile users. It is difficult to maintain the transmit power below eye safe levels (10 dBm [53])[1] and maintain a reasonable SNR at the mobile receivers without actively steering the beam.

We have demonstrated the beam-steering operation using a real-life scenario which is shown in Fig. 5.5a. There is a user who is connected to an AP, which is receiving 2 Gbps downstream data from the AP. The user walks from one end of a 10 m long room to the other end at a speed of 1 m/s. For this scenario, we have observed the throughput of the network with a fixed beam, a steered beam, and a steered beam with an error of $\pm 10°$. In this case we assume that the user has its precise location and periodically sends it to the VAP in the control channel. Then the VAP can execute the beam-steering algorithms to

[1] Approximate only. Exact value greatly depends on the type and parameters of the transmitter

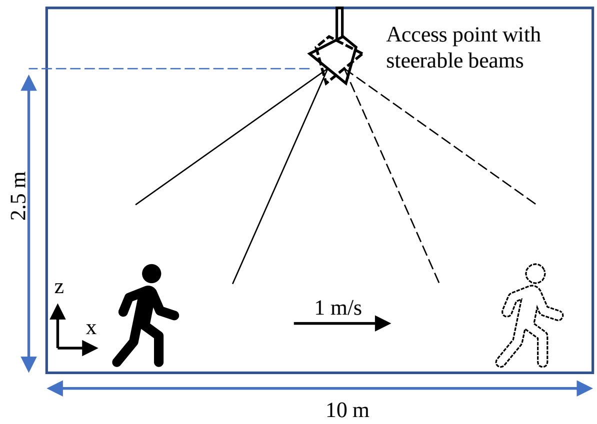

(a) Simulated scenario

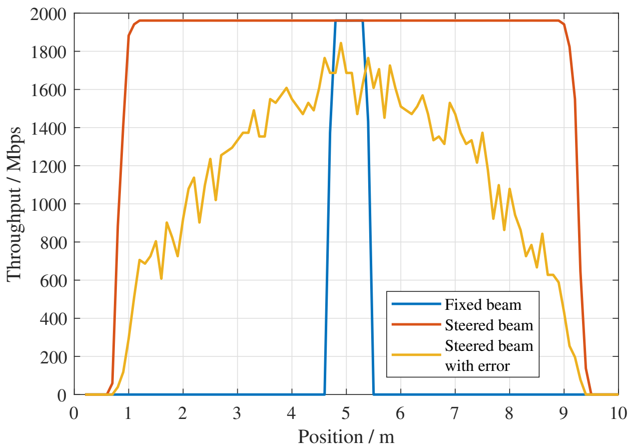

(b) Throughput

Figure 5.5: Variation of the network throughput with the mobile user with a fixed beam, a steered beam and a steered beam with random misalignment.

align the transceivers for maximum received power.

As it can be seen from the Fig. 5.5b the throughput of the link is highly limited if the beam is not steered towards the user. The fixed beam only reaches acceptable SNR to send packets at x=4.5 m and again drops after x=5.5 m. Therefore, the effective coverage is only 1 m in the linear path. On the contrary, the steered beam establishes the link at x=0.5 m. The user quickly reaches the full data rate and maintains it consistent until x=9.5 m. This case depicts the ideal beam-steering operation which could be difficult to achieve with the hardware imperfections. Finally, the yellow curve shows the throughput of the user with an erroneously steered beam. The beam steering error is uniformly distributed in [-10°, 10°] range. It can be seen that the misalignments have caused significant performance degradation in the system throughput.

Similarly, the proposed module can simulate other issues in beam-steering like mechanical overshoots, lags, offsets and misalignments in other axes. Such experiments are useful in designing robust beam-steering and user tracking algorithms.

5.4.2 Gaussian and Uniform Beams

Simulating the received power distribution of the coverage areas is a key component of any network simulator. With the comprehensive mobility models in ns-3, it is possible to implement various deployments with different layouts. In this subsection we will explain the process of building the coverage area shown below. We used this layout in the Subsection 4.4.3.

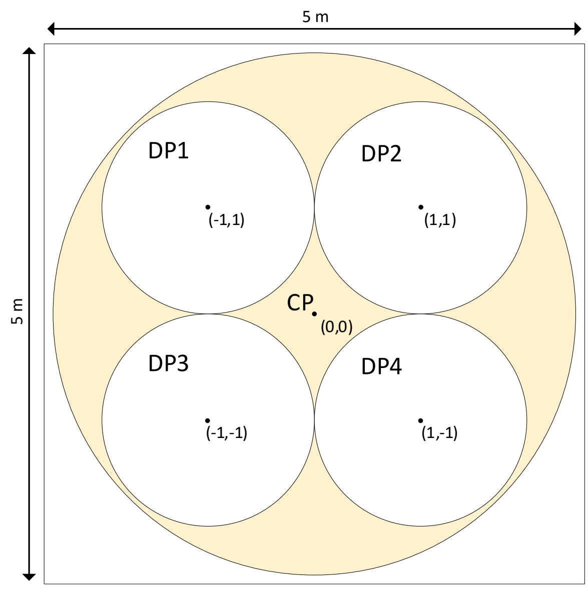

Figure 5.6: Layout of the coverage area.

Here we have a 5 $m \times 5$ m coverage area with a CP centred at the middle. Considering the middle point as (0, 0) of (x, y) coordinates, we have four DP beams located at (1, 1), (1, -1), (-1, 1), and (-1, -1).

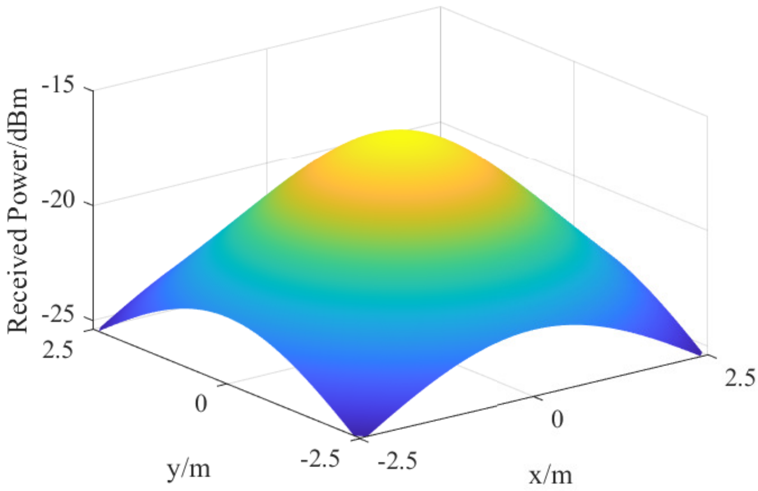

(a) Gaussian CP

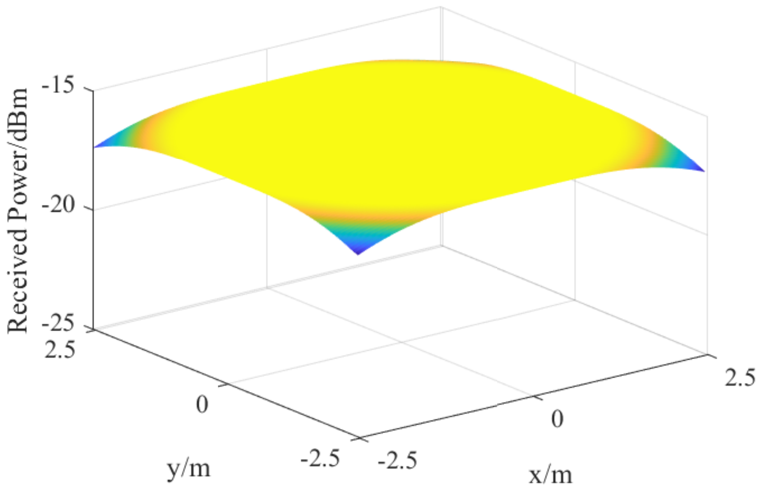

(b) Uniform CP

Figure 5.7: Received power distributions of the CP.

First, we will implement the CP in two different forms; Gaussian and uniform, which are shown in Fig. 5.7. The Gaussian CP has the peak power at the centre and drops drastically towards the cell edge. The power at the peak is around -16 dBm while the corners where the minimum power is recorded shows around -25 dBm. On the contrary, the uniform CP demonstrates a properly flat power distribution throughout the coverage area.

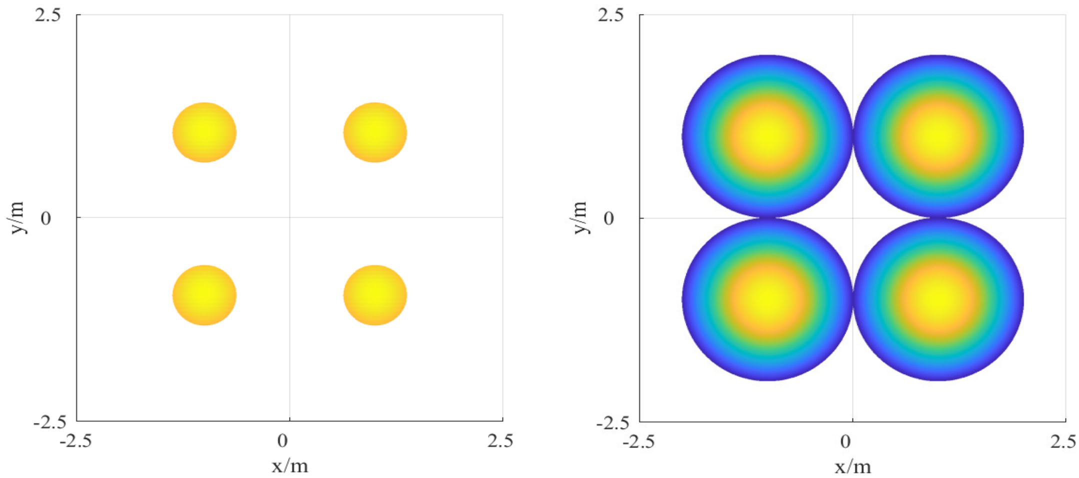

(a) Basic DP (b) Beam-steered DP

Figure 5.8: Received power distributions of the DP.

Next, we will show the implementation of the DP beams. DP beams are very narrow beams and do not cover a useful area in their basic form (without beam-steering). For instance, Fig. 5.8a shows the coverage of a basic DP beam. The transmitter semi-angle is 5°. It is necessary to maintain the transmitter emission power below eye safe level to comply with the safety standards. Hence, in order to improve the coverage area to a more practical range, we have enabled beam-steering to the DP beams. Fig. 5.8b depicts the power distribution with the beam-steered DP beams. The area of one beam was limited to a 1 m radius circle to avoid inter-DP interference. It is possible to increase the radius by allocating different wavelength to the four DP beams.

Finally, the Fig. 5.9 shows the combined power distributions of the DP and CP for Gaussian CP and uniform CP. As stated earlier, it is effortless to deploy networks with different number of beams and users. Further, one can combine the mobility models in ns-3 and simulate network performance under mobile users.

The proposed module can simulate two types of power distributions, Gaussian and uniform at the moment and it is fairly straightforward to add additional power distributions depending on the transmitter characteristics.

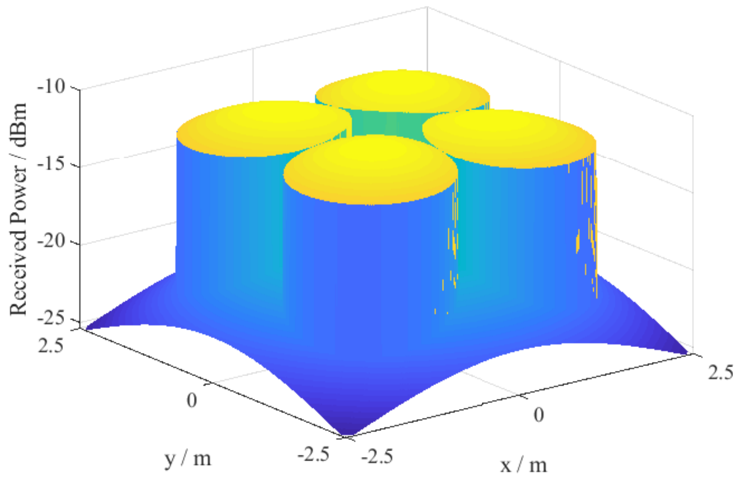

(a) Gaussian CP with Beam-steered DP

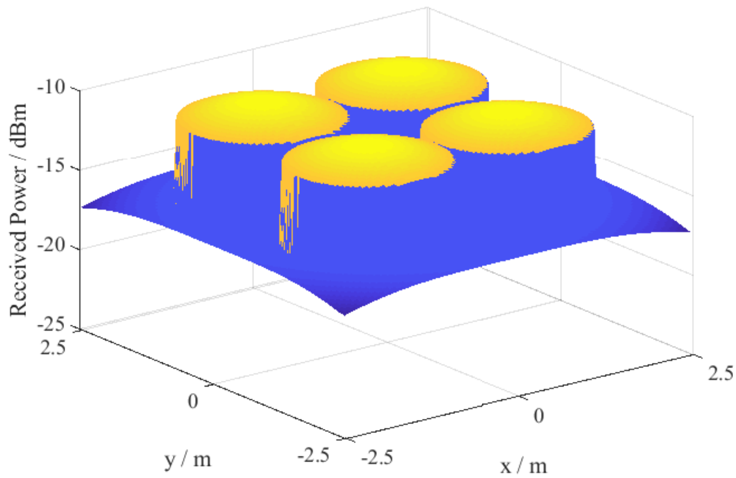

(b) Uniform CP with Beam-steered DP

Figure 5.9: Power distribution of the coverage area with Gaussian and uniform CP beams with beam-steered DP.

5.5 Conclusion

We have introduced our ns-3 module in detail in this chapter. Discrete-event simulators are vital for upcoming technologies to evaluate their performance individually and collectively with other technologies. For instance, the upcoming technologies need to evaluate their own protocols such as MAC protocols before hardware trails. However, more importantly, it is important to see how the upcoming technologies fit or behave in the existing networking ecosystem. This involves experimentation with network interfacing, loading balancing, interference management and many other aspects. Therefore, we have implemented our module in ns-3, which is a widely accepted and a module-rich environment that supports Wi-Fi, 4G LTE to 5G NR networks. In this chapter, we have detailed the implementation of the proposed module, the capabilities and limitation and potential future expansions of the proposed ns-3 OWC module.

Chapter 6

Contention-free MAC Protocol for OWC Networks

6.1 Introduction

THE medium access control protocols used in existing WLANs are predominately based on the CSMA/CA mechanism [78]. However, the CSMA/CA protocol drastically drops in efficiency with increasing traffic collisions. Therefore, under high data rate scenarios with bursty traffic arrivals, contention-based MAC protocols will not perform well. Hence, many RF counterparts of OWC such as IEEE 802.15.3 and IEEE 802.11ad have already adopted contention-free access periods in their MAC protocols [3,127]. Furthermore, existing MAC protocols have relatively small frame sizes due to low aggregation and small packet sizes [128]. However, at multi-gigabit data rates, the combined effect of low aggregation and small packet sizes can lead to high overheads and hence result in poor network efficiency [129].

Considering the drawbacks of contention-based MAC protocols, in this chapter, we propose a contention-free MAC protocol for OWC networks. When it comes to contention-free MAC protocols, one of the main concerns is the overhead caused by the bandwidth requests and grant messages [130]. The FLOWN architecture proposed in Chapter 4 has the capability to split the data plane and control plane into two channels. With this feature we overcome the inefficiencies caused by the control messages.

Further, the beacon interval of a contention-free MAC protocol plays a key role in the network performance as network delay is highly influenced by this parameter. Most existing WLANs have a fixed beacon interval. For example, Wi-Fi networks have a fixed beacon interval of 102.4 ms. One can only adjust it by logging into the Wi-Fi router. However, with the increasing amount of delay-sensitive traffic in the networks, it is necessary to use an adaptive beacon interval period to ensure that stringent delay requirements under varying traffic conditions can be met [131]. Therefore, we equip the proposed contention-free MAC protocol with an adaptive beacon interval mechanism to cater the diverse delay-sensitive applications.

Our contributions of this chapter can be listed as four main points.

- We introduce the superframe structure of the contention-free MAC protocol.
- We provide the data packet, beacon and header structures. Data packets and headers are designed to support high-level aggregation.
- We introduce an adaptive beacon interval mechanism to adjust the beacon interval of the MAC protocol to suit the traffic delay requirements.
- Finally, we introduce an exhaustive allocation method to serve the delay-sensitive traffic with guaranteed quality-of-service.

The rest of the chapter is organised as follows. The proposed MAC protocol is presented in Section 6.2, which is followed by the performance evaluation in Section 6.3. Section 6.4 provides the concluding remarks for the Chapter 6.

6.2 Proposed Contention-free MAC Protocol

The FLOWN architecture uses a separate control plane (CP) for the control and management messages in the network while the data plane (DP) is completely used for data transmission only, except for a few beam-training messages. The following subsections describe the structures of the superframe, data packets and headers designed for the proposed MAC protocol.

6.2.1 Superframe Structure

The superframe structure is illustrated in Fig. 6.1. The CP time consists of CP beacon intervals (CPBI) which are kept constant in length. The DP beacon intervals (DPBI) are always submultiples of CPBI. DPBI will be adaptively adjusted to suit the traffic delay requirements according to the proposed mechanism in Subsection 6.2.4. Furthermore, different DP sectors might use different DPBI values as show in Fig. 6.1 to cater the traffic requirements of the users associated with a particular sector. It is worth noting that CP beacons take longer time to transmit compared to DP beacons due to the lower order modulation format it uses.

In CP downlink operation, the CP will send the uplink grants to the users after waiting for an interframe spacing (IFS) delay from a CP beacon. The grants are calculated according to the buffer status messages received at the end of the last DPBI. Therefore, the grants are sent only to the users with non-zero buffer lengths. After sending the grant messages, the CP will open an association period where new users or any user who lost connection can request association to the network. This period is contention-based and could be extended if there are many users. Towards the end of the DPBI, the CP will send status inquiry messages to all the users. The status inquiry messages will also piggyback the acknowledgements for the uplink frames. The users will respond to the status inquiry with their buffer status and piggyback the acknowledgements for the downlink frames.

In the DP downlink, the AP will send the user frames according to the throughput and delay requirements of the users. It is worth noting that users who just joined the network will need a beam training period with the DP downlink in order to train the infrared beams. The AP can schedule this whenever the DP downlink is free without affecting the downlink performance.

The uplink transmission of the DP is completely managed by grant messages. The users follow the uplink schedule without contending for the channel access. For example, in sector 1 shown in Fig. 6.1, only user 1, and 2 have downlink data during first DPBI, whereas, user 1, 2, and 4 have uplink data in the same beacon interval.

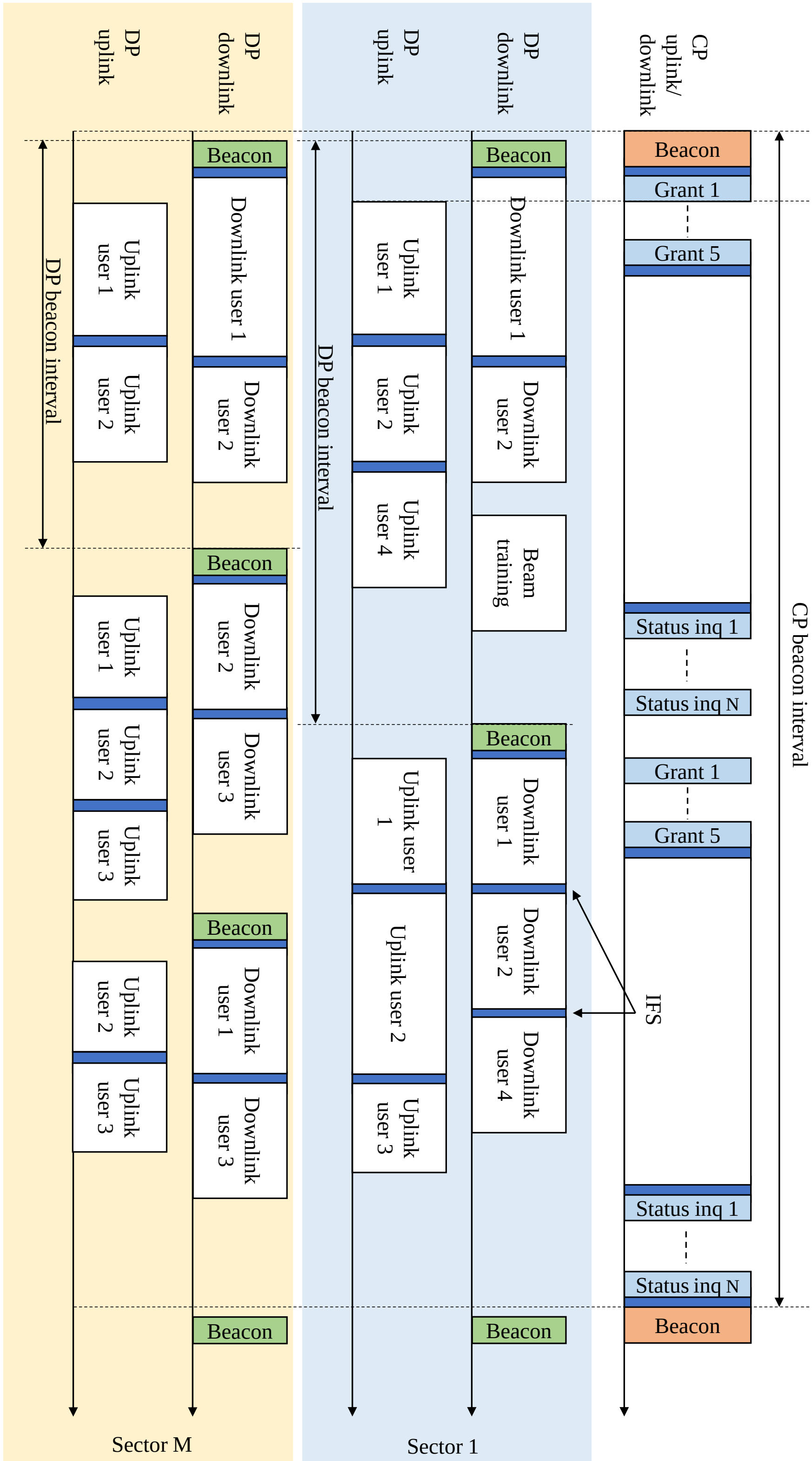

Figure 6.1: Superframe structure of the proposed contention-free MAC protocol.

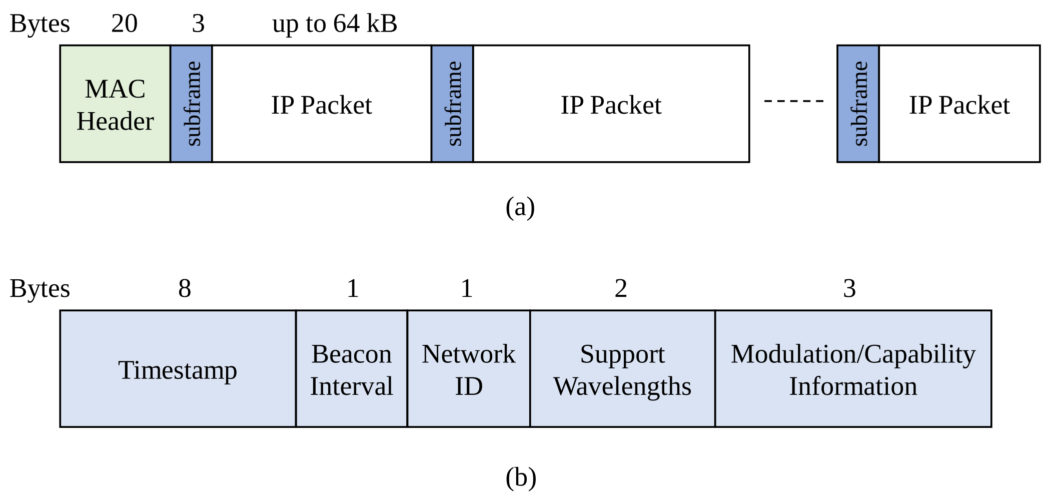

Figure 6.2: (a) Data packet structure (b) Beacon structure

6.2.2 Packet Structures

A typical WLAN will accept IP packets from the distribution network and form MAC frames with or without aggregation. Considering the high data rates, the proposed MAC protocol has aggregation turned on by default, effectively increasing the data rate. However, care must be taken in the scheduling algorithms to avoid unnecessary delays in waiting for packets for aggregation.

As shown in the Fig. 6.2a, a typical data packet is comprised a MAC header and several data packets (IP packets), separated by subframe headers. As stated earlier, the proposed headers support full-size IP packets up to 64 kB. The aggregated frame length can be as large as 16 MB. Maximum aggregation allowed in the existing WLANs is 4 MB. Nevertheless, the upper limit is always set by the channel conditions and delay tolerances. It is worth noting that some packets will be padded with zeros to memory align, which makes the packet processing faster.

The beacon structure shown in Fig. 6.2b depicts the fields found in a beacon frame. Both CP and DP use the same beacon frame. The timestamp field carries time-of-origin of the particular beacon frame. Timestamps are useful in synchronisation. The beacon interval field is used to extract the current DPBI duration. The network ID will be used by the CP to advertise the network, while the DP uses it to announce the channel number.

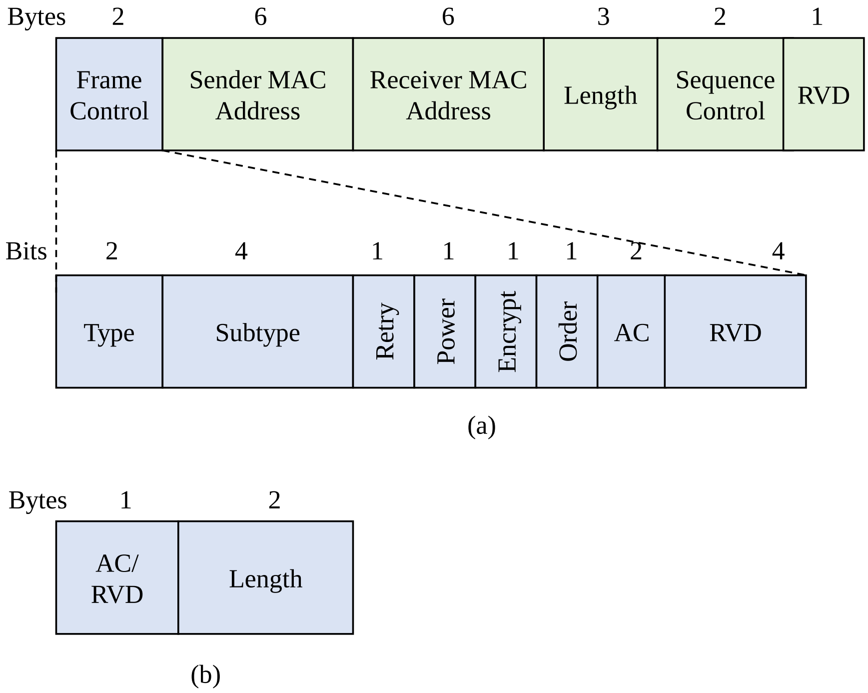

Figure 6.3: (a) MAC header (b) Subframe header.

Supported wavelength, modulation and capability info fields are used to advertise the wavelength, modulation, and beamforming/data rate capabilities, respectively. In addition, these fields can be used in the future for transmitting other network information as well.

6.2.3 Headers

The MAC header of the proposed protocol is 20 bytes long. As shown in Fig. 6.3a, it comprises the sender and receiver MAC addresses and a 16-bit wide sequence control field. The 24-bit long length field allows aggregated lengths up to 16 MB which are not used in present WLANs. There is a reserved byte at the end of the header which can be used in the future. The frame control field is explained in Table 6.1, which includes several bits to convey different network information.

The subframe headers depicted in Fig. 6.3b are used in aggregated frames to separate the IP packets. The first two bits of the subframe header contains the access category

Table 6.1: Frame control field of the MAC header

Field	Usage
Type	00 - data 01 - control 10 - management 11 - reserved
Subtype	0000 - single data frame 0001 - aggregated data frame 0010 - beacon frame 0011 - grant message 0100 - status inquiry 0101 - beam training request 0110 - beam training frame
Retry	Retransmitted frame
Power	Power saving mode
Encrypt	Encrypted frame
Order	Order to be preserved
AC (Access category)	00 - control/management 01 - low 10 - medium 11 - high
RVD	Reserved

information while the rest of the byte is reserved. The last two bytes are used to convey the length of the packet which can be up to 64 kB.

6.2.4 Adaptive Beacon Interval Mechanism

The DP beacon interval of a contention-free MAC protocol significantly affects the delay performance of the entire network. A fixed DPBI is not suitable for a delay-sensitive high data rate network like optical wireless for several reasons. When the DPBI is fixed, MAC protocol will not improve the delay performance of the network even if there is a possibility to do so. However, fixing a very small DPBI to the entire network will unnecessarily increase the transmissions in the CP, resulting in smaller aggregated packets and will cause high power consumption in both AP and users.

On the other hand, DPBI affects the buffer utilisation of the users. In a multi-gigabit network, it is crucial to maintain the DPBI such that user buffers do not overflow due to the enormous traffic load. Therefore, it is essential to have a mechanism to adjust the DPBI according to the traffic requirements of the network. Therefore, we proposed an adaptive beacon interval mechanism.

DPBI duration can be calculated by considering the scheduled transmissions in the network. The users are expected to keep the AP up to date on the data rate and maximum delay tolerance of their applications. Therefore, the following information is expected to be readily available at the AP.

Maximum user data rates,

$$\{S_{max,u1}, S_{max,u2}, ..., S_{max,uN}\}$$

Maximum delay tolerances,

$$\{D_{max,u1}, D_{max,u2}, ..., D_{max,uN}\}$$

Traffic specification messages such as TSPEC messages used in IEEE 802.11e can be used to communicate this information to the AP.

The scheduling MAC results in an average delay of the DPBI duration. Hence the DPBI duration, T_{DPBI}, can be selected as follows,

$$T_{DPBI} = min\{D_{max,u1}, D_{max,u2}, ..., D_{max,uN}\} \tag{6.1}$$

However, T_{DPBI} must be within the acceptable range which is defined by factors such as minimum packet sizes.

$$T_{DPBI,min} \ll T_{DPBI} \ll T_{DPBI,max} \tag{6.2}$$

Based on the selected DPBI duration, the scheduling MAC will consider the requested data rate and calculate the maximum channel bandwidth allocation, $Alloc_{max,k}$, for the k^{th} user. The instantaneous channel bandwidth could be different since it is calculated every DPBI using instantaneous buffer sizes.

$$Alloc_{max,k} = \frac{S_{max,k}}{\sum_{i=1}^{N} S_{max,i}}[T_{DPBI} - (N-1)IFS - O] \tag{6.3}$$

where IFS stands for the inter-frame spacing which is 32 ns, O is the overhead caused by everything else such as the beacon message itself, and N is the number of active users.

Buffers of the users are used to store the packets until they are clear to transmit the packets. Longer DPBIs cause the users to store many packets while shorter DPBIs can drastically reduce the memory requirements for buffers. We can estimate the buffer utilisation of the k^{th} user, Buf_k, as follows,

$$Buf_k = S_{max,k} \times T_{DPBI} \tag{6.4}$$

There should be lower and upper limits for T_{DPBI} to avoid undesirable operation in the network. Lower limit of T_{DPBI} can be derived considering the minimum duration needed to transmit at least one packet plus the overhead.

$$T_{DPBI,min} = N \times \frac{max\ IP\ packet}{R} + (N-1)IFS + O \tag{6.5}$$

where R is the physical layer data rate and maximum IP packet size is typically 1500 bytes. Upper limit of T_{DPBI} is not as strict as the lower limit. If the users can tolerate the delay, it is possible to allow for a longer DPBI. However, practically, a longer T_{DPBI} is going to need larger buffer sizes. Therefore, it is useful to use Eq. 6.4 to determine the maximum buffer size and set the upper limit for T_{DPBI}.

6.2.5 Exhaustive Allocation for Delay Sensitive Applications

Users that have strict delay requirements are scheduled with exhaustive allocations such that all the packets received in a DPBI will be transmitted in the same DPBI. The exhaustive allocation size is determined by the maximum throughput specification sent by the user. Otherwise the normal allocations will only allocate the requested number of bytes to be transmitted in the DPBI. However, there will be packets arriving between the time the request was received and the actual transmission. These packets will not be included in the next transmission for normal allocations and this will result in higher delays. Therefore, as mentioned above, we proposed to use exhaustive allocation for delay sensitive application.

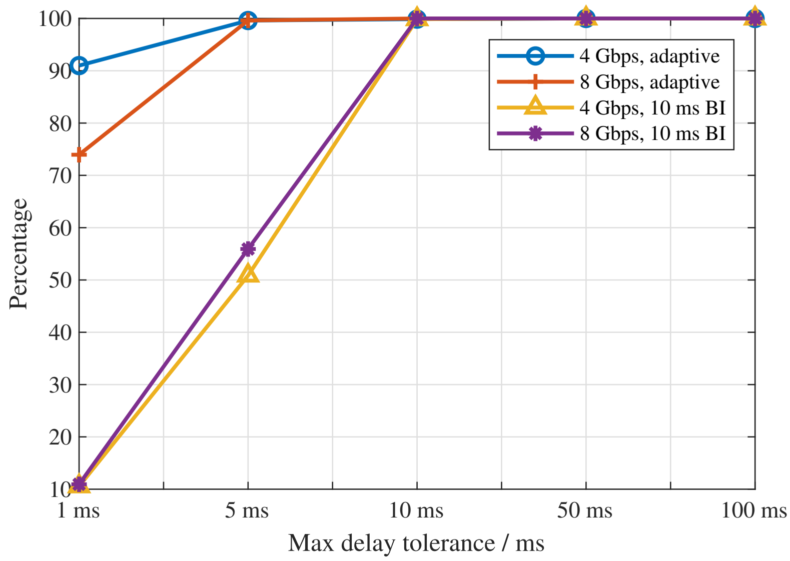

Figure 6.4: Percentage of packets that meet the delay tolerances for fixed DPBI and adaptive DPBI.

Exhaustive allocations inevitably cause low channel utilisations due to unused bandwidth. Nonetheless, a network will have comparatively small number of exhaustive allocations and with accurate maximum throughput specifications, the channel utilisation can be improved.

6.3 Performance Evaluation

We have two simulation scenarios to evaluate the performance of the proposed MAC protocol. Firstly, we present the performance evaluation of the adaptive DPBI mechanism. Secondly, we present the results of the exhaustive allocations with a mix of normal and delay-sensitive (DS) users. All the simulations were performed in ns-3 simulation platform. The presented results were averaged over three random number seeds except for the histograms, which are snapshots of one simulation run.

6.3.1 Adaptive DPBI Mechanism

In this simulation scenario we simulate two cases where we have 5 users transmitting 4 Gbps and 8 Gbps of Poisson distributed traffic in the uplink. Fig. 6.4 shows the percentage of traffic that meets their delay tolerances with adaptive DPBI and fixed DPBI. As shown, the adaptive DPBI outperforms fixed DPBI in all the scenarios we have considered. It can be seen that when adaptive DPBI is used, 100% of the traffic meet their delay tolerances except for 1 ms delay tolerance case. This can be improved by setting a DPBI below 1 ms. However, below 1 ms DPBIs are not considered in this work since the traffic dynamics are different at below 1 ms. For instance, buffers always have comparatively small number of packets. Hence, one aggregated packet can exhaust a whole buffer whereas for above 1 ms scenarios, there will be multiple transmissions inside an allocation.

In contrast, the fixed DPBI will quickly drop in delay performance when the max delay tolerance is smaller than the fixed DPBI. In this case the fixed DPBI is set to 10 ms. Only 10% of the packets achieve a delay less than 1 ms when the DPBI is fixed.

6.3.2 Exhaustive Allocations

For this simulation scenario we have considered two delay-sensitive users requiring exhaustive allocations and three normal users. The offered load is split between delay-sensitive and normal as 40% and 60%, respectively. Figure 6.5 shows the simulation results of the considered scenario.

Fig. 6.5a shows that the throughput of the network is fairly independent of the DPBI of the network. A smaller DPBI would require the users to send small amounts of data more often, while a larger DPBI would require the users to send comparatively large amount of data every once in a while. However, the throughput is calculated for fixed time intervals such as 1 second, therefore, the average throughput stays the same regardless of the DPBI. It is worth noting that the network was only offered up to 9 Gbps to prevent overloading.

On the contrary, the delay of the network, shown in Fig. 6.5b, increases with both offered load and DPBI. Normal traffic experiences a significant increment in the delay with increasing offered load from 0.27 ms for the $DPBI = 1\ ms$ to 20 ms when the the DPBI is 100 ms. On average the increment is around 40% for the normal traffic. On the other hand, the delay-sensitive traffic increases only 0.15 ms for the $DPBI = 1\ ms$ case and 5.7 ms for the $DPBI = 100\ ms$ case, averaging an increment of only 22%. Similarly, the traffic delay increases with the increasing DPBI due to the larger service interval. However, the delay-sensitive traffic stays well below the normal traffic because of the exhaustive allocations.

Buffer utilisation is an important aspect that is not sufficiently explored in the context of multi-gigabit WLANs. The average buffer utilisation is heavily dependent on the DPBI and the offered load as shown in Fig. 6.5c. The buffer requirements significantly increase with the DPBI due to the high accumulation of packets in the buffers. Similarly, increasing offered load require larger buffers to store the packets until transmitted. Combined with large DPBI, a user could require a buffer as large as 30 MB at the highest loading. On the other hand, delay-sensitive traffic require less buffer space compared to normal traffic since the delay-sensitive buffers are cleared quickly.

Histograms of the packet delay are shown in the next two figures to give better insights to the behaviour of the exhaustive allocations. Fig. 6.6a and Fig. 6.6b show the effect of increasing the offered load for $DPBI = 5\ ms$ and $DPBI = 50\ ms$, respectively. As it can be seen, delay-sensitive packets always meet their delay requirements, except for high data rates cases in $DPBI = 5\ ms$. However, the percentage is less than 1%, even though it is exaggerated in the log scale. The spike near the origin represents a significant portion of the delay-sensitive traffic. Therefore, the average delay for the 5 ms case varies from 1.7 ms to 2.2 ms and for the 50 ms case, it varies from 16.7 ms to 19.5 ms.

By contrast, the normal traffic consistently increases the delay with increasing offered load. Majority of the packets tend to be in the middle of the distribution. Therefore, only around 65%-76% of the normal traffic packets fall below the delay tolerance. This results in the average delay ranges of 2.9 ms - 4.2 ms and 28.3 ms - 38.4 ms for the 5 ms and 50 ms cases, respectively.

The presented results highlight the importance of the versatility of the MAC protocol used in upcoming multi-gigabit WLANs. The proposed MAC protocol with exhaustive allocations demonstrated highly favourable capabilities to serve the upcoming high data rate and delay-sensitive user applications.

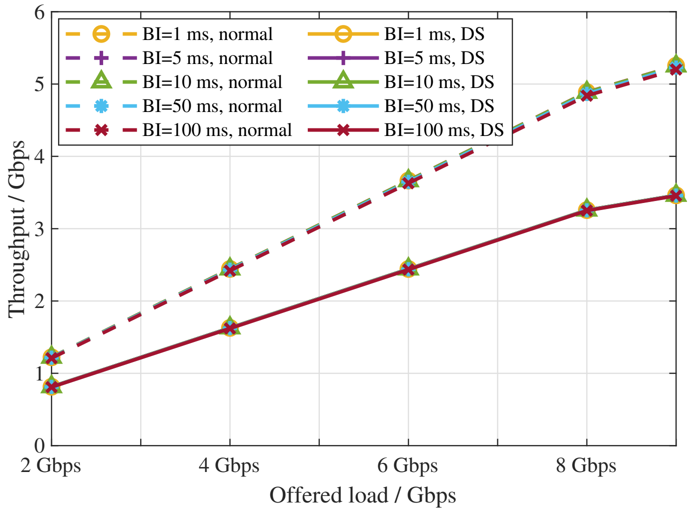

(a)

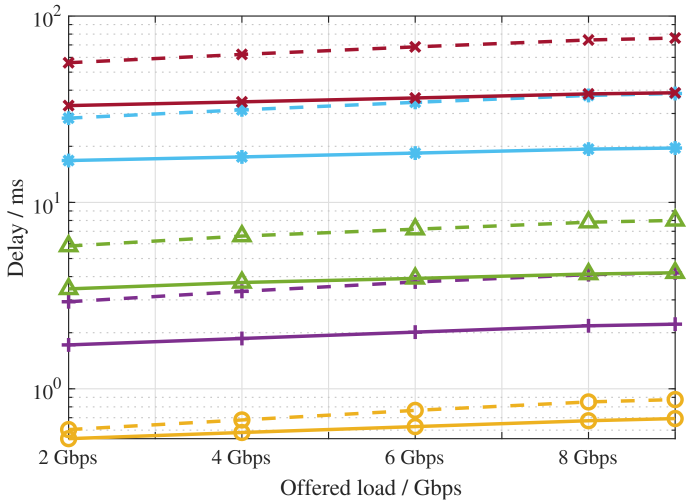

(b)

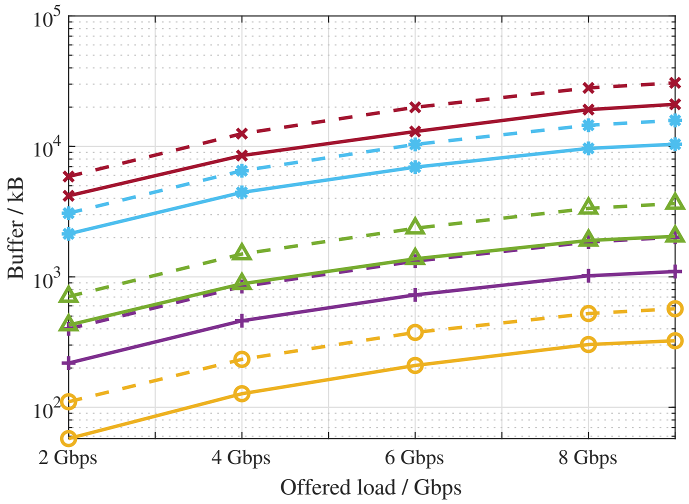

(c)

Figure 6.5: (a) Throughput, (b) delay, and (c) buffer utilisation of the normal and delay-sensitive users with increasing load.

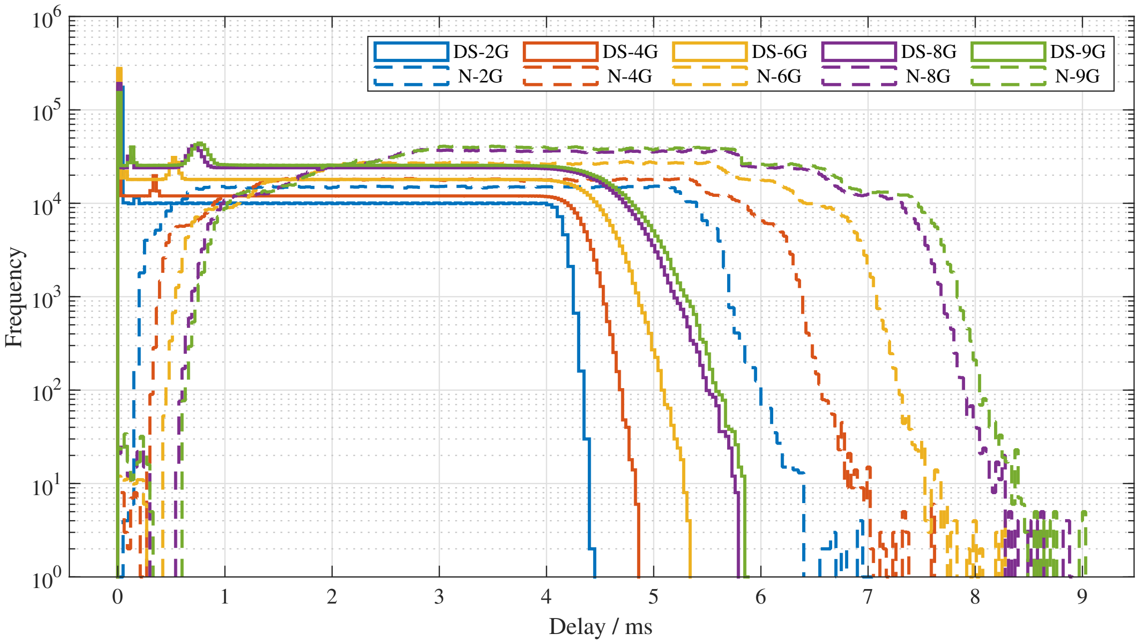

(a)

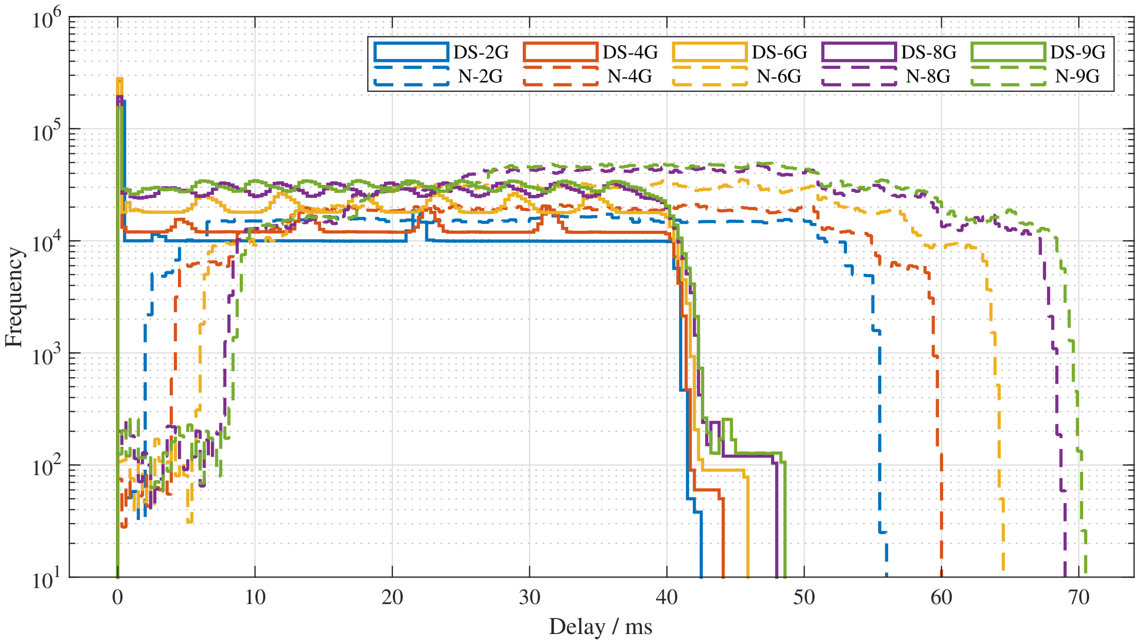

(b)

Figure 6.6: Packet delay histograms of the delay-sensitive and normal traffic for (a) 5 ms DPBI and (b) 50 ms DPBI cases for different network loads.

6.4 Conclusion

Optical wireless communication can offer data transmission at multi-gigabit data rates to the WLAN domain. So far WLANs operated in contention-based MAC protocols providing "best-effort" service. However, we have shown that the contention-based MAC protocols degrade in performance with increasing load at multi-gigabit data rates. Therefore, it is vital to explore and study contention-free MAC protocols for the upcoming multi-gigabit WLANs. In this chapter, we have presented the design of a contention-free MAC protocol for optical wireless communication which has versatile features such as adaptive beacon intervals and exhaustive allocations to meet the upcoming stringent traffic demands.

Chapter 7

Conclusions and Future Directions

7.1 Conclusions

This thesis studied the challenges in the upper layer operation of optical wireless communication networks. With the physical layer research progressing fast, the upper layer network protocols and architectures need to be examined to utilise the full potential of the physical layer. The existing network protocols such as CSMA/CA do not meet the performance requirements of multi-gigabit WLANs. Similarly, the overall network architecture needs to be redesigned such that the users can experience the performance improvements in end-to-end connections.

To that end, we first evaluated the widely used Wi-Fi contention-based MAC protocol in a multi-gigabit OWC network. We modified the Wi-Fi module of the ns-3 simulator for this study. These simulations demonstrated that at multi-gigabit data rates, the contention-based MAC protocols becomes prohibitively inefficient due to packet collisions. Therefore, we proposed a dynamic contention window tuning mechanism to alleviate the performance degradation caused by packet collisions. Further, the service differentiation of Wi-Fi MAC protocol is not suitable for the upcoming traffic types like virtual reality. Hence, we introduced a new service differentiation mechanism that can ensure the priority of the upcoming traffic types. The improved contention-based MAC protocol was evaluated with increasing traffic load and a dynamic scenario where users join and leave the network randomly. The results show that the improved version is more resilient to packet collisions and sudden changes in traffic load.

Secondly, we have introduced a novel network architecture that can support all the upcoming multi-gigabit WLANs in homogeneous and heterogeneous deployments. The proposed architecture has a central office where all the software and hardware resources are housed. The centralisation makes the resource allocation, management and upgrades of the overall network flexible. The access points in the coverage areas are connected to the central office via a fibre network conceivably avoiding any capacity bottlenecks in the distribution network. The access points have minimum processing power since the majority of the processing functions are carried out in the virtual access points inside the central office. The virtual access points are equipped with advanced functionalities like full-duplex and split-plane operation which make them suitable for the upcoming advanced WLANs. We have demonstrated the performance of gain of the full-duplex operation by comparing a full-duplex OWC network and a Wi-Fi network. In addition to the plain capacity improvement, we have shown that the uplink downlink symmetrical performance is achieved under full-duplex operation. Finally, we have demonstrated the split-plane operation with the control plane being used as a secondary channel for data transmissions. We have showed that depending on the mobility of the users, they can gain around 100 Mbps to 200 Mbps by using the control plane as a secondary channel.

Thirdly, we have implemented a simulation module for OWC in ns-3. Most of the network layer research is carried out in standard simulators such as ns-3, OMNeT++ and NetSim. These simulators already include widely used routing and network protocols such as TCP and UDP. Therefore, the simulations are quite close to real-life implementations. On the other hand, it is easy to verify/extend/contribute to a piece of research when it is done in a standard simulator. We realised that there is a lack of simulation modules for OWC in standard simulators. The proposed module can implement different network deployments, channel models, physical layer components and upper layer protocols. It was used in all the simulation studies of this thesis except Chapter 3. In addition to that, we have demonstrated some of the other capabilities like beam-steering and transmitter types in Chapter 5 that were not covered in the other chapters.

Finally, we have introduced a contention-free MAC protocol for OWC networks as the contention-based networks cannot fully utilise the channel resources due to the inevitable collisions and waiting periods. The proposed MAC protocol was designed from the ground up to be flexible and efficient. It features an adaptive service interval that can be tuned to the delay requirements of the current users. We have provided the closed-form solutions to calculate the service interval depending on the delay requirements. Further, we have introduced an exhaustive allocation mechanism that allows the delay-sensitive users to exhaust their queues in every service interval. With these two mechanisms, the contention-free MAC protocol can ensure high level of quality-of-service for upcoming user applications. Moreover, the novel packet structures of the proposed MAC protocol are designed to support aggregated packets as large as 16 MB to reduce the overhead. We define a universal MAC header to reduce the packet processing delay in the hardware level. Therefore, the proposed MAC protocol attempt to improve the performance of the network in both operational and implementation levels.

7.2 Future Directions

Generalised Split-plane Architectures for Heterogeneous WLAN

With the WLANs becoming heterogeneous networks, it is beneficial to have split-plane support in each WLAN technology such that the network architectures like FLOWN or Inter-MAC can offer their full potential. It would require studying the IEEE 802.11 and visible light communication standards to determine how to split the data and control planes, simulate the split-plane operation of these standards to evaluate the performance and eventually implement it in hardware. Once the implementations achieve desired performance, it can be integrated in the standards.

Hybrid MAC Protocol

We have proposed contention-based and contention-free MAC protocols for OWC networks. Depending on the requirements of the user applications, it would be efficient to select the type of MAC protocol that needs to be used. For instance, a non-priority IoT device might not need to be served in a contention-free scheduled manner. Therefore, it would be worthwhile designing a hybrid MAC protocol by combining the contention-based and contention-free MAC protocols such that the channel resources are intelligently divided between the two access modes and also considering the QoS requirement of the end users.

Improvements to the ns-3 Module

The proposed ns-3 module provides a comprehensive simulation platform to analyse the operation and performance of OWC networks. However, the proposed ns-3 module can be further improved to include additional simulation environments to support broader research community beyond OWC. For example, multiple channel models can be added and with minor modifications, it is possible to add visible light communication channel models as well. In the physical layer it is possible to add more devices such as different types of laser diodes, photodiodes, lenses, and filters. Furthermore, the parameters of the devices can be made adjustable for the ease of investigations. In addition to that, the ns-3 module can be extended to support underwater OWC systems by adding underwater propagation channel models and transceiver models.

The list of upper layer protocols implemented in the module can be further extended to other candidate protocols. For example, address resolution protocol (ARP) can be implemented which is not included in the current version of proposed ns-3 module.

Capacity Analysis and Load Balancing Heterogeneous WLANs

The WLANs ecosystem has been dominated by Wi-Fi for over 20 years now. There has not been much research that study WLANs in heterogeneous settings, except for some work in visible light communication [101]. Therefore, our understanding of the capabilities and challenges of heterogeneous WLANs are very limited.

For instance, with the increasing virtualisation of the networking resources, it would be worthwhile to develop consolidated physical layers which have RF and optical transceivers. It will allow the upper layers to efficiently allocate suitable physical layer resources based on the traffic requirements. Such architectures need to be studied further in order to understand the capacity that they can provide for diverse users.

Horizontal and Vertical Handover

The OWC networks are going to deploy a large number of small cells in a heterogeneous network environment giving rise to frequent handovers between OWC networks (horizontal handover) as well as other networks (vertical handover). With the OWC links operating at high data rates, it is necessary to implement handover algorithms that are fast and smooth to avoid link quality degradation. Similarly, when the wireless link is handed over to another network, it is necessary to make sure the candidate network is capable of handling the data flow. Therefore, the handover issues will need an overall examination and needs to be incorporated into the network architecture.

Appendix A
ns-3 Classes

A.1 OwcAggregator

The `OwcAggregator` class is used to aggregate IP packets into a MAC frame. The aggregator will add subframe headers in between the IP packets. The aggregated frame will be padded at the end for memory aligning. The main functions of this class are `Aggregate` and `Deaggregate`, which are self-explanatory. The full form of the functions are as follows.

```
bool
OwcAggregator::Aggregate (Ptr<const Packet> packet, Ptr<Packet>
aggregatedPacket, uint16_t ac, uint8_t aggType) const
```

```
OwcAggregator::DeaggregatedSdus
OwcAggregator::Deaggregate (Ptr<Packet> aggregatedPacket)
```

A.2 OwcCoCtrlMac

The `OwcCoCtrlMac` class was explained in Subsection 5.3.5. Here we have listed a few additional functions and their tasks.

Sends the CP beacon at the beginning of every CP beacon interval.

```
void OwcCoCtrlMac::SendOneBeacon ()
```

Sends the uplink grants immediately after the CP beacon.

```
void
OwcCoCtrlMac::SendGrant(Mac48Address to, uint32_t bytes, Time
start)
```

Sends queue (buffer) status inquiries towards the end of each beacon interval.

```
void OwcCoCtrlMac::SendStatusInquiry (Mac48Address to)
```

Responds to users who requested to associates to the AP.

```
void
OwcCoCtrlMac::SendAssociationResponse (Mac48Address to, uint8_t
sectorId)
```

A.3 `OwcCoDataMac`

Similarly, a few additional classes from the `OwcCoDataMac` class.
Sends the DP beacon at the beginning of every DP beacon interval.

```
void OwcCoDataMac::SendOneBeacon ()
```

Schedules the downlink transmission depending on the queue statuses and traffic priorities.

```
void OwcCoDataMac::ScheduleDownlinkTransmisssions (void)
```

A.4 OwcCoMac

Base class for `OwcCoDataMac` and `OwcCoCtrlMac` classes. The `Enqueue` function is declared in this class as a virtual function.
Trace sources of all the MAC classes have the same names. Their functionality is also the same. Therefore, they are listed here in the base class. Please refer to the source code to find the minor differences.

```
MacTx - Packet transmitted successfully from the MAC layer
MacTxDrop - Packet dropped while attempting to transmit, ex:
physical layer busy, scheduling clashes
MacRx - Packet received successfully at the MAC layer
MacRxDrop - Packet dropped while attempting to receive, ex:
corrupted headers
```

A.5 OwcNetDevice

The `OwcNetDevice` class is a base class used for deriving `OwcUeNetDevice` and `OwcCoNetDevice` classes. The `NetDevice` classes are used to model the network interface cards (NIC) in real systems. `NetDevice` classes interact with packet sources and sinks such as web browsers.
The base class implements the `Receive` function which is used to register the callback for receiving packets.

```
void OwcNetDevice::Receive (Ptr<Packet> p, Mac48Address from)
```

Derived classes individually implement their own `Send` functions to send packets. The `OwcUeNetDevice` will directly call its MAC object to enqueue the packets while the

`OwcCoNetDevice` will send the packets to the `OwcRouter` for forwarding to the relevant sector.

```
bool
OwcUeNetDevice::Send (Ptr<Packet> packet, const Address& dest,
uint16_t protocolNumber)
```

```
bool
OwcCoNetDevice::Send (Ptr<Packet> packet, const Address& dest,
uint16_t protocolNumber)
```

A.6 OwcMacHeader

The MAC header is defined in the `OwcMacHeader` class. Structure of the MAC header is shown in Fig. 6.2 and explained in Subsection 6.2.3. The functions inside the `OwcMacHeader` class are mostly Getters and Setters used to retrieve and set header fields.
Following enumerated types (enums) are used inside the source code to denote different packet types.

```
enum OwcMacType
{
OWC_MAC_DATA,
OWC_MAC_MGMT,
OWC_MAC_CTL,
};
```

```
enum OwcMacSubType
{
OWC_MAC_DATA_ONE,
```

```
OWC_MAC_DATA_AGG,
OWC_MAC_DATA_AGG_MULTI,

OWC_MAC_MGMT_DP_BEACON,
OWC_MAC_MGMT_CP_BEACON,
OWC_MAC_MGMT_ASSOCIATION_REQ,
OWC_MAC_MGMT_ASSOCIATION_RES,
OWC_MAC_MGMT_DISASSOCIATION,

OWC_MAC_CTL_ACK,
OWC_MAC_CTL_BEAMFORM_REQ,
OWC_MAC_CTL_BEAMFORM_RES,
OWC_MAC_CTL_GRANT,
OWC_MAC_CTL_INQ,
OWC_MAC_CTL_STAT,
};
```

A.7 OwcChannel

The theoretical aspects of the channel are explained in detail in the Subsection 5.3.1. Among the many functions inside the `OwcChannel`, the `Send` function is interesting and worth explaining.

```
void
OwcChannel::Send (Ptr<OwcPhy> sender, Ptr<const Packet> packet,
double txPower,Time duration, uint8_t chn) const
```

This particular function is called by the `OwcPhy` object. As it can be seen from the function description, it receives the transmit power, duration and channel number (chn). The operation of the `Send` function is as follows.

1. First it will take the list of users who are connected to the channel `chn`.
2. Then it will consult the propagation loss model to calculate the received power at the receiving end for each user.
3. Finally, it will schedule the `Receive` function of each user after a `duration` time from now.

This function sends the packet to every user in the particular channel similar to real transmitters. Only in the MAC layer do the packets get dropped if they are not intended to them.

A.8 OwcMacQueue

A new queue class was written for the OWC module for flexibility with a few appealing features adopted from the `WifiMacQueue` class in the Wi-Fi module. Some of the commonly used functions are listed below.
Sets the maximum time-to-live for a packet.

```
void SetMaxDelay (Time delay)
```

Enqueue and dequeue functions. `OwcMacQueueItem` is the format that packets are store in the queue. It is a tuple of the packet, MAC header and time stamp.

```
bool Enqueue (Ptr<OwcMacQueueItem> item)
Ptr<OwcMacQueueItem> Dequeue (void)
```

Other dequeuing functions that can filter packets based on the address and priority (tid).

```
Ptr<OwcMacQueueItem> DequeueByAddress (Mac48Address dest)
Ptr<OwcMacQueueItem> DequeueByTidAndAddress (uint8_t tid,
Mac48Address dest)
```

Peek functions are used to peek into the queue without dequeuing the packets. They are used by the scheduling algorithms.

```
Ptr<const OwcMacQueueItem> Peek (void) const
Ptr<const OwcMacQueueItem> PeekByTidAndAddress (uint8_t tid,
Mac48Address dest)
```

Following functions are used to get the statistics of the queue. *N* denotes 'number of' and the rest of the function names are self-explanatory.

```
uint32_t GetNPacketsByAddress (Mac48Address dest)
uint32_t GetNBytesByAddress (Mac48Address dest)
uint32_t GetNPacketsByTidAndAddress (uint8_t tid, Mac48Address
dest)
bool IsEmpty (void)
uint32_t GetNPackets (void) uint32_t GetNBytes (void)
```

A.9 OwcPhy

The physical layer was explained in detail in the Subsection 5.3.3. Here we list the two enumerated types used to store the channel state and the type of the physical layer.

```
enum ChannelState
{
OWC_CHANNEL_TXING,
OWC_CHANNEL_RXING,
OWC_CHANNEL_IDLE,
};
```

```
enum ChannelType
{
OWC_DATA_CHANNEL,
OWC_CTRL_CHANNEL,
};
```

Explanation of the `OwcPhy` trace sources.

```
PhyTx - Packet transmitted successfully from the physical layer
PhyTxDrop - Packet dropped while attempting to transmit, ex:
channel busy
PhyRx - Packet received successfully at the physical layer
PhyRxDrop - Packet dropped while attempting to receive, ex:
another transmission started midway
```

A.10 OwcMgtHeaders

The `owc-mgt-header.cc` file contains all the management header classes used in the proposed module. There are four basic headers at the moment as shown in Fig. A.1. With the further development these classes will change and new classes will be added.

A.11 OwcSector

A `OwcSector` object maintains pointers to its physical layer, MAC layer and attached `NetDevice` objects.

A.12 OwcVap

The `OwcVap` class is used to model the virtual access points. These objects have a list of `OwcSector` objects to contain the data sectors. Further, the control sector is stored in a

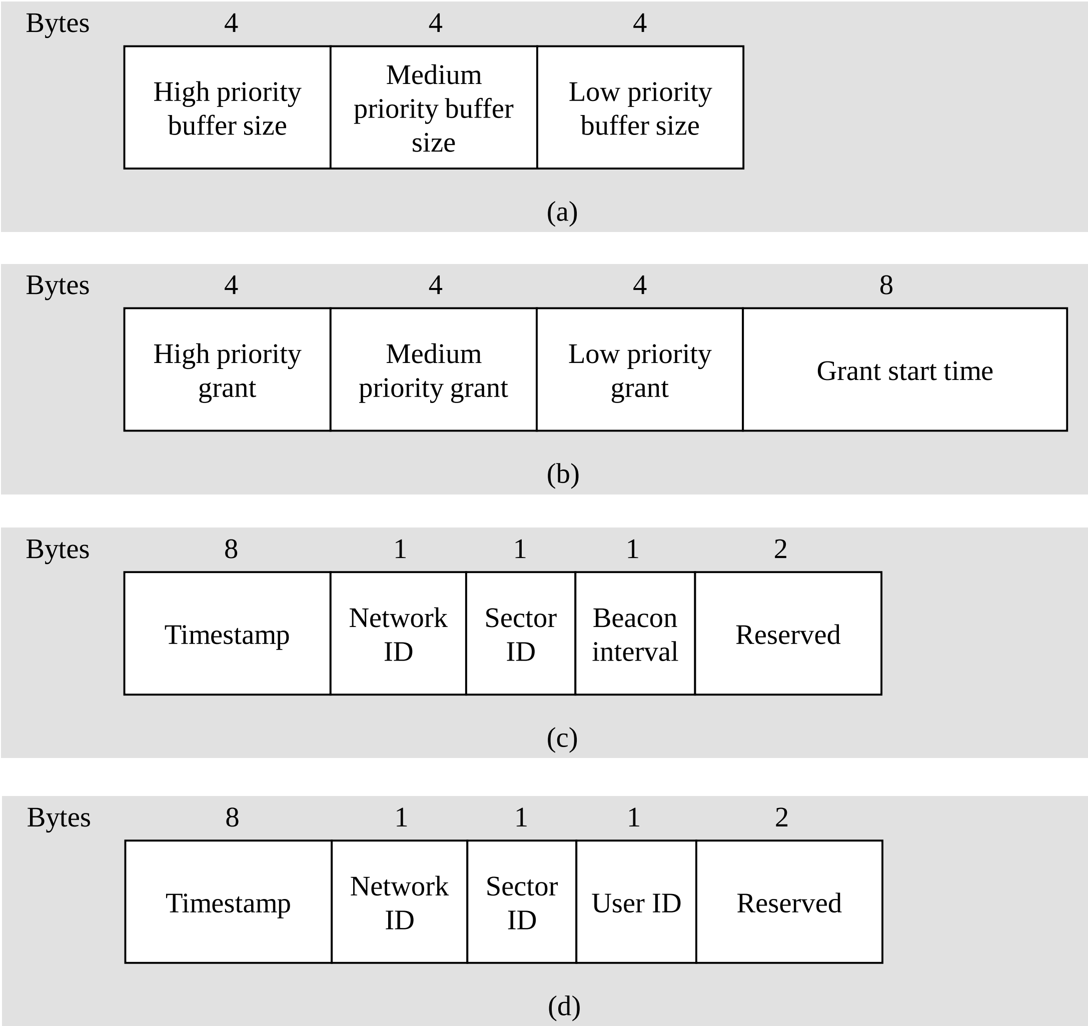

Figure A.1: (a) Buffer status header (b) Grant header (c) Association request and (d) Association response.

separate variable.

A.13 `OwcHelper`

Helper classes are used throughout the ns-3 project to ease the network deployment issues. As explained in 5.2, helper classes bundle the network deployment functions together and provide an interface to customise. For instance, the following code snippet from a simulation script sets up the central office and 5 users. If one were to do it without helper classes, it would be 114 lines of code. Therefore, helper classes are useful in writing simulation scripts quickly and plainly.

```
owcApNode.Create (1);
owcStaNodes.Create (5);

OwcHelper owclink;

NetDeviceContainer staDevices;
staDevices = owclink.Install (owcStaNodes);

NetDeviceContainer apDevices;
apDevices = owclink.InstallCoDevice (owcApNode.Get(0));
```

Bibliography

[1] L. Liu, R. Zhong, W. Zhang, Y. Liu, J. Zhang, L. Zhang, and M. Gruteser, "Cutting the cord: Designing a high-quality untethered VR system with low latency remote rendering," *Proceedings of the 16th Annual International Conference on Mobile Systems, Applications, and Services*, pp. 68–80, 2018.

[2] A. Bekkali, T. Kobayashi, K. Nishimura, N. Shibagaki, K. Kashima, and Y. Sato, "Millimeter-wave-based fiber-wireless bridge system for 8k UHD video streaming and gigabit Ethernet data connectivity," *Journal of lightwave technology*, vol. 36, no. 18, pp. 3988–3998, 2018.

[3] "IEEE standard for information technology–telecommunications and information exchange between systems–local and metropolitan area networks–specific requirements-part 11: Wireless LAN medium access control (MAC) and physical layer (PHY) specifications amendment 3: Enhancements for very high throughput in the 60 GHz band," *IEEE Std 802.11ad-2012 (Amendment to IEEE Std 802.11-2012, as amended by IEEE Std 802.11ae-2012 and IEEE Std 802.11aa-2012)*, pp. 1–628, 2012.

[4] T. Nitsche, C. Cordeiro, A. B. Flores, E. W. Knightly, E. Perahia, and J. C. Widmer, "IEEE 802.11 ad: directional 60 GHz communication for multi-gigabit-per-second Wi-Fi," *IEEE Communications Magazine*, vol. 52, no. 12, pp. 132–141, 2014.

[5] S. Arnon, *Visible light communication*. Cambridge University Press, 2015.

[6] R. X. Ferreira, E. Xie, J. J. McKendry, S. Rajbhandari, H. Chun, G. Faulkner, S. Watson, A. E. Kelly, E. Gu, R. V. Penty *et al.*, "High bandwidth GaN-based micro-LEDs

for multi-Gb/s visible light communications," *IEEE Photonics Technology Letters*, vol. 28, no. 19, pp. 2023–2026, 2016.

[7] "IEEE standard for local and metropolitan area networks–part 15.7: Short-range wireless optical communication using visible light," *IEEE Std 802.15.7-2011*, pp. 1–309, 2011.

[8] 'IEEE 802.15.13 Multi-Gigabit/s Optical Wireless Communications Task Group', http://www.ieee802.org/15/pub/TG13.html, Accessed June 2020.

[9] K. Wang, A. Nirmalathas, C. Lim, and E. Skafidas, "High-speed optical wireless communication system for indoor applications," *IEEE Photonics Technology Letters*, vol. 23, no. 8, pp. 519–521, 2011.

[10] A. Gomez, K. Shi, C. Quintana, R. Maher, G. Faulkner, P. Bayvel, B. C. Thomsen, and D. O'Brien, "Design and demonstration of a 400 Gb/s indoor optical wireless communications link," *Journal of Lightwave Technology*, vol. 34, no. 22, pp. 5332–5339, 2016.

[11] Z. Cao, L. Shen, Y. Jiao, X. Zhao, and T. Koonen, "200 Gbps OOK transmission over an indoor optical wireless link enabled by an integrated cascaded aperture optical receiver," in *2017 Optical Fiber Communications Conference and Exhibition (OFC)*. IEEE, 2017, pp. 1–3.

[12] H. Le Minh, D. O'Brien, G. Faulkner, O. Bouchet, M. Wolf, L. Grobe, and J. Li, "A 1.25-Gb/s indoor cellular optical wireless communications demonstrator," *IEEE Photonics Technology Letters*, vol. 22, no. 21, pp. 1598–1600, 2010.

[13] 'Network Simulator-3', https://www.nsnam.org/, Accessed June 2020.

[14] N. Abramson, "Development of the ALOHANET," *IEEE transactions on Information Theory*, vol. 31, no. 2, pp. 119–123, 1985.

[15] G. Anastasi, L. Lenzini, and E. Mingozzi, "HIPERLAN/1 MAC protocol: stability and performance analysis," *IEEE Journal on Selected Areas in Communications*, vol. 18, no. 9, pp. 1787–1798, 2000.

[16] IEEE, "IEEE standard for wireless LAN medium access control (MAC) and physical layer (PHY) specifications," *IEEE Std 802.11-1997*, pp. 1–445, 1997.

[17] W. Lemstra, V. Hayes, and J. Groenewegen, *The innovation journey of Wi-Fi: The road to global success*. Cambridge University Press, 2010.

[18] R. Fisher, "60 GHz WPAN standardization within IEEE 802.15.3c," in *2007 International Symposium on Signals, Systems and Electronics*. IEEE, 2007, pp. 103–105.

[19] M. S. Gast, *802.11 ac: a survival guide: Wi-Fi at gigabit and beyond*. " O'Reilly Media, Inc.", 2013.

[20] Cisco, "802.11ac: The Fifth Generation of Wi-Fi Technical White Paper," Cisco, Tech. Rep., 2018.

[21] B. Bellalta, "IEEE 802.11 ax: High-efficiency WLANs," *IEEE Wireless Communications*, vol. 23, no. 1, pp. 38–46, 2016.

[22] E. Khorov, A. Kiryanov, A. Lyakhov, and G. Bianchi, "A tutorial on IEEE 802.11 ax high efficiency WLANs," *IEEE Communications Surveys & Tutorials*, vol. 21, no. 1, pp. 197–216, 2018.

[23] D.-J. Deng, Y.-P. Lin, X. Yang, J. Zhu, Y.-B. Li, J. Luo, and K.-C. Chen, "IEEE 802.11 ax: Highly efficient WLANs for intelligent information infrastructure," *IEEE Communications Magazine*, vol. 55, no. 12, pp. 52–59, 2017.

[24] 'Wi-Fi-6E', https://www.qualcomm.com/wi-fi-6e, Accessed June 2020.

[25] 'Wi-Fi Alliance brings Wi-Fi 6 into 6 GHz', https://www.wi-fi.org/news-events/newsroom/wi-fi-alliance-brings-wi-fi-6-into-6-ghz, Accessed June 2020.

[26] P. Zhou, K. Cheng, X. Han, X. Fang, Y. Fang, R. He, Y. Long, and Y. Liu, "IEEE 802.11 ay-based mmWave WLANs: Design challenges and solutions," *IEEE Communications Surveys & Tutorials*, vol. 20, no. 3, pp. 1654–1681, 2018.

[27] R. Bhusal and S. Moh, "Qualitative and quantitative comparison of IEEE 802.15.3c and IEEE 802.11ad for multi-gbps local communications," *Wireless personal communications*, vol. 75, no. 4, pp. 2135–2149, 2014.

[28] A. G. Bell, "The photophone," *Science*, vol. 1, no. 11, pp. 130–134, 1880.

[29] Y. Tanaka, T. Komine, S. Haruyama, and M. Nakagawa, "Indoor visible light data transmission system utilizing white LED lights," *IEICE transactions on communications*, vol. 86, no. 8, pp. 2440–2454, 2003.

[30] T. Komine and M. Nakagawa, "Integrated system of white LED visible-light communication and power-line communication," *IEEE Transactions on Consumer Electronics*, vol. 49, no. 1, pp. 71–79, 2003.

[31] P. H. Pathak, X. Feng, P. Hu, and P. Mohapatra, "Visible light communication, networking, and sensing: A survey, potential and challenges," *IEEE communications surveys & tutorials*, vol. 17, no. 4, pp. 2047–2077, 2015.

[32] D. C. O'brien, L. Zeng, H. Le-Minh, G. Faulkner, J. W. Walewski, and S. Randel, "Visible light communications: Challenges and possibilities," in *2008 IEEE 19th International Symposium on Personal, Indoor and Mobile Radio Communications*. IEEE, 2008, pp. 1–5.

[33] S. Rajagopal, R. D. Roberts, and S.-K. Lim, "IEEE 802.15.7 visible light communication: modulation schemes and dimming support," *IEEE Communications Magazine*, vol. 50, no. 3, pp. 72–82, 2012.

[34] S.-K. Liaw, H. Chou, C.-J. Wu, M.-J. Chien, and C. Teng, "500 Mb/s OOK visible light communications using RGB-based LEDs," in *2015 International Symposium on Next-Generation Electronics (ISNE)*. IEEE, 2015, pp. 1–2.

[35] C.-H. Yeh, C.-W. Chow, and L.-Y. Wei, "1250 Mbit/s OOK wireless white-light VLC transmission based on phosphor laser diode," *IEEE Photonics Journal*, vol. 11, no. 3, pp. 1–5, 2019.

[36] Q. Wang, Z. Wang, and L. Dai, "Multiuser MIMO-OFDM for visible light communications," *IEEE Photonics Journal*, vol. 7, no. 6, pp. 1–11, 2015.

[37] M. S. Mossaad, S. Hranilovic, and L. Lampe, "Visible light communications using OFDM and multiple LEDs," *IEEE Transactions on Communications*, vol. 63, no. 11, pp. 4304–4313, 2015.

[38] M. Z. Afgani, H. Haas, H. Elgala, and D. Knipp, "Visible light communication using OFDM," in *2nd International Conference on Testbeds and Research Infrastructures for the Development of Networks and Communities, 2006. TRIDENTCOM 2006.* IEEE, 2006, pp. 6–pp.

[39] T. Nguyen, A. Islam, T. Yamazato, and Y. M. Jang, "Technical issues on IEEE 802.15. 7m image sensor communication standardization," *IEEE Communications Magazine*, vol. 56, no. 2, pp. 213–218, 2018.

[40] V. Jungnickel, "Text proposal for high bandwidth PHY," Available at https://mentor.ieee.org/802.15/documents (June 2020), from the document archive of IEEE P802.15 Working Group for Wireless Personal Area Networks (WPANs).

[41] M. Uysal, F. Miramirkhani, T. Baykas, and K. Qaraqe, "IEEE 802.11bb reference channel models for indoor environments," Tech. Rep., 2018.

[42] P. Hu, P. H. Pathak, A. K. Das, Z. Yang, and P. Mohapatra, "PLiFi: Hybrid WiFi-VLC networking using power lines," in *Proceedings of the 3rd Workshop on Visible Light Communication Systems*, 2016, pp. 31–36.

[43] M. B. Rahaim, A. M. Vegni, and T. D. Little, "A hybrid radio frequency and broadcast visible light communication system," in *2011 IEEE GLOBECOM Workshops (GC Wkshps).* IEEE, 2011, pp. 792–796.

[44] E. Edirisinghe, P. Karunarathna, D. Dissanayake, and G. Godaliyadda, "Design and implementation of a bi-directional visible light communication system," in *2015 IEEE 10th International Conference on Industrial and Information Systems (ICIIS).* IEEE, 2015, pp. 519–524.

[45] ’5G vs. Wi-Fi 6: A Powerful Combination for Wireless’, https://www.intel.com/content/www/us/en/wireless-network/5g-technology/5g-vs-wifi.html#: :text=As%20with%20LTE%2C%20mobile%20carriers, predecessor%2C%20Wi%2DFi%205.z, Accessed June 2020.

[46] ’What’s Best? Wi-Fi 6 (802.11ax) or 5G’, https://www.qorvo.com/design-hub/blog/whats-best-wifi-6-80211ax-or-5g, Accessed June 2020.

[47] J. M. Kahn and J. R. Barry, “Wireless infrared communications,” *Proceedings of the IEEE*, vol. 85, no. 2, pp. 265–298, 1997.

[48] H. Elgala, R. Mesleh, and H. Haas, “Indoor optical wireless communication: potential and state-of-the-art,” *IEEE Communications Magazine*, vol. 49, no. 9, pp. 56–62, 2011.

[49] C. Oh, E. Tangdiongga, and A. Koonen, “Steerable pencil beams for multi-Gbps indoor optical wireless communication,” *Optics Letters*, vol. 39, no. 18, pp. 5427–5430, 2014.

[50] ’Electromagnetic Spectrum’, https://www.infratec.eu/sensor-division/service-support/glossary/infrared-radiation/, Accessed June 2020.

[51] G. A. Mahdiraji and E. Zahedi, “Comparison of selected digital modulation schemes (OOK, PPM and DPIM) for wireless optical communications,” in *2006 4th Student Conference on Research and Development*. IEEE, 2006, pp. 5–10.

[52] R. Mesleh, H. Elgala, and H. Haas, “On the performance of different OFDM based optical wireless communication systems,” *IEEE/OSA Journal of Optical Communications and Networking*, vol. 3, no. 8, pp. 620–628, 2011.

[53] T. Koonen, F. Gomez-Agis, Z. Cao, K. Mekonnen, F. Huijskens, and E. Tangdiongga, “Indoor ultra-high capacity optical wireless communication using steerable infrared beams,” in *2017 International Topical Meeting on Microwave Photonics (MWP)*. IEEE, 2017, pp. 1–4.

[54] W. Ke, A. Nirmalathas, C. Lim, S. Tingting, L. Tian, K. Alameh, and E. Skafidas, "Short-range optical wireless communications for indoor and interconnects applications," *ZTE Communications*, vol. 14, no. 2, pp. 13–22, 2019.

[55] P. Brandl, S. Schidl, A. Polzer, W. Gaberl, and H. Zimmermann, "Optical wireless communication with adaptive focus and MEMS-based beam steering," *IEEE Photonics Technology Letters*, vol. 25, no. 15, pp. 1428–1431, 2013.

[56] B. Glushko, A. Shar, M. Medina, D. Kin, and S. Krylov, "MEMS-based tracking for an indoor optical wireless communication bidirectional link," *IEEE Photonics Technology Letters*, vol. 28, no. 5, pp. 550–553, 2016.

[57] G. Wang, U. Habib, Z. Yan, N. J. Gomes, Q. Sui, J.-B. Wang, L. Zhang, and C. Wang, "Highly efficient optical beam steering using an in-fiber diffraction grating for full duplex indoor optical wireless communication," *Journal of Lightwave Technology*, vol. 36, no. 19, pp. 4618–4625, 2018.

[58] I. Abdalla, M. B. Rahaim, and T. D. Little, "Interference in multi-user optical wireless communications systems," *Philosophical Transactions of the Royal Society A*, vol. 378, no. 2169, p. 20190190, 2020.

[59] K. Wang, A. Nirmalathas, C. Lim, and E. Skafidas, "High speed 4$\times$ 12.5 Gbps wdm optical wireless communication systems for indoor applications," in *Optical Fiber Communication Conference*. Optical Society of America, 2011, p. JWA081.

[60] G. W. Marsh and J. M. Kahn, "Channel reuse strategies for indoor infrared wireless communications," *IEEE Transactions on Communications*, vol. 45, no. 10, pp. 1280–1290, 1997.

[61] S. S. Bawazir, P. C. Sofotasios, S. Muhaidat, Y. Al-Hammadi, and G. K. Karagiannidis, "Multiple access for visible light communications: Research challenges and future trends," *Ieee Access*, vol. 6, pp. 26 167–26 174, 2018.

[62] M. H. Shoreh, A. Fallahpour, and J. A. Salehi, "Design concepts and performance analysis of multicarrier CDMA for indoor visible light communications," *Journal of Optical Communications and Networking*, vol. 7, no. 6, pp. 554–562, 2015.

[63] C. Chen, W.-D. Zhong, H. Yang, and P. Du, "On the performance of MIMO-NOMA-based visible light communication systems," *IEEE Photonics Technology Letters*, vol. 30, no. 4, pp. 307–310, 2017.

[64] V. Vitsas and A. C. Boucouvalas, "Performance analysis of the advanced infrared (AIr) CSMA/CA MAC protocol for wireless lans," *Wireless Networks*, vol. 9, no. 5, pp. 495–507, 2003.

[65] P. Chatzimisios and A. C. Boucouvalas, "Packet delay analysis of the advanced infrared (AIr) CSMA/CA MAC protocol in optical wireless LANs," *International Journal of Communication Systems*, vol. 18, no. 3, pp. 307–331, 2005.

[66] T. Fickenscher, J. Holborn, and D. Thiel, "Underwater wireless optical communication for swimmer feedback using IrDA transceiver," *Electronics letters*, vol. 47, no. 24, pp. 1335–1336, 2011.

[67] S. Asadallahi, H. H. Refai, and P. G. LoPresti, "Performance comparison of CSMA/CA advanced infrared (AIr) and a new point-to-multipoint optical MAC protocol," in *2012 8th International Wireless Communications and Mobile Computing Conference (IWCMC)*. IEEE, 2012, pp. 1149–1153.

[68] H. Zhu, M. Li, I. Chlamtac, and B. Prabhakaran, "A survey of quality of service in IEEE 802.11 networks," *IEEE Wireless Communications*, vol. 11, no. 4, pp. 6–14, 2004.

[69] G. Bianchi, "Performance analysis of the IEEE 802.11 distributed coordination function," *IEEE Journal on Selected Areas in Communications*, vol. 18, no. 3, pp. 535–547, 2000.

[70] C. Cordeiro, D. Akhmetov, and M. Park, "Ieee 802.11 ad: Introduction and performance evaluation of the first multi-gbps wifi technology," in *Proceedings of the 2010*

ACM international workshop on mmWave communications: from circuits to networks, 2010, pp. 3–8.

[71] Y. Xiao, X. Shen, and H. Jiang, "Optimal ack mechanisms of the ieee 802.15. 3 mac for ultra-wideband systems," *IEEE Journal on Selected Areas in Communications*, vol. 24, no. 4, pp. 836–842, 2006.

[72] J.-P. Javaudin, M. Bellec, D. Varoutas, and V. Suraci, "OMEGA ICT project: Towards convergent gigabit home networks," in *2008 IEEE 19th International Symposium on Personal, Indoor and Mobile Radio Communications*. IEEE, 2008, pp. 1–5.

[73] V. Guerra, J. Rabadan, R. Perez-Jimenez, M. Brzozowski, V. Sark, R. Singh, G. Faulkner, D. O'Brien, G. Vercasson, T. Weszely *et al.*, "WORTECS: enabling untethered virtual reality through optical wireless communication," in *2020 South American Colloquium on Visible Light Communications (SACVC)*. IEEE, 2020, pp. 1–6.

[74] M. Shahjalal, M. Z. Chowdhury, M. K. Hasan, M. T. Hossan, and Y. M. Jang, "A generalized SDN framework for optical wireless communication networks," in *2018 International Conference on Information and Communication Technology Convergence (ICTC)*. IEEE, 2018, pp. 848–851.

[75] N. McKeown, T. Anderson, H. Balakrishnan, G. Parulkar, L. Peterson, J. Rexford, S. Shenker, and J. Turner, "OpenFlow: enabling innovation in campus networks," *ACM SIGCOMM Computer Communication Review*, vol. 38, no. 2, pp. 69–74, 2008.

[76] T. Koonen, J. Oh, K. Mekonnen, Z. Cao, and E. Tangdiongga, "Ultra-high capacity indoor optical wireless communication using 2D-steered pencil beams," *Journal of Lightwave Technology*, vol. 34, no. 20, pp. 4802–4809, 2016.

[77] Y. Wang, N. Chi, Y. Wang, L. Tao, and J. Shi, "Network architecture of a high-speed visible light communication local area network," *IEEE Photonics Technology Letters*, vol. 27, no. 2, pp. 197–200, 2014.

[78] IEEE, "IEEE standard for information technology– telecommunications and information exchange between systems local and metropolitan area networks– specific requirements–part 11: Wireless lan medium access control (MAC) and physical layer (PHY) specifications–amendment 4: Enhancements for very high throughput for operation in bands below 6 ghz." *IEEE Std 802.11ac-2013 (Amendment to IEEE Std 802.11-2012, as amended by IEEE Std 802.11ae-2012, IEEE Std 802.11aa-2012, and IEEE Std 802.11ad-2012)*, pp. 1–425, 2013.

[79] S. Joumessi-Demeffo, S. Sahuguède, A. Julien-Vergonjanne, and P. Combeau, "Performance trade-offs of an optical wireless communication network deployed in an aircraft cockpit," *IEEE Open Journal of the Communications Society*, 2020.

[80] J. Choi, J. Yoo, S. Choi, and C. Kim, "EBA: An enhancement of the IEEE 802.11 DCF via distributed reservation," *IEEE Transactions on Mobile Computing*, vol. 4, no. 4, pp. 378–390, 2005.

[81] E. Ziouva and T. Antonakopoulos, "CSMA/CA performance under high traffic conditions: throughput and delay analysis," *Computer communications*, vol. 25, no. 3, pp. 313–321, 2002.

[82] Cisco, "The zettabyte era-trends and analysis," Cisco, Tech. Rep., 2017.

[83] S. Edirisinghe, C. Lim, A. Nirmalathas, E. Wong, K. Wang, and K. Alameh, "Dynamic tuning of contention window for optical wireless networks," *2018 Optical Fiber Communications Conference and Exposition (OFC)*, pp. 1–3, 2018.

[84] S. Mangold, S. Choi, G. R. Hiertz, O. Klein, and B. Walke, "Analysis of IEEE 802.11 e for QoS support in wireless LANs," *IEEE wireless communications*, vol. 10, no. 6, pp. 40–50, 2003.

[85] O. Abari, D. Bharadia, A. Duffield, and D. Katabi, "Cutting the cord in virtual reality," in *Proceedings of the 15th ACM Workshop on Hot Topics in Networks*, 2016, pp. 162–168.

[86] 'GitHub Repository', https://github.com/essedirisinghe/OWC, Accessed June 2020.

[87] R. Pries, S. Menth, D. Staehle, M. Menth, and P. Tran-Gia, "Dynamic contention window adaptation (DCWA) in IEEE 802.11e wireless local area networks," *2008 Second International Conference on Communications and Electronics*, pp. 92–97, 2008.

[88] Cisco Systems, "Voice over wireless LAN 4.1 design guide," 2010.

[89] L. Romdhani, Q. Ni, and T. Turletti, "Adaptive EDCF: enhanced service differentiation for IEEE 802.11 wireless ad-hoc networks," *Wireless communications and networking, 2003. WCNC 2003. 2003 IEEE*, vol. 2, pp. 1373–1378, 2003.

[90] S. Vittorio and L. L. Bello, "An approach to enhance the QoS support to real-time traffic on IEEE 802.11 e networks," *Proceedings of the 6th International Workshop on Real Time Networks (RTN'07)*, 2007.

[91] L. Gannoune and S. Robert, "Dynamic tuning of the contention window minimum (cwmin) for enhanced service differentiation in ieee 802.11 wireless ad-hoc networks," *Personal, Indoor and Mobile Radio Communications, 2004. PIMRC 2004. 15th IEEE International Symposium on*, vol. 1, pp. 311–317, 2004.

[92] I. Syed and B.-h. Roh, "Adaptive backoff algorithm for contention window for dense IEEE 802.11 WLANs," *Mobile Information Systems*, 2016.

[93] S. Prasetya, B. Rahmat, and E. Susanto, "Quality of service improvement with 802.11e EDCA scheme using enhanced adaptive contention window algorithm," *2015 IEEE International Conference on Communication, Networks and Satellite (COMNESTAT)*, pp. 80–85, 2015.

[94] C. Zhang, P. Chen, J. Ren, X. Wang, and A. V. Vasilakos, "A backoff algorithm based on self-adaptive contention window update factor for IEEE 802.11 DCF," *Wireless networks*, vol. 23, no. 3, pp. 749–758, 2017.

[95] S. Edirisinghe, C. Ranaweera, E. Wong, C. Lim, and A. Nirmalathas, "A novel network architecture for indoor optical wireless communication," in *2019 Global LIFI Congress (GLC)*. IEEE, 2019, pp. 1–6.

[96] C. Ranaweera, M. G. Resende, K. Reichmann, P. Iannone, P. Henry, B.-J. Kim, P. Magill, K. N. Oikonomou, R. K. Sinha, and S. Woodward, "Design and optimization of fiber optic small-cell backhaul based on an existing fiber-to-the-node residential access network," *IEEE Communications Magazine*, vol. 51, no. 9, pp. 62–69, 2013.

[97] R. Bian, I. Tavakkolnia, and H. Haas, "10.2 Gb/s visible light communication with off-the-shelf LEDs," in *2018 European Conference on Optical Communication (ECOC)*. IEEE, 2018, pp. 1–3.

[98] A. Nirmalathas, T. Liang, S. Edirisinghe, C. Lim, E. Wong, K. Wang, and K. Alameh, "High-speed optical wireless communications for local area networks," in *2018 23rd Opto-Electronics and Communications Conference (OECC)*. IEEE, 2018, pp. 1–2.

[99] T. Koonen, F. Gomez-Agis, F. Huijskens, K. A. Mekonnen, Z. Cao, and E. Tangdiongga, "High-capacity optical wireless communication using two-dimensional IR beam steering," *Journal of Lightwave Technology*, vol. 36, no. 19, pp. 4486–4493, 2018.

[100] R. C. Kizilirmak, O. Narmanlioglu, and M. Uysal, "Centralized light access network (c-LiAN): A novel paradigm for next generation indoor VLC networks," *IEEE Access*, vol. 5, pp. 19 703–19 710, 2017.

[101] D. A. Basnayaka and H. Haas, "Hybrid RF and VLC systems: Improving user data rate performance of VLC systems," in *2015 IEEE 81st Vehicular Technology Conference (VTC Spring)*. IEEE, 2015, pp. 1–5.

[102] K. Lin and K. Hirohashi, "High-speed full-duplex multiaccess system for LED-based wireless communications using visible light," in *Proc of the International Symposium on Optical Engineering and Photonic Technology (OEPT)*, 2009, pp. 1–5.

[103] K. A. Mekonnen, J. H. Van Zantvoort, N. Calabretta, N. Tessema, E. Tangdiongga, and T. Koonen, "High-capacity dynamic indoor network employing optical-wireless and 60-GHz radio techniques," *Journal of Lightwave Technology*, vol. 36, no. 10, pp. 1851–1861, 2018.

[104] 'Preparing the Enterprise for Wi-Fi 6', https://www.cisco.com/c/en/us/solutions/cisco-on-cisco/enterprise-wifi-6.html, Accessed June 2020.

[105] 'Enterprise Wi-Fi connectivity', https://www.arubanetworks.com/en-au/products/networking/access-points/, Accessed June 2020.

[106] P. Calhoun, M. Montemurro, and D. Stanley, "Control and provisioning of wireless access points (CAPWAP) protocol specification," *IETF RFC 5415*, 2009.

[107] M. Jain, J. I. Choi, T. Kim, D. Bharadia, S. Seth, K. Srinivasan, P. Levis, S. Katti, and P. Sinha, "Practical, real-time, full duplex wireless," in *Proceedings of the 17th annual international conference on Mobile computing and networking*. ACM, 2011, pp. 301–312.

[108] S. Jin and S. Choi, "A seamless handoff with multiple radios in IEEE 802.11 WLANs," *IEEE Transactions on Vehicular Technology*, vol. 63, no. 3, pp. 1408–1418, 2013.

[109] ECMA-387, "High rate 60 GHz PHY, MAC and HDMI PALs," ECMA International, Tech. Rep., 2010).

[110] E. M. Mohamed, K. Sakaguchi, and S. Sampei, "Wi-Fi coordinated WiGig concurrent transmissions in random access scenarios," *IEEE Transactions on Vehicular Technology*, vol. 66, no. 11, pp. 10 357–10 371, 2017.

[111] I. BAROŇÁK and M. Halas, "Mathematical representation of VoIP connection delay," *Radioengineering*, vol. 16, no. 3, p. 77, 2007.

[112] 'MCS Table', https://www.semfionetworks.com/blog/mcs-table-updated-with-80211ax-data-rates, Accessed June 2020.

[113] MATLAB, *version 9.8.0 (R2020a)*. Natick, Massachusetts: The MathWorks Inc., 2020.

[114] 'OPNET Modeler', https://support.riverbed.com/content/support/software/opnet-model/modeler.html, Accessed June 2020.

[115] 'NetSim', https://www.tetcos.com/index.html, Accessed June 2020.

[116] 'OMNeT++ Discrete Event Simulator', https://omnetpp.org/, Accessed June 2020.

[117] A. Aldalbahi, M. Rahaim, A. Khreishah, M. Ayyash, R. Ackerman, J. Basuino, W. Berreta, and T. D. Little, "Extending ns3 to simulate visible light communication at network-level," in *2016 23rd International Conference on Telecommunications (ICT)*. IEEE, 2016, pp. 1–6.

[118] A. Aldalbahi, "Simulation, performance and interference analysis of multi-user visible light communication systems," 2017.

[119] M. Bilgi and M. Yuksel, "Packet-based simulation for optical wireless communication," in *2010 17th IEEE Workshop on Local & Metropolitan Area Networks (LANMAN)*. IEEE, 2010, pp. 1–6.

[120] H. Assasa and J. Widmer, "Implementation and evaluation of a WLAN IEEE 802.11 ad model in ns-3," in *Proceedings of the Workshop on Ns-3*, 2016, pp. 57–64.

[121] M. Mezzavilla, M. Zhang, M. Polese, R. Ford, S. Dutta, S. Rangan, and M. Zorzi, "End-to-end simulation of 5G mmWave networks," *IEEE Communications Surveys & Tutorials*, vol. 20, no. 3, pp. 2237–2263, 2018.

[122] L. Tian, S. Deronne, S. Latré, and J. Famaey, "Implementation and validation of an IEEE 802.11 ah module for ns-3," in *Proceedings of the Workshop on ns-3*, 2016, pp. 49–56.

[123] 'Wireshark. Go Deep.', https://www.wireshark.org/, Accessed June 2020.

[124] 'ns-2 wiki', http://nsnam.sourceforge.net/wiki/index.php/Main_Page, Accessed June 2020.

[125] E. Dinc, O. Ergul, and O. B. Akan, "Soft handover in OFDMA based visible light communication networks," in *2015 IEEE 82nd Vehicular Technology Conference (VTC2015-Fall)*. IEEE, 2015, pp. 1–5.

[126] T. Y. Elganimi, "Performance comparison between OOK, PPM and PAM modulation schemes for free space optical (FSO) communication systems: analytical study," *International Journal of Computer Applications*, vol. 79, no. 11, 2013.

[127] IEEE, "IEEE standard for high data rate wireless multi-media networks," *IEEE Std 802.15.3-2016 (Revision of IEEE Std 802.15.3-2003)*, pp. 1–510, 2016.

[128] O. Sharon and Y. Alpert, "A new aggregation based scheduling method for rapidly changing IEEE 802.11 ac wireless channels," *arXiv preprint arXiv:1803.10170*, 2018.

[129] C.-W. Pyo, F. Kojima, J. Wang, H. Harada, and S. Kato, "MAC enhancement for high speed communications in the 802.15.3c mmWave WPAN," *Wireless personal communications*, vol. 51, no. 4, p. 825, 2009.

[130] A. Lindgren, A. Almquist, and O. Schelén, "Quality of service schemes for IEEE 802.11 wireless LANs–an evaluation," *Mobile networks and applications*, vol. 8, no. 3, pp. 223–235, 2003.

[131] Y. Lv, M. P. I. Dias, L. Ruan, E. Wong, Y. Feng, N. Jiang, and K. Qiu, "Request-based polling access: Investigation of novel wireless LAN MAC scheme for low-latency e-health applications," *IEEE Communications Letters*, vol. 23, no. 5, pp. 896–899, 2019.